理學博士學位論文

방선균 *Streptomyces coelicolor*에서 아연의 획득과 방출을 조절하는 Zur의 전사 조절기작

Regulation of zinc import and export genes by zinc-responsive Zur in *Streptomyces coelicolor*

2017年 8月

서울大學校 大學院

生命科學部

崔 乘 桓

Regulation of zinc import and export genes by zinc-responsive Zur in *Streptomyces coelicolor*

by

Seung-Hwan Choi

under the supervision of

Professor Jung-Hye Roe, Ph.D.

A Thesis submitted in Partial Fulfillment of the Requirements for the Degree of

Doctor of Philosophy

August, 2017

SCHOOL OF BIOLOGICAL SCIENCES

GRADUATE SCHOOL

SEOUL NATIONAL UNIVERSITY

ABSTRACT

In various bacteria Zur (Zinc-uptake-regulator), a zinc-specific regulator of Fur family, regulates genes for zinc uptake to maintain zinc homeostasis. It has also been suggested to control zinc mobilization by regulating some ribosomal proteins. The antibiotics-producing soil bacterium *Streptomyces coelicolor* contains four genes for Fur family regulators, and one (named as *zur*) is located downstream of the *znuACB* operon encoding a putative zinc uptake transporter. Zinc specifically represses the level of *znuA* transcript by Zur. Zn-Zur also represses genes for ribosomal proteins L31 (*rpmE*) and L33 (*rpmG*) for zinc mobilization. Previous ChIP-chip analysis and expression analysis in delta-zur mutant revealed a unique target of Zur, SCO6751, which is predicted to be a zinc-exporter and the expression of which is activated by Zur. The activation mechanism of SCO6751, which later was named *zitB*, was investigated. The *zitB* over-expressing cells showed white phenotype, being defective in sporulation, and decreased intracellular zinc content. Zinc-dependent gene activation by Zur occurred in two phases: at sub-femtomolar zinc concentrations (phase I) with concomitant repression of zinc-uptake genes, and at over micromolar zinc conditions (phase II). DNase I footprinting on *zitB* DNA was performed with fixed amount of Zur (2.7 μM) and varying $ZnSO_4$ from 2.5 to 10 μM. The results demonstrated that the Zur-footprint extended further upstream as zinc increased, up to -138 nt from TSS. This expansion in Zur-binding region is likely to lie behind the induction of *zitB* by zinc in phase II. It can be postulated that high concentrations of zinc could have caused some changes in Zur and its DNA-binding behavior. Whether high zinc induces Zur oligomerization in the absence of DNA was examined. Zur appears not to form oligomers beyond dimer by itself under high zinc condition. The physiological role of *zitB*

upstream sequence in vivo was examined. The effectiveness of the *zitB* upstream region in zinc-dependent gene activation was examined *in vivo* by using a heterologous reporter gene (GUS). Recombinant p*zitB*-GUS fusion plasmids that contain the *zitB* regulatory region up to Zur binding motif (from +50 ~ -60 nt) or including expanded Zur-binding region (up to -228 nt) were constructed on pSET152-based integration vector. The S1 mapping of GUS transcripts demonstrated that the *zitB* regulatory region with the Zur-box motif only allowed only marginal gene activation, whereas the longer *zitB* upstream sequence enabled full activation of the reporter gene expression. A molecular model of the Zur_2-DNA complex in low zinc condition was presented. As the level of zinc increases to micromolar range, oligomeric Zur binding was observed in vitro. At micromolar zinc, formation of hexameric or octameric Zur bindings were captured by EMSA with limited amount of Zur. From EMSA, the formation of super-retarded complex with higher concentration of Zur indicated the possibility of multimerization of Zur, with or without DNA conformational change, to underlie the activation mechanism of phase II. Taken together these findings reveal a novel mode of zinc-dependent gene activation and an ingenious strategy to use a single metallo-regulator to control both the uptake and export genes over a wide range of zinc concentrations.

Keywords: *Streptomyces coelicolor*, Fur family, Zur, zinc homeostasis, *znuA*, zinc-exporter, *zitB*, activation mechanism, mechanism structure model.

CONTENTS

LIST OF FIGURES

LIST OF TABLES

LIST OF ABBREVIATIONS

ABC	ATP binding cassette
bp	base pair
BSA	bovine serum albumin
Da	dalton
DTT	dithiothreitol
EDTA	ethylenediamietetraacetate
nt	nucleotide
OD	optical density
PAGE	polyacrylamide gel electrophoresis
PCR	polymerase chain reaction
TPEN	N,N,N′,N′-Tetrakis-(2-pyridylmethyl)ethylenediamine
ABC	ATP binding cassette
EMSA	electrophoretic mobility shift assay
Fur	ferric uptake regulator
GUS	β-glucuronides
zitB	zinc ion transport
ICP-MS	inductively coupled plasma-mass spectrometry
IPTG	isopropyl-β-D-thiogalactopyranoside
aa	amino acid
WT	wild type
Zur	zinc uptake regulator

CHAPTER I

INTRODUCTION

I.1. Biology of *Streptomyces coelicolor*

Streptomycetes are the most widely studied and well-known genus of the actinomycete family and ubiquitous Gram-positive soil bacteria with a unique capacity for the production of varied and complex secondary metabolites. They are crucial in soil environment because of their broad range of metabolic processes. They usually inhabit soil and are important decomposers. They are crucial in soil because of their broad range of metabolic processes and biotransformations. These include degradation of the insoluble remains of other organisms, such as lignocellulose and chitin, making Streptomycetes central organisms in carbon recycling (McCarthy and Williams, 1992). The importance of Streptomycetes to medicine results from their production of over two-thirds of naturally derived antibiotics in current use (Bentley *et al*., 2002).

Unusually for bacteria, Streptomycetes undergo complex multicellular developmental life cycle. *Streptomyces* life cycle starts from germination of spore and formation of highly branched vegetative mycelium. The hyphae are divid ed into multigenomic compartments by the infrequent formation of veget ative septa. After a period of active growth, aerial mycelium develops from substrate mycelium on the surface of colony, and eventually differentiates into unigenomic spores (Mc Gregor *et al.,* 1954) (Fig. I-1). Genetic studies on morphological differentiation started from the isolation of mutants with altered morphology: *bld* (bald) mutants which fail in aerial mycelium formation, and *whi* mutants which are defective in sporulation (Merric, 1976; Potúčková *et al*., 1995, Pope *et al*., 1996; Keleman *et al*., 1996; Nodwell *et al*., 1996). The morphological differentiation is often temporally associated with physiological differentiation, the production of secondary metabolites, as synthesis generall y occurs after the main period of rapid growth and assimilative metaboli sm (Chater, 1984; Demain *et al*., 1983; Matsumoto *et al*., 1995; Onaka *et al*.,).

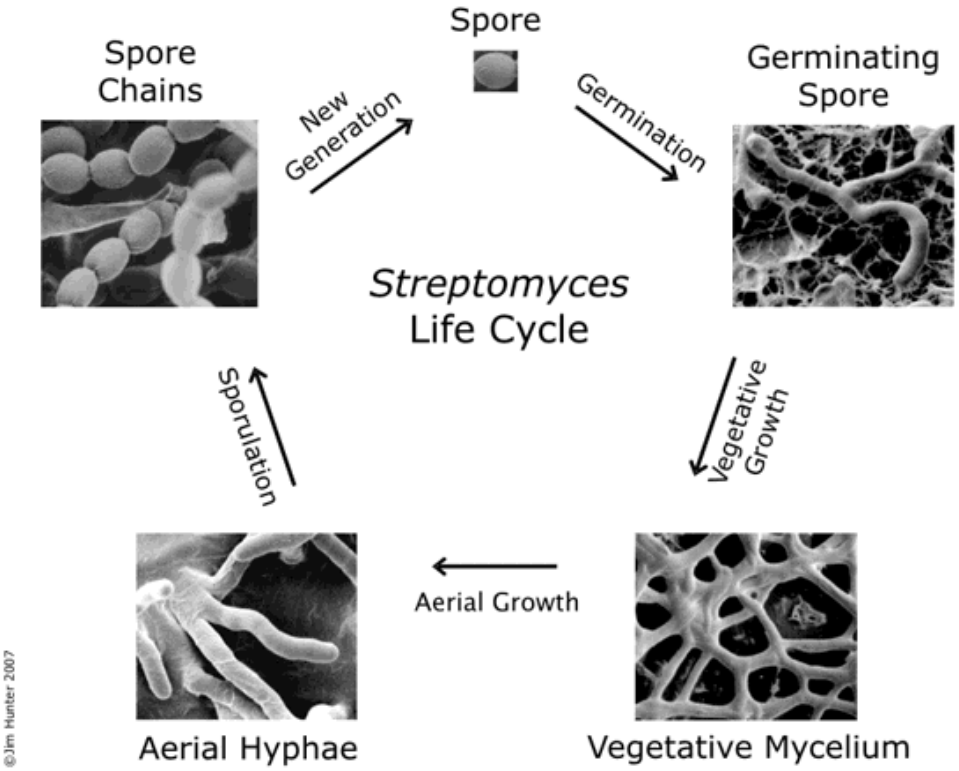

Fig. I-1. The life cycle of *Streptomyces coelicolor*.

From a single spore a vegetative mycelium germinates, this is followed by aerial growth with the production of aerial hyphae. These hyphae in turn will undergo synchronous septation to produce unigenomic spore compartments, which will disperse and thus commence a new cycle.

Streptomyces species have been the subject of genetic investigation for over 50 years, with many studies focusing on the developmental cycle and the production of secondary metabolites. Among them, *Streptomyces coelicolor* is genetically the best known representative of the genus. The complete DNA sequence of *S. coelicolor* M145 has been published, (Bentlely *et al*., 2002). The linear chromosome is 8,667,507 bp long and is predicted to contain 7,825 genes, about twice as many as typical free-living bacteria, making it the largest bacterial genome yet sequenced. The genome shows a strong emphasis on regulation, with 965 proteins (12.3%) predicted to have regulatory function. This is not only attractive feature but also for a challenging puzzle for future investigation to elucidate gene regulation in this organism.

I.2. Bacterial Fur family Metalloregulators

I.2.1. Fur

Fur (Ferric-uptake-regulator) was first characterized as an iron-responsive repressor of iron-transport systems in *Escherichia coli* (Hantke, 1981; Bagg and Neilands, 1987a, b). The studies of the *E. coli* Fur and its role have been summarized in several reviews (Bagg and Neilands, 1987a, *b*; Escolar *et al*., 1999; Hantke, 2001; Braun, 2003; Troxell and Hassan, 2013). Together, these studies led to a clear and compelling model for Fur mediated repression of target genes under iron-replete conditions. This regulation model posits that the coordination of one Fe^{2+} per monomer enables the dimeric Fur protein to bind a specific 19 bp DNA sequence, called the "Fur box", within the promoter of the regulated genes. The affinity of Fur protein for Fe^{2+} is poised to allow accumulation of sufficient intracellular Fe to activate essential iron-containing and iron-utilizing enzymes (e.g. enzymes for heme and FeS cluster synthesis).

However, when iron levels exceed those needed for metallo-enzyme function, Fur protein represses further uptake and thereby helps prevent iron overload. Typically, the binding of iron-loaded Fur hinders the access of RNA polymerase resulting in the repression of downstream genes (Fig. I-2; mechanism 1). Numerous studies support the validity of this general model and it likely accounts for a significant fraction of the iron-dependent regulation effected by Fur. However, recent results indicate that regulation by Fur, and Fur-like proteins, can be much more complex.

The role of *E. coli* Fur (*Ec*Fur) as an Fe^{2+}-dependent repressor, as inferred from early genetic studies, was first demonstrated using an in vitro coupled-transcription translation system (Bagg and Neilands, 1987a, b). In vitro, numerous other divalent cations can also activate the Fur protein to bind DNA. For reasons of convenience, the majority of studies employ Mn^{2+} (which unlike Fe^{2+} is stable in aerobic solutions) as a corepressor. The ability of Fur to bind DNA in response to Mn^{2+} likely underlies the observation that *fur* mutants have an increased ability to grow in the presence of elevated levels of Mn^{2+} (Hantke, 1987). The implication is that excess Mn^{2+} in the growth medium can bind Fur and inappropriately repress iron homeostasis functions thereby impeding growth. Direct biochemical measurements have also provided evidence for a regulatory metal ion binding site with an apparent dissociation constant for metal ions in the low micromolar range (Mills and Marletta, 2005). The affinity of Fur for ferrous iron is comparable to the estimated levels of free (loosely bound and chelatable) iron present in the cytosol (Keyer and Imlay, 1996), consistent with a role for Fur as the primary monitor and regulator of intracellular iron levels. Presumably, occupancy of this regulatory metal-binding site alters the conformation of the protein to allow interaction with operator DNA. The Fur family of proteins is widespread within the Bacteria

with ~800 homologs represented in the current compilations of the PFAM (PFO1475; 764 matches) and EMBL InterPro (IPR002481; 837 matches) databases. A structural Zn^{2+} ion is also shown in this example; although not all Fur proteins have structural zinc. Approximately one half of these identified representatives are from the proteobacteria and another ~200 from the Firmicutes. The emerging consensus is that most of these proteins are likely to function as metal-dependent, DNA-binding repressors. However, within this family the metal-dependence and metal-specificity varies widely, even among the small minority of members that has been functionally characterized. Thus, it is important to appreciate that proteins annotated as "ferric uptake repressor", or with a related descriptor, may or may not actually sense iron. Examples of Fur family members that respond to other metals include sensors of zinc (Zur), manganese (Mur), and nickel (Nur). The ability of Fur family members to function physiologically as sensors of Zn^{2+} was discovered concurrently in *B. subtilis* (*Bs*Zur) and *E. coli* Zur (*Ec*Zur) (Gaballa and Helmann, 1998; Patzer and Hantke, 1998).

I.2.2. Nur

A nickel-uptake-regulator (Nur) was discovered in *Streptomyces coelicolor* thereby adding a nickel responsive member to the Fur family (Ahn *et al*., 2006, An *et al*., 2009) (Fig I-3.). Nur exhibits significant similarity to other members of Fur family having 27% identity (48% similarity) to *Ec*Fur. Nur has four of the five conserved amino acids predicted to constitute the regulatory metal-sensing site (based on functional studies of PerR; Lee and Helmann, 2006b), with the fifth replaced by His. This is the likely location for a Ni^{2+}-selective regulatory site. In addition, both CXXC motifs that comprise the structural Zn^{2+}-site in *Bs*PerR are well conserved in Nur. In contrast, the predicted regulatory metal

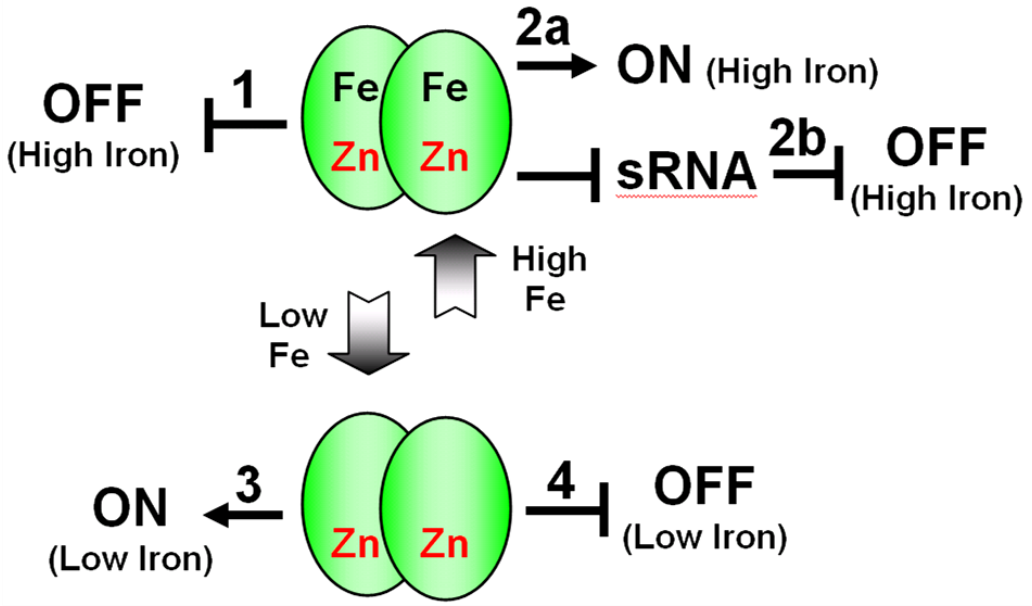

Fig. I-2. Regulatory models of bacterial Fur proteins.

Fur proteins have been described to regulate gene expression by four general mechanisms. In most cases, it is the iron-loaded form of Fur protein (top) that binds to DNA operator sites. DNA-bound Fur can directly repress transcription (mechanism 1) or activate gene expression either directly or indirectly via small RNA molecules (mechanisms 2a and 2b, respectively). In *H. pylori*, the iron-free form of Fur also binds DNA and represses expression of an iron storage protein (mechanism 4). In the case of *B. japonicum* Irr, apo-protein binds DNA in the absence of a metal ion cofactor and can either activate (mechanism 3) or repress (mechanism 4) the expression of target genes for a comparison among Fur family proteins). In general, when Fur functions as a repressor, the Fur box overlaps the promoter region, whereas activation is associated with a Fur box just upstream of the promoter. Note that Zur, Mur, and Nur regulate gene expression by mechanism 1 (although the regulatory metal ion is Zn^{2+}, Mn^{2+}, or Ni^{2+}, respectively, rather than Fe^{2+}).

site inferred from *Pa*Fur is poorly conserved with only one match out of four. Nur negatively regulates the FeSOD gene *sodF* and the putative nickel-transporter gene cluster *nikABCDE*, by binding to promoter regions in the presence of nickel (Ahn *et al*., 2006).

Although the expression of NiSOD encoded by *sodN* is induced by the presence of nickel, Nur does not regulate a direct activator for *sodN*, and use a *sodF* sRNA-mediated mechanism (Kim *et al*., 2014). Unlike many other Fur family proteins (e.g. Fur, Mur, and PerR), which can be activated by several metal ions in vitro, Nur is highly specific for Ni^{2+} both in vitro and *in vivo*.

I.2.3. Mur

The Fur homolog in *Rhizobium leguminosarum* represses the transcription of the ABC-type Mn^{2+} transporter *sitABCD* (*mntABCD*) operon under manganese depleted conditions, but not under excess iron conditions (Diaz-Mireles *et al*., 2004). Thus, this protein was named Mur (manganese uptake regulator). *Rl*Mur apparently lacks a structural Zn^{2+} binding site and instead binds two Mn^{2+} ions per dimer with micromolar dissociation constants (Bellini and Hemmings, 2006). Activated *Rl*Mur binds to a unique binding site (MRS; Mur responsive sequence) distinct from canonical Fur boxes (Diaz-Mireles *et al*., 2005). However, *Rl*Mur partially regulates the *bfd* gene (having a canonical Fur box) in a Fe-dependent manner in an *E. coli fur* mutant background. In vitro, *Rl*Mur can also use Fe^{2+}, Co^{2+}, or Zn^{2+} as activating metals, and the consequent metallated Mur binds to both MRS and canonical fur boxes as one and two homodimers (Bellini and Hemmings, 2006).

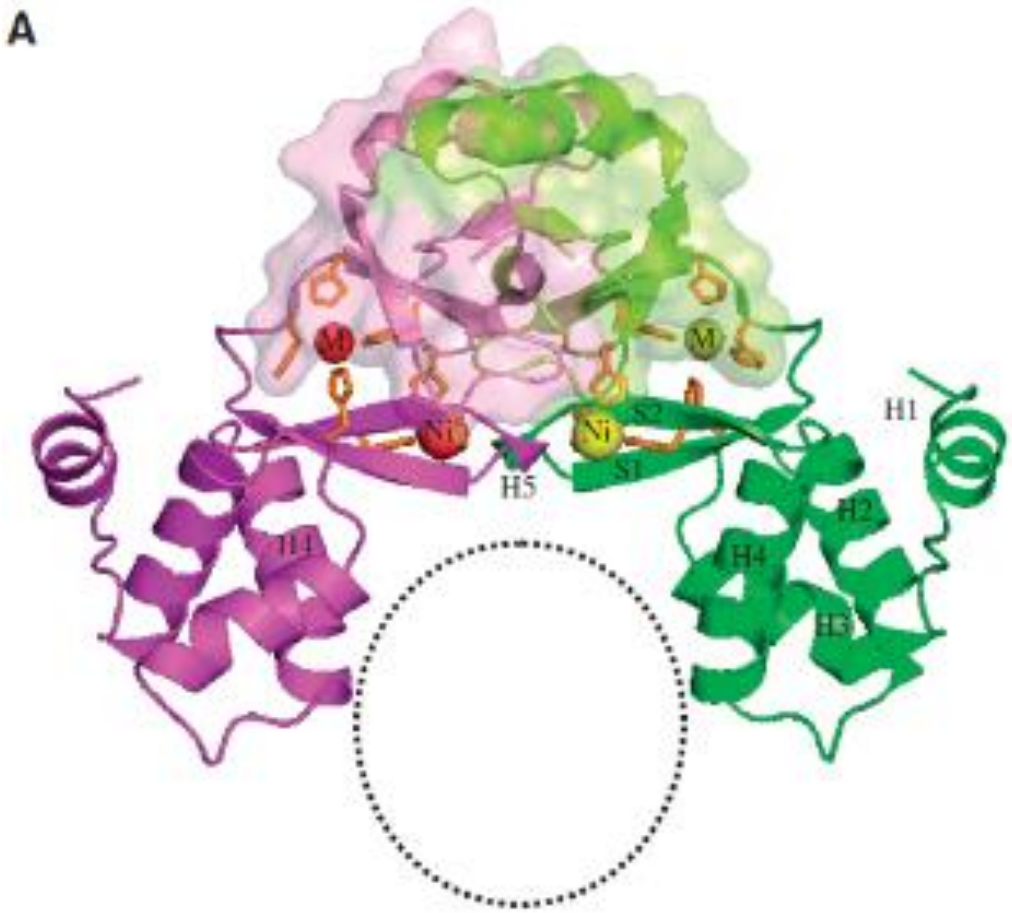

Fig I-3. Structure of Nur and metal sites.

Ribbon diagram of Nur with the dimeric core veiled by transparent surface. Nickel ions and metalcoordinating residues are represented by spheres and sticks, respectively. M and Ni indicate M- and Ni-sites, respectively. A black circle indicates the plausible DNA-binding site. For clarity, secondary structure elements only for DB-domain are labeled.

Thus, Mur may in fact have an overlapping DNA-recognition specificity with Fur. The ability of Mur to respond selectively to Mn^{2+} (in *R. leguminosarum)* and to Fe^{2+} (in *E. coli*) is a reminder that many metalloregulators will bind a fairly broad range of metal ions (as confirmed in in vitro binding studies), but their *in vivo* responsiveness is dictated by the available levels of metals in the cytosol. Similar results were noted when the iron-specific repressor DtxR was expressed in *B. subtilis* (Guedon and Helmann, 2003), and in studies of metalloregulators of the ArsR/SmtB family (Tottey *et al*., 2005).

I.2.4. Zur

Subsequently, genomic analyses have allowed tentative assignments of likely Zur regulons in numerous other bacteria (Panina *et al*., 2003). *Ec*Zur represses the expression of an ABC-type Zn-specific uptake system (ZnuACB) by binding to the bidirectional promoter region of *znuA* and *znuCB*. When cells are starved for zinc, derepression of this high affinity uptake system aids in zinc acquisition (Patzer and Hantke, 2000). In *B. subtilis*, *Bs*Zur was discovered in the course of functional characterization of the multiple Fur paralogs encoded in genome (Gaballa and Helmann, 1998). In response to zinc sufficiency, *Bs*Zur represses a zinc uptake ABC transporter (encoded by the *ycdHI-yceI* operon) and a complex operon encoding proteins of largely unknown function (*yciABC*) (Gaballa *et al*., 2002). Although initially the YciABC system was postulated to function as low affinity zinc-uptake system or permease (Gaballa *et al*., 2002), recent data suggest a different role for these proteins under zinc limited conditions. YciC is a putative metallochaperone which is postulated to allow metal insertion into YciA (Shin *et al*., 2016)

Biochemically, *Ec*Zur is the best characterized member of the Zur sub-family

of regulators (Outten and O'Halloran, 2001; Outten *et al*., 2001; Gilston BA, *et al*, 2014). Like *Ec*Fur, *Ec*Zur contains two distinct metal-binding sites with different affinity and coordination environment. Zur containing only one Zn^{2+} ion per monomer (Zur:Zn_1) does not bind DNA. In the presence of excess Zn^{2+}, Zur (presumably Zur:Zn_2) can bind to the *znuC* promoter and sterically hinders the binding of RNA polymerase (Outten and O'Halloran, 2001). The structural Zn^{2+} ion in Zur:Zn is tightly bound and difficult to replace with other metal ions. The coordination environment of this Zn^{2+} ion has been determined to be $S(N/O)_3$ by XAS, and is proposed to involve two Cys residues in the $C_{103}XXC_{106}$ motif by analogy with *Ec*Fur. The second metal binding site in *Ec*Zur can bind either Zn^{2+} or Co^{2+} and is readily exchangeable. The geometry of this regulatory site was assigned as tetrahedral $S(N/O)_3$ by combined XAS and UV-vis spectroscopy studies using Zur:Zn,Co (Outten *et al*., 2001). The apparent affinity of *Ec*Zur for Zn^{2+}, as determined using TPEN as a Zn^{2+} buffer, was $1 \sim 2 \times 10^{-16}$ M: a value indicating that there is no free zinc in the cell at equilibrium (Outten and O'Halloran, 2001; Gilston BA, *et al,* 2014). It remains to be determined whether or not other Zur homologs have a similar high affinity.

I.3. Zur in *Streptomyces coelicolor*

Zur in *S. coelicolor* is a zinc uptake regulator Zur that regulates a putative high affinity zinc uptake system and some ribosomal proteins predicted to be involved in zinc mobilization. The regulation of zinc uptake systems by Zur has been demonstrated in a broad range of bacteria including *E. coli* (Patzer and Hantke, 1998), *B. subtilis* (Gaballa and Helmann, 1998; Gaballa et al., 2002), and *M. tuberculosis* (Maciag *et al*., 2007). Zur has been also hypothesized to control the mobilization of zinc from several paralogous ribosomal proteins on the basis

of comparative genomic analysis of Zur regulons (Panina *et al*., 2003). According to this model, the ribosomal proteins that contain zinc-binding motif (C+) can serve as zinc-storage forms, and can be replaced with their Zur-regulated paralogues without zinc-binding motif (C-). This hypothesis was experimentally supported in B. subtilis for a ribosomal large subunit protein L31 where Zur-regulated paralogue YtiA (C-) replaces RpmE (C+) under zinc-deficient condition (Akanuma *et al*., 2006, Nanamiya *et al*., 2004). Recent observations in *M. tuberculosis* from microarray and in vitro binding experiments demonstrated that Zur regulates genes for C- paralogues of L33 (RpmG), S14 (RpsN) and S18 (RpsR), supporting this hypothesis (Maciag *et al*., 2007). Zur regulates the synthesis of C- paralogues of L31 and L33 in *S. coelicolor* (Shin *et al*., 2007). Considering the position of Zur binding site within the intergenic region of *rpmG* (SCO3428) and *rpmB* (SCO3429), it is very likely that *rpmB* encoding a C-paralogue of L28 is also regulated by Zur along with its downstream gene *rpsN2* (SCO3430) encoding a C- paralogue of S14. These observations strengthen the generalization of the proposal that bacteria utilize the strategy of using zinc-specific regulator such as Zur to control paralogous ribosomal proteins without zinc-binding ability, enhancing zinc storage through ribosomal proteins under zinc-sufficiency, and zinc mobilization from these proteins by replacing them with zinc-less paralogues under zinc-deficiency.

Identification of the proposed Zur binding consensus in the study depends on the assumption that a Zur dimer recognizes an inverted repeat sequence (Shin *et al*., 2007). Simple sequence alignment of footprinted region does not reveal any salient inverted repeat sequences among the conserved nucleotides. Identification of an inverted repeat motif within the small (30 bp) protected region in *rpmG* gene provided a lead sequence to identify two such motifs within the broader (57 bp) protected region in *znuA* gene. It is possible that the binding

of one Zur dimer to either of those two sites could create broad footprint pattern, even though I cannot rule out the possibility that two Zur dimers bind to two sites simultaneously. The currently proposed Zur-binding consensus sequence in 7-1-7 format (TgaaTat-g-atTttCA) resembles closely with the *B. subtilis* Fur box consensus (TGATAAT-N-ATTATCA; (Fuangthong and Helmann, 2003)) but is distant from *B. subtilis* Zur box (TCGTAAT-N-ATTACGA) or PerR box (TTATAAT-N-ATTATAA). The *S. coelicolor* Zur box sequence matches closely with the proposed Zur box consensus in *M. tuberculosis* (TGAAAAT-N-ATTTTCA; (Maciag *et al*., 2007)). When the amino acid sequence of the DNA-binding helix in Fur homologues were compared according to the structure model determined for *Pseudomonas aeruginosa* Fur (Ratledge and Dover, 2000), *S. coelicolor* Zur shares 13 identical amino acids out of 17 with *M. tuberculosis* Zur, and 9 residues with *B. subtilis* Fur. On the other hand, it shares only 5 identical residues with *B. subtilis* Zur or PerR, consistent with the distance in conservation of binding sequence. By allowing one nucleotide mismatch and maintaining over 50% AT content within the more variable 11 nt central sequences ($TGN_{11}CA$), I was able to draw out several candidate target genes of Zur regulation. DNA binding activity of purified Zur was reduced to oxidants and EDTA. In previous report, reduction state of the Zur protein very important to dimerization and the Zur binding activity. In *E. coli*, Zur is active only in the reduced form. These results suggest that zinc ions needs to Zur binding and the Zur oxidized protein can not bind on the *znuA* promoter region. In other word, only reduced and zinc containing Zur dimer form can repressed the high affinity zinc uptake system while, when the oxidizing molecules such as H_2O_2 and Diamide oxidized the Zur protein in the cell, high affinity zinc uptake system will be repress. Therefore, zinc ions were imported into the cell, just like the *zur* mutant cells. Specifically, there are some current controversies in Fur family

regulator, regarding the site and consequences of regulatory metal ion binding, the diverse mechanisms used by bacterial Fur proteins to regulate their target genes, and the roles of Fur-like regulators that sense other metal ions and oxidative stress signals. In order to clarify these issues, some biochemical properties of Zur (such as oligomeric status, sequence specificity, zinc responsibility, metal contents, and zinc binding residues on modeled structure) were examined (Shin *et al*., 2011)

Through mutation studies, zinc binding to the C-site ensures dimeric structural integrity of Zur. This observation coincides with previous reports that zinc binding ensures dimeric structure for Fur from *E. coli* (Pecqueur *et al*., 2006; D'Autréaux *et al*., 2007) and that the Cys4-Zn site, which corresponds to the C-site, is critically required to maintain dimeric structure of *Bs*PerR and Fur from Helicobacter pylori (*Hp*Fur)(Lee and Helmann, 2006; Vitale *et al*., 2009). On the other hand, mutations at M- and D-sites did not affect dimerization as well as the characteristics of secondary structure. Therefore, it can be safely assumed that both M- and D-sites serve regulatory roles to modulate Zur activity. D-site occupation has been observed in *Pa*Fur (Pohl *et al*., 2003) and *Vc*Fur (Sheikh and Taylor, 2009). In these iron-responsive Fur proteins, the conserved C-terminal cysteines are lacking, and metals were found to occupy M- and D-sites. Because D-sites are occupied by zinc and M-sites can accommodate iron, the D-site in these proteins is regarded to serve a structural role. On the other hand, a recent report on the structure of active zinc-bound variant of HpFur, which contains C-terminal cysteines, revealed the occupation of the D-site in addition to M- and C-sites (Dian *et al*., 2011). In this structure, the D-site 14hermophil has been proposed to be nonessential for DNA binding, but to serve a secondary role to modulate binding affinity, consistent with what we discovered in the present study. Although the domain structures of *Sc*Zur are virtually identical to those

of *Mt*Zur, a remarkable difference exists between dimeric conformations of the two structures. *Sc*Zur assumes an arch-shaped DNA binding-competent closed conformation, whereas *Mt*Zur is reported to assume an inactive open conformation (Lucarelli *et al*., 2007). In this context, the difference in metal content at the D-site between the two Zur proteins attracts our attention. According to the structural report of *Mt*Zur, a zinc ion at the D-site was refined with a low occupancy because of an initially high temperature factor (Lucarelli *et al*., 2007). In contrast, the temperature factor and the occupancy of a zinc ion at the D-site in *Sc*Zur are comparable to those of coordinating residues, clearly indicating the presence of a zinc ion at the D-site. The fact that His84 in the hinge loop participates in metal coordination at the D-site (Fig. I-4.) suggests that metal-binding to this site may affect the metal-induced swing motion of the DB-domain. Based on our observations, I postulate a simplified model for modulating Zur activity through two regulatory zinc sites. Zinc binding to the M-site at the interdomain hinge loop activates Zur to bind its targets. Because the M-site has been revealed to accommodate various divalent cations, such as zinc, nickel, manganese, and iron, in diverse active Fur family members (Pohl *et al*., 2003; Sheikh and Taylor, 2009; Jacquamet *et al*., 2009; Giedroc, 2009), it fits the previously proposed activation model (Giedroc, 2009). Without M-site occupation, Zur cannot bind and repress any of its target genes, causes disturbance in zinc homeostasis, and affects sporulation, most likely because of elevated synthesis of coelibactin (Hesketh *et al*., 2009). Nevertheless, it appears that M-site occupation may not be sufficient to guarantee binding to all target genes of Zur. The *in vivo* and *in vitro* observations that the D-site mutations affected target genes differently and that a higher amount of zinc was needed to allow Zur to bind to the more sensitive promoters (*znuA* and *rpmF*) can be interpreted to imply that additional zinc binding to the D-site is needed to

repress some targets, such as the sensitive group of genes. Therefore, in this model, the M- and D-sites can serve as an on-off switch and a tuner, respectively, for activity modulation. However, considering that Zur binds to its target sites with different affinity and that the presence of bound DNA can affect zinc-binding affinity of Zur, the more sensitive induction of a subset of genes upon smaller zinc depletion can be speculated to arise also from the weaker affinity of sensitive promoters to Zur. Even though the precise mechanism is currently beyond our understanding, the combined effect of two regulatory metal-binding sites and differential DNA-binding affinity of Zur seems to be behind the scenes. Even though they formulated the model based on negatively regulated target genes of Zur as a repressor, it can also be applied for positively regulated genes by Zur as an activator. No such gene has been reported yet in S. coelicolor, but they expect these genes exist, considering the example of positively regulated zinc-exporter gene by Zur in *Xanthomonas* (Huang *et al*., 2008)

I.4. Zinc homeostasis in *Streptomyces coelicolor*

Transition metals such as iron, zinc, copper, and manganese are key constituents of the cell but are toxic when in excess. In bacteria, their intracellular "free" levels are maintained within a narrow range (Finney and O'Halloran, 2003; Reyes-Caballero *et al*., 2011; Foster *et al*., 2014). This homeostasis is achieved primarily through regulating transcription of genes for metal acquisition, utilization, trafficking, and exporting by specific metal- sensitive regulators (Waldron *et al*., 2009; Giedroc and Arunkumar, 2007). Almost all metal acquisition genes are regulated by repressor-type regulators combined with cognate metals as co-repressors. Depletion of the specific co-zinc is an abundant transition metal that serves catalytic, structural, redox-modulatory, and regulatory roles (Riccardi *et al*., 2008). Its high binding affinity, next to

copper among Irving-Williams series of metals, can cause competitive mismetallation, toxifying cells when in excess (Foster *et al*., 2014; Xu *et al*., 2012). Bacteria encounter a wide fluctuation of zinc concentrations in the environment. Zinc-chelation and sequestration by competing microbes or host cells easily create zinc deficiency (Braymer and Giedroc, 2014), whereas nutrient-rich and metal-rich environments in animal guts and soils present toxic amounts of zinc. The zinc depletion is mostly sensed by Zur, a member of ferric uptake regulator (Fur) family proteins, conserved across major bacterial phyla such as proteobacteria, firmicutes, cyanobacteria, and actinobacteria (Hantke, 2005). Zinc-bound Zur acts as a repressor for genes encoding high-affinity zinc importer (*znuABC*) and ribosomal proteins to mobilize zinc (Panina *et al*., 2003). Zinc surplus is sensed by various regulators such as ZntR of the MerR family and CzrA/SmtB/AztR of the ArsR family to induce zinc-efflux genes[5]. In *E. coli*, where zinc homeostasis is best studied, the uptake regulator Zur was reported to respond to extremely low level of "free" cytoplasmic buffered zinc, in femtomolar range (Outten and O'Halloran TV, 2001), whereas the efflux regulator ZntR responds to free zinc of femtomolar to nanomolar range (Outten and O'Halloran , 2001; Wang *et al*., 2012). In *S. coelicolor* and *B. subtilis*, Zur was also reported to respond to femtomolar zinc, to control zinc uptake/mobilization genes (Shin *et al*., 2011; Ma *et al*., 2011). In Gram-positive antibiotic-producing *Streptomyces coelicolor*, cellular differentiation (sporulation) and antibiotic production is critically affected by zinc and perturbation of zinc homeostasis (Kallifidas *et al*., 2010; Hesketh *et al*., 2009; Shin *et al*., 2007). Zinc acquisition genes encoding high affinity ABC transporter and its homolog (*znuABC* and *znuB2C2*), cysteine-less ribosomal protein paralogs to mobilize zinc (*rpmG/B*, *rpmF*), and a zincophore called coelibactin (SCO7676-92) are repressed by zinc-bound Zur (Kallifidas *et al*., 2010; Shin *et al*., 2007).

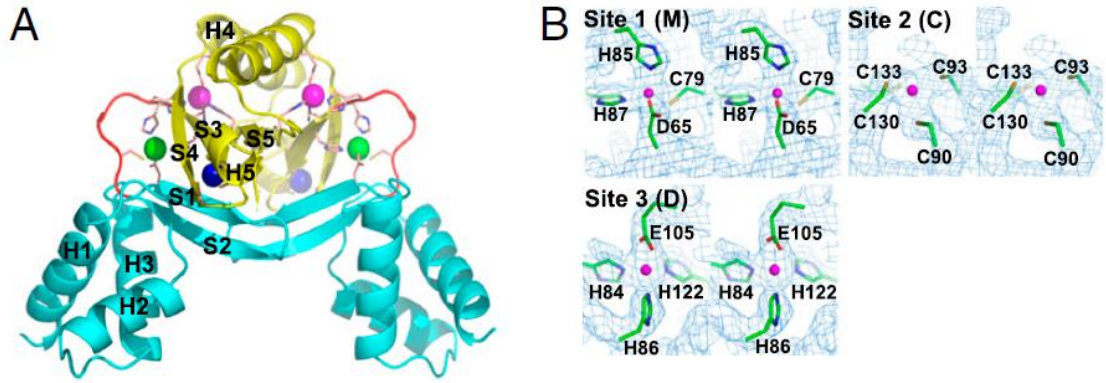

Fig. I-4. Structure of ScZur.

(**A**) Overall structure of ScZur determined at 2.4 Å resolution. The D- and DB-domains are colored by yellow and cyan, respectively. The hinge loop is in red. Zinc ions and metal-coordinating residues are represented by spheres and sticks, respectively. Pink, green, and blue spheres indicate zinc ions bound to the D-, M-, and C- sites, respectively. For clarity, secondary structure elements for one monomer are labeled.

(**B**) Electron-density maps of three zinc-binding sites. Stereoview of the final 2Fo – Fc electron density maps contoured at 1σ, showing the M-, C-, and D-sites. Zn and Zn-coordinating residues are shown in spheres and sticks, respectively.

Structural studies revealed two regulatory zinc-binding sites in addition to a structural one in Zur (Shin *et al*., 2011). Existence of two regulatory sites with slightly different zinc-binding affinity was proposed to enable graded expression of Zur target genes in response to zinc availability in femtomolar concentration ranges (Shin *et al*., 2011).

In order to understand the function of Zur in its entirety, a genome-scale assessment of its direct target genes was in need. From ChIP-chip analysis, they identified a large number of Zur-binding sites in the chromosome, and found a novel zinc-dependent gene that encodes a zinc-exporter, which is activated by Zur over a wide range of zinc concentrations. The principle behind the zinc-dependent modulation of Zur activity from femtomolar to micromolar zinc, to perform a dual role as a repressor and an activator, was investigated.

I.5. Aims of this study

S. coelicolor is the model species for the study of many fundamental genetic phenomena in Streptomycetes. Its unique character, the complex life cycle during growth, made it as a good model system to study the relationship between oxidative stress, metal homeostasis and differentiation. The genome information of *Streptomyces coelicolor,* predicts the presence of four Fur homologues (Bentley *et al*., 2002). Among the Fur homologues, Zur regulates target genes including *znuABC* operon and putative zinc exporter; SCO6751 for zinc homeostasis.

This work mainly focuses on a novel mode of achieving zinc homeostasis by Zur that binds to both the import and the export genes at the Zur-box sequences, how to regulate the zinc exporter with difference of *znuA* regulation mechanism

and exerts a repressor or an activator function over a wide range of zinc concentration changes.

CHAPTER II

MATERIALS AND METHODS

I.1. Bacterial strains and culture conditions

II.1.1. *Streptomyces coelicolor*

S. coelicolor A3(2) M145 was used as wild type in most studies. Streptomyces cells were grown as described previously (Kieser et al., 2000). For liquid culture, spore suspension was inoculated in YEME medium (1% glucose, 0.5% Bacto Peptone, 0.3% malt extract, 0.3% yeast extract, 10.3% sucrose, 5 mM $MgCl_2$), Nutrient Broth (NB, 0.4% beef extract, 0.4% beef peptone; commercially supplied as Nutrient Broth by Biolife) media were used. R2YE (10.3% sucrose, 1% glucose, 1% $MgCl_2$, 0.024% K_2SO_4, 0.001% casamino acid (Difco), 0.5% yeast extract, 20 mM TES (N-tris[hydroxymethyl]methyl-2-aminoenthanesulfonic acid, pH 7.0), 20 mM $CaCl_2$, 0.005% K2HPO4, and 0.3% proline), NA (nutrient agar plate; 8% nutrient broth, 2.2% agar), and SFM (soy flour mannitol plate; 2% soy flour, 2% mannitol, 2% agar) were used. To apply zinc stress in liquid culture, various concentrations of zinc was treated to exponentially growing cell (OD_{600} = 0.3 ~ 0.5).

II.1.2. *Escherichia coli*

Escherichia coli strain DH5α was routinely used for manipulation of DNA. For overexpression of recombinant proteins using T7 polymerase-based system, *E. coli* BL21 (DE3) pLysS was used according to the manufacturer's recommendations (Novagen). To gain methylation-negative DNA, *E. coli* ET12567 (MacNeil *et al.*, 1992) was used, and for direct transformation of *S. coelicolor*, DNA was introduced into *E. coli* ET12567 harboring pUZ8002 (lab collection) to supply the donor (*trans*-) function when having a compatible *oriT*-containing plasmid. *E. coli* BW25113 (Datsenko and Wanner, 2000) was used to

propagate the recombination plasmid pIJ790 and *S. coelicolor* cosmids (Redenbach *et al*., 1996). *E. coli* strains were grown in LB (1% tryptone, 0.5% yeast extract, 1% NaCl) or SOB (2% tryptone, 0.5% yeast extract, 0.05% NaCl, 2.5 mM KCl) containing 20 mM $MgSO_4$ under aeration at 37℃ or 30℃. Carbenicillin (Carb, 100 μg/ml), aparmycin (Apr, 50 μg/ml), chloramphenicol (Cm, 25 μg/ml), or kanamycin (Kan, 50 μg/ml) were added to growth media when required. L-arabinose (10 mM final concentration) was added as indicated to SOB medium to induce genes under control of the pBAD promoter (Datsenko and Wanner, 2000).

II.2. DNA manipulations

Purification of plasmid DNA from *E. coli*, digestion with restriction enzymes, gel electrophoresis, ligation, and transformation of *E. coli* competent cells were carried out as described previously (Sambrook *et al.*, 1989). Purification of genomic or plasmid DNA from *S. coelicolor* were done following the method described by Kieser et al., 2000. All plasmids used in this study are listed in Table II-2.

II.3. Polymerase Chain Reaction (PCR)

Each 50μL reaction mixture contained the followings; 1×Taq polymerase reaction buffer, 150 μM MgCl2, 200 μM dNTP, 500 nM each of 5′ and 3′ primers, 10-100 ng of template DNA, and 5 U of *Taq* polymerase. Reaction was carried out in thermal cycler (Thermo) by denaturing at 95℃, annealing at different temperature for different samples, and extending at 72℃ and cycle is 30 cycle.

Table II-1. ***S. coelicolor*** **strains used in this study.**

Strains	Genotype or description[a]	Source or reference
M145	Prototrophic SCP1$^-$ SCP2$^-$ Pgl$^+$	Hopwood *et al*., 1985
S700	M145 *zur*::Apr^R	Shin *et al.,* 2007
Vec-con	M145 *pSET162*::Apr/Tsr^R	This study
ZitBover	M145 *pSET162-ErmEp-zitB*	This study
long	M145 *pSET162-zitBpL-GUS*	This study
short	M145 *pSET162-zitBpS-GUS*	This study

Table II-2. *E. coli* strains used in this study.

Strains	Genotype or description	Source or reference
DH5α	F- *lacU169*(ϕ80*lacZ*M15) *endA1 recA1 hsdR17 deoR supE44 thi-1* λ- *gyrA96 relA1*	Hanahan, 1983
BL21(DE3)pLysS	F- *ompT* r_{B^-} m_{B^-} (DE3)/pLysS	Studier, 1991
ET12567(pUZ8002)	F- *dam13*::Tn9 *dcm6 hsdM hsdR recF143*::Tn10 *galK2 galT22 ara-14 lacY1 xyl-5 leuB6 thi-1 tonA31 rpsL136 hisG4 tsx-78 mtl-1 glnV44*	McNeil *et al.*, 1992
BW25113	K12 derivative: *araBAD*, *rhaBAD*	Datsenko and Wanner, 2000

II.4. Construction of the *zitB* over-expression and zitBp::GUS with the wild type

To construct of *zitB* overexpression strain in *S.coelicolor* M145 and ∆zur, using integrative pSET162 vector. Constitutive promoter PermE was amplified from pSE34 using ermE forward primer (5′- GAA TTC GAG CTC GGT ACC AG-3′; the EcoRI site is underlined) and ermE reverse primer (5′- CAT ATG TAC CAA CCG GCA CG-3′; the NdeI site is underlined). *zitB* was amplified using primer pairs, SCO6751 over; forward primer (5′- ATG CCA TAT GTT CAG TGC CGC GTT GCC C -3′; the NdeI site is underlined) and SCO6751 over; reverse primer (5′- ATG CGG ATC CGC CGC GTC ACG GGC TCA -3′; the BamHI site is underline). The ligated 1329-bp PCR product was cloned into pSET152-derived integration vector pSET162. To construct *zitBp*::GUS reporter strain, the *zitB* promoter regions from +49 to –60 (zitB-60GUS) or to -228 (zitB-228GUS) were PCR-amplified and cloned in front of the reporter gene with SD sequence and coding region of β-glucuronides (GUS) in pSET152-derived integration vector pGUS (provided by A. Luzhetskyy). Recombinant plasmids were introduced into *E. coli* ET12567 carrying pUZ8002, followed by conjugal transfer to *S. coelicolor* M145. Apramycin-resistant exconjugants were selected, and the correct integration of *ermEp::zitB* or *zitBp::GUS* into the chromosome via the *att* site was confirmed by PCR and nucleotide sequencing.

II.5. RNA analysis

II.5.1. Preparation of RNA from *S. coelicolor*

RNA was isolated from *S. coelicolor* cells grown in YEME as described previously (Kieser *et al*., 2000). Cells were resuspended in Kirby mixture [1%

sodium triisopropyl naphthalene sulfate, 6% sodium 4-aminosalicylate, 6% phenol equilibrated with 10 mM Tris-HCl buffer (pH 8.3)] and disrupted by sonication with a micro tip (Sonica) at 20% of the maximum amplitude (600 W, 20 kHz) for 10 sec. After centrifugation, supernatant was precipitated with equal volume of isopropanol and 1/10 volume of sodium acetate (pH 5.3). The RNA pellet was washed with 70% ethanol and dried. Finally the dried pellet was dissolved in TDW and the concentration of RNA was quantified by measuring at 260 nm and 260/280 ratio. The quantified RNAs were visualized in 1.3% agarose TBE gel.

II.5.2. Preparation of probes

Probes for *zitB, znuA* transcripts were generated by PCR using *S. coelicolor* cosmids (SCC5F2A for *zitB*; SCC121 for *znuA*; John Innes Centre) using primer pairs whose ends correspond to -103 to +149 for the zitB, and -127 to +130 for znuA. (For Primer pairs were as follows: *zitB* forward primer, 5′- CCT CGC AAC ACT CTG ACC TG -3′ and *zitB* reverse primer, 5′- GGG TGA TCG ACA GCG CCA CG -3′, *znuA* forward primer, 5′- GCG AGA TGC TTC CAG AGA ATG -3′ and *znuA* reverse primer, 5′- GTA GAA CGA CGC GAC GAC GTC -3′). The probe DNA fragments were labeled with [γ-^{32}P] ATP and T4 polynucleotide kinase. Hybridization and S1 nuclease mapping was carried out according to standard procedures. For high resolution mapping, the protected DNA fragments were loaded on 6% (w/v) polyacrylamide gel containing 7 M urea, along with sequencing ladders generated from the same probe DNA.

II.5.3. S1 nuclease mapping assay

S1 nuclease protection assay was done as described previously (Smith, 1991). 20 to 50 μg of RNA was dried down with 30,000-40,000 cpm of radioactive ly labeled probe DNA. The pellet was dried and carefully dissolved in 2 0 μl of hybridization buffer [40 mM PIPES (pH 6.4), 400 mM NaCl, 1 m M EDTA, 80% (v/v) formamide]. The solution was incubated at 80℃ for 10 min and slowly cooled to 52℃. Following overnight incubation, 300 μ l of S1 nuclease mix containing 100 units of S1 nuclease in S1 nuclease buffer [280 mM NaCl, 30 mM NaOAc (pH 4.4), 4.5 mM ZnOAc] was add ed and incubated at 37℃ for 1h. The reaction was terminated by addi tion of 75 μl of S1 nuclease termination solution (2.5 M NH_4Oac, 0.05 M EDTA). The DNA-RNA hybrid was precipitated by adding 400 μl of isop ropanol and the pellet was washed with 70% (v/v) ethanol, vacuum drie d, and then resuspended in 10 μl of 28hermoph loading dye. The sample s were boiled for 2 min and subjected to electrophoresis on a 5% (w/v) polyacrylamide gel containing 8 M urea. Then the gel was dried, exposed to film or phosphor screen, and quantified with image analyzer (FLA-2000, Fuji).

II.6. Overproduction and purification of *S. coelicolor* Zur from *E. coli*

The coding region of the *zur* gene was amplified from the *S. coelicolor* cosmid SCC121 using mutagenic primers, Zur-up (5′- GGA GGA ATC ATA TGA CCA CCG CTG-3′; *Nde* I site underlined) and Zur-down (5′- CCG TTC AGG CGG ATC CAG GGG C -3′; *Bam*HI site underlined). The 470 bp PCR product was digested with *Nde*I and *Bam*HI and inserted into pET3a (Novagen) digested with the same enzymes. To construct complementation plasmids for Zur point

mutants, the plasmid containing of pGEM-Teasy::P*zur-zur* was used as template for site directed mutagenesis and then, 0.456 kb NdeI–BamHI fragments of pGEM-Teasy::P*zur-zur* possessing *zur* point mutations were sub-cloned into the pET3a vector for in vitro activity of Zur variants. The resulting recombinant plasmid (pET3aZur) was transformed into *E. coli* BL21 (DE3). For purification of Zur, an overnight culture from a single colony was used to inoculate 1 liter of LB media. Cells were grown with vigorous shaking at 37°C to OD_{600} of 0.5 and were induced with 1 mM (final concentration) isopropyl-β-D-thiogalactopyranoside (IPTG) for 6 hrs at 30°C. Harvested cells were resuspened with binding buffer (20 mM Tris-HCl, pH 7.9, 0.5 M NaCl and 5 mM imidazole) and cell-free extracts were prepared. Cell extracts were loaded onto nickel-charged Chelex-100 column, washed with six volumes of binding buffer, followed by six volumes of washing buffer (20 mM Tris-HCl, pH 7.9, 0.5 M NaCl and 60 mM imidazole). Zur was eluted with ten volumes of elution buffer (20 mM Tris-HCl pH 7.9 and 0.5 M NaCl) containing linear imidazole gradients from 100 to 500 mM. Fractions containing Zur were pooled and dialyzed against buffer A (20 mM Tris-HCl, pH 7.8, 100 mM NaCl, 5% (v/v) glycerol and 5 mM EDTA) to remove imidazole and nickel, buffer B (20 mM Tris-HCl, pH 7.8, 50 mM NaCl, 10% glycerol and 0.1 mM DTT), and finally against storage buffer (20 mM Tris-HCl, pH 7.8, 50 mM NaCl, 30% glycerol and 2 mM DTT). The concentration of purified Zur was determined by the Bradford method. The protein was stored at –80°C.

II.7. Protein analysis

II.7.1. Chemical cross-linking assay

Cross-linking was performed with purified Zur proteins. The reaction was

initiated by adding glutaraldehyde, freshly prepared from a 10-fold stock solution in distilled water, to a final concentration of 0.01-0.1 % V/V. Before analysis by SDS/PAGE, samples were stored on ice overnight. For SDS/PAGE, protein samples were supplemented with fivefold SDS sample buffer (300 mM Tris/HCl, pH 6.8, 5% SDS, 50% glycerol, 0.5% bromophenol blue) either containing or lacking dithiothreitol (DTT). Gels were stained with coomassie blue staining.

II.7.2. Western blot analysis

Following SDS PAGE, the gel was soaked in transfer buffer [25 mM Tris, 192 mM glycine, 20% (v/v) methanol] for 10 min, and then electrotransferred to nitrocellulose membrane BA79 (Schleicher & Schuell) at 60 V for 60 min in Trans-Blot Cell (Bio-Rad). Membrane was blocked in Tris-buffered saline buffer containing 0.1% Triton X-100 (TBST) supplemented with 0.5% BSA, for more than 1 h. The blocked membrane was incubated with antibody diluted in the same buffer for 1 h, and then washed with TBST for 10 min twice. Washed membrane was incubated with anti-mouse IgG secondary antibody 1:10,000 diluted in TBST, and washed with TBST for 10 min twice. Detection of the signal was done using Western ECL detection system (Amersham BioSciences).

II.8. Mobility shift assay for DNA-binding proteins

II.8.1. Probe preparation

The 25 bp *zitB* probe (from -39 to -63 nt from the TSS) was generated by annealing the sense (5'- GCA CAT GAC AAC GGT GTT CAG TGC C -3') and

anti-sense (5′- GGC ACT GAA CAC CG TTG TCA TGT GC -3′) strands of synthetic oligonucleotides. The 33 bp *zitB* DNA probe (from -35 to -67) was amplified by PCR with the forward (5′- CAA GGC ACA TGA CAA CGG TGT T -3′) and reverse (5′- ACG CGG CAC TGA ACA CCG TTG T -3′) primers. The 46 bp *zitB* DNA probe (from -80 to -35) was amplified by PCR by using the forward primer (5′- CGT TTC CGC AGG TCA AGG C -3′) and the reverse primer used to generate 33 bp DNA probe. The 120 bp probe (from nt -148 to -29) was amplified by using the forward (5′- GTC GGA CCG GTC CCC CTG AC -3′) and reverse (5′- CGG GCA ACG CGG CAC TGA AC -3′) primers. The purified DNA was labeled with [γ-^{32}P]-ATP by using T4 polynucleotide kinase. Zur protein was purified from *E. coli* BL21 (DE3) cells containing pET3a-based recombinant plasmid using Ni-NTA column, as previously described.

II.8.2. DNA-protein binding reaction and detection

Binding reactions were performed with approximately 5.5 fmole of labeled DNA probes and 90 or 900 nM purified Zur in 20 µl of the reaction buffer [20 mM Tris-HCl, pH 7.8, 50 mM KCl, 1 mM DTT, 0.1 mg/ml BSA, 5% glycerol, and 0.1 µg of poly(dI-dC), with 0 to 20 µM $ZnSO_4$]. Following incubation at room temperature for 20 min, the binding mixture was subjected to electrophoresis at 4°C on a 5% polyacrylamide gel at 130 V in TB (89 mM Trizma base, 89 mM boric acid) buffer. After electrophoresis, the gel was dried and exposed to a phosphor screen (BAS MP 2040) and quantified with a Phosphorimage analyzer (FLA-2500; Fuji).

II.9. Dnase I footprinting with capillary electrophoresis

The probe DNA was prepared by PCR using a 5′ 6-FAM labeled fluorescent forward primer. For 267 bp *zitB* probe, the forward (5′- GAC AAA CCG CGC CCC CAG AC -3′) and the reverse (5′- GAC GCC GGT ACA CAC GAG GAG -3′) primers encompassing a region from nt -237 to +38 (relative to TSS) were used. The PCR products were gel-purified by using the standard crush and soak method. Binding reactions were performed as in EMSA, except using 250 ng probe DNA in 40 µl reaction mixture. After 10 min incubation at room temperature, 40 µl of 5 mM $CaCl_2$ and 10 mM $MgCl_2$ was added, followed by adding 200 U of RQI Rnase-free Dnase I (Promega) for 1 min. The cleavage reaction was stopped by adding 90 µl stop solution (200 mM NaCl, 30 mM EDTA, 1% sodium dodecyl sulfate, 125 µg/ml of glycogen), followed by DNA extraction and precipitation. Samples were analyzed by ABI 3730 DNA analyzer (Life Technologies).

II.10. *In vitro* transcription assay

The housekeeping sigma factor HrdB of *S. coelicolor* was purified from *E. coli* BL21 containing the recombinant plasmid pET15b-ScHrdB that contains the entire coding region of the *hrdB* gene (1554 bp) amplified from cosmid SC5B8 (provided by John Innes Center). Run-off transcription assay was done as described by Kang et al, with some modifications. Template DNAs for *zitB* (- 287 - + 52) and *znuA* (- 107- + 87) were prepared by PCR. Purified DNA (0.05 pmole), Zur (1 pmole), *E. coli* RNA polymerase core enzyme (1 Unit; NEB, M0550S), and sigma factor HrdB from *S. coelicolor* (1.12 µM) were incubated in 20 µl transcription buffer (20 mM Tris-HCl, pH 7.8, 50 mM KCl, 1 mM DTT, 0.1 mg/ml BSA, 5% glycerol) at 30°C for 5 min, in the absence or presence of $ZnSO_4$

(1 to 20 μM). Transcription reactions were allowed to occur at 37°C for 5 min by adding unlabeled ATP, UTP and GTP to 400 μM, and CTP to 40 μM, with 5 μCi of [α-^{32}P] CTP (400 Ci/mmole, Amersham). Cold CTP (1.2 mM) was then added for 10 min. The reaction was terminated by adding 50 μl precooled stop solution (375 mM sodium acetate, pH 5.2, 15 mM EDTA, 0.1 mg/ml calf thymus DNA), followed by ethanol precipitation. RNA samples were loaded onto 6% (w/v) polyacrylamide gel containing 7 M urea, followed by gel drying and autoradiography as done for S1 mapping analysis.

II.11. ChIP-sequencing analysis

Wild-type cells were grown to OD_{600} of 0.4 ~ 0.5 in YEME medium. Cells were treated with formaldehyde 1 % and incubated for 10 min at RT on the rocker for cross-linking. Followed by added Gglycine 125 mM for 5 min for quenching and then centrifugated at 3000g at 4℃ for 5 min. The samples were washed with TBS in 2 times. For sonication 500 μL IP buffer was added into the samples and then 30 % power for 5 sec pulse to cooling cycles for 15 times, respectively. The input DNA 100 μg were kept at -20℃ and IP DNA samples 1000 μg was rotated with anti-body, protein A/G bead 20 μL, BSA 2 μg and IP buffer up to 200 μL at 4℃ for over-night. The samples were washed with 1 mL Low salt (50mM HEPES-KOH pH 7.5, 150 mM NaCl, 1mM EDTA pH 8.0, 1 % tripton X-100 and 0.1 % Sodium Deoxycholate), 1mL high salt (50mM HEPES-KOH pH 7.5, 500 mM NaCl, 1mM EDTA pH 8.0, 1 % tripton X-100 and 0.1 % Sodium Deoxycholate), 1mL LiCl (50mM Tris-HCl pH 8.0, 250 mM LiCl, 1mM EDTA pH 8.0, 1 % NP-40 and 1 % Sodium Deoxycholate) and 1mL TE for 10min, respectively. Followed by samples were centrifugated and supernatant were taken. 20 μg Rnase was treated at 37℃ for 1 hour. For reverse cross-liking,

samples were added with 350 mM NaCl and 50 μg proteinase K at 65℃ for over-night. DNA preparation was done PCI extraction and 10 μg glycogen with 100 % EtOH and then eluted with 100 μL TDW.

II.12. ICP-MS analysis of metals

Wild-type cells containing parental pSET162 vector or pSET162-*ermEp::zitB* were grown to OD_{600} of 0.4 ~ 0.5 in YEME medium. Harvested cells were washed three times with 10% glycerol, and subjected to metal analysis by ICP-MS (NexION 350D, Perkin-Elmer SCIEX) at The National Center for Inter-University Research Facilities (NCIRF) at SNU and Korea Basic Science Institute (KBSI).

II.13. Modeling *Sc*Zur/DNA complexes

There are two available structures of the Fur family proteins in complex with DNA; Fur from *Magnetospirillum gryphiswaldense* (*Mg*Fur) and Zur from *E. coli* (*Ec*Zur). Since the tetrameric conformation of *Mg*Fur in the complex seems to be more adequate for the formation of hexameric or octameric oligomer in the DNA-bound conditions, I used the *Mg*Fur/DNA complexes for modeling study. The structure of *S. coelicolor* Zur (*Sc*Zur) experimentally determined without DNA is nicely superposed on both *Mg*Fur and *Ec*Zur in the complexes with similar root mean square deviations for corresponding Cα atoms. The *Sc*Zur/DNA (25 bp) complex model was built up based on the crystal structure of the dimeric *Mg*Fur/DNA (25 bp) complex. Since the available crystal structure of *Sc*Zur does not represent the DNA-bound state, I modeled the *Sc*Zur structure with the *Mg*Fur structure in the *Mg*Fur/DNA complex as a template

using SWISS-MODEL. Then the modeled *Sc*Zur structure was superposed onto the *Mg*Fur structure in the *Mg*Fur/DNA complex. After changing DNA sequences matching with the *zitB* sequence, the relative positions of *Sc*Zur and DNA were refined by DISCOVERY (Molecular Simulation, Inc.). To make the *Sc*Zur/DNA (33 bp) complex model, the modeled *Sc*Zur structure was superposed onto each *Mg*Fur structure in the tetrameric *Mg*Fur (two dimers)/DNA (25 bp) complex, and the DNA of 25 base pairs was changed to the 33 base pair DNA with the *zitB* sequence. The positions of two *Sc*Zur molecules were manually modified to minimize steric clashes with DNA and subsequently the relative positions of *Sc*Zur and DNA were refined by DISCOVERY (Molecular Simulation, Inc.).

CHAPTER III

RESULTS

III.1. Zur is an abundant protein with extensive binding sites in the genome of *S. coelicolor*

III.1.1. Confirmation of the amount of Zur protein in the cell under varying zinc concentration

Prior to analyzing Zur-regulated genes, I determined the amount of Zur protein in the cell under varying zinc concentrations. Cells were either untreated or treated with chelator TPEN (5.0 – 5.9 μM) or $ZnSO_4$ (100 μM) for 1 h before obtaining cell extracts. Western blot analysis revealed that the amount of intracellular Zur stayed nearly constant throughout these treatments (Fig. III-1.). Compared with known amounts of purified Zur, the intracellular Zur was determined to be ~3.5 ng in 5 μg total proteins in each cell sample. This corresponds to about 3.7 μM Zur, based on the assumption that about 43% of dry cell weight is from the protein, and the wet cell weight is about 5.6 fold of the dry weight, and that the cell density is 1. This analysis revealed that Zur is an abundant protein, and its level does not fluctuate upon changes in zinc concentration over a wide range.

III.1.2. Zur-binding peaks throughout the whole genome from ChIP-chip analysis

The binding sites of Zur throughout the genome were determined by ChIP-chip experiments as described below. Regions of the genome significantly enriched by Zur binding were identified at 172 positions. They were ranked by relative peak intensity, the average of the $\log_2$ ratios of the 10 highest consecutive probes in each selected region. These sites encompassed all the previously determined Zur-regulated promoters; *znuA, znuB2/C2, rpmF, rpmG/B*, and

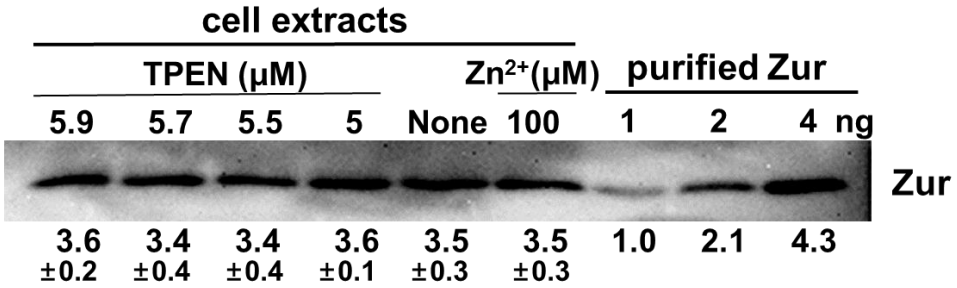

Fig. III-1. The abundance of Zur in *S. coelicolor*.

Analytical Western blot analysis of Zur. Exponentially grown *S. coelicolor* M145 cells were either untreated or treated with varying concentrations of chelator TPEN (5.9, 5.7, 5.5, 5.0 μM) or 100 μM $ZnSO_4$ for 1 h before cell harvest. Crude cell extracts were analyzed by Western analysis, in parallel with quantified amount of purified Zur (1, 2, 4 ng), using polyclonal antibodies against Zur. The amount of Zur in each loaded sample was estimated in ng, taking the band intensity of 1 ng purified Zur as 1.0. Average values with standard deviations from three independent experimental samples were presented.

promoters of SCO7676 and 7681/7682 in a gene cluster for synthesizing enterobactin-type zincophore (Fig. III-2.).

III.1.3. Determination of Zur binding motif

MEME (Multiple EM for Motif Elicitation; http://meme-suite.org/) analysis of these Zur-enriched regions revealed a 15-bp Zur-binding motif tGaNNatSatNNtCa, which can be viewed as a 7-1-7 palindrome (Fig. III-2B.). It is an improved version of the consensus Zur-box motif from previous ones determined from three to six Zur-binding sites (Fig. III-3.). This sequence shares some features within the central 15-bp of the computational Zur-box motif (21-bp palindrome) obtained from the *znuA* genes of 17 actinobacterial genomes, taaTGaNAANNNTTNtCANta. In 169 out of 172 sites, the Zur-box motif was located within 100 bp from the peak midpoint, indicating that the highly represented Zur-binding sites exhibit pronounced sequence-specificity. Among the 172 sites, 113 were located within 500 bp upstream of an ORF, although 72 out of which resided also within the coding region of a neighboring ORF. Only 41 sites were genuinely located in the intergenic region.

III 2. SCO6751 (*zitB*) encoding a putative zinc efflux pump is positively regulated by Zur

III.2.1 The zinc-specific and Zur-dependent induction of the *zitB* gene

Among the top 1% Zur binding sites, I identified a candidate member of Zur regulon (SCO6751), which encodes a putative metal efflux pump of the cation diffusion facilitator (CDF) superfamily (Fig. III-2A). When compared with other

Fig. III-2. Zur-binding peaks throughout the whole genome.

(**A**) Zur-binding peaks throughout the whole genome from ChIP-chip analysis. The peak intensity values (y-axis) were calculated from the average of the $\log_2$ ratios of 10 highest consecutive probe signals for each Zur-enriched site. Known promoter sites of Zur-repressed genes were indicated with red arrows. A new promoter site with Zur-binding consensus sequence was indicated with a blue arrow.

(**B**) The Zur binding motif was extracted from the highly enriched 172 Zur-binding regions by MEME (Multiple EM for Motif Elicitation).

A

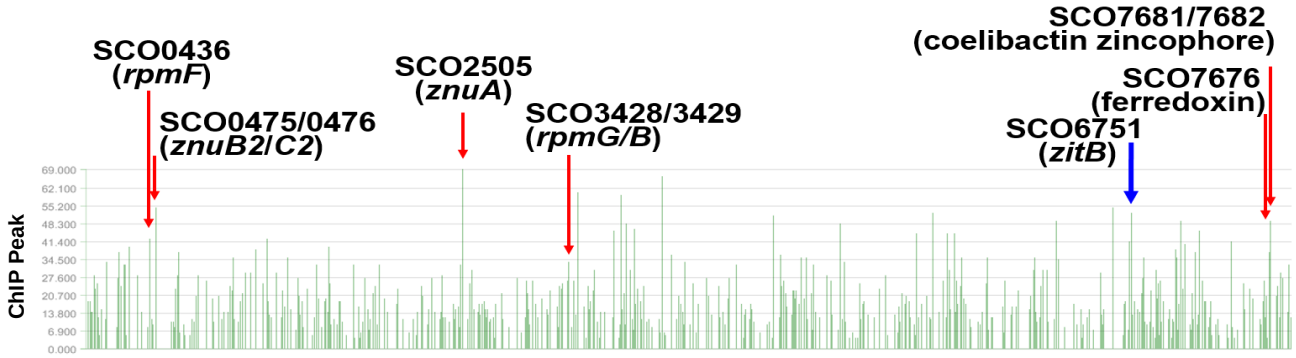

B

Zur-binding motif from top 1% peak regions

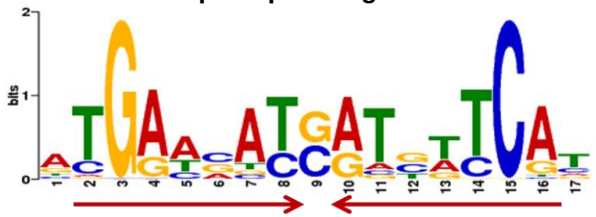

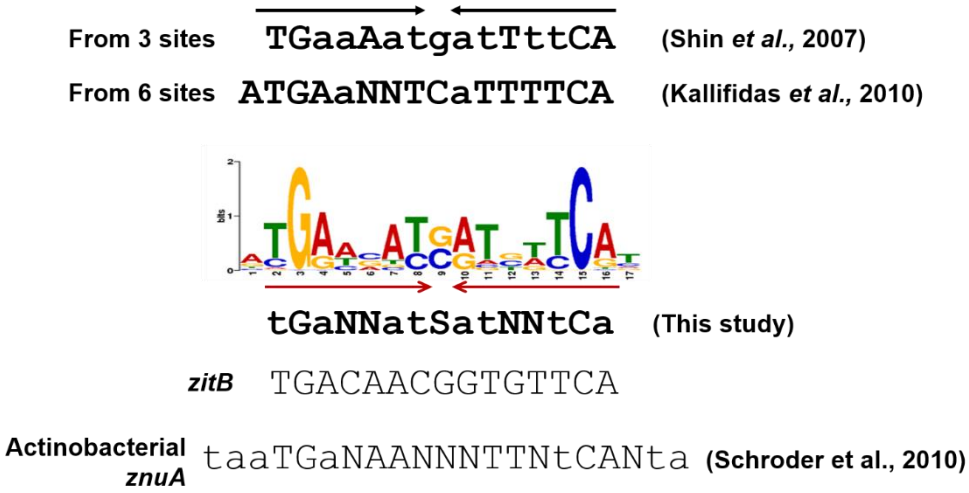

Fig. III-3. Comparison of Zur-binding consensus sequences.

The Zurbox consensus sequences determined from three Zur-bound sites (Shin et al. 2007), from 6 bound sites (Kallifidas et al., 2010), and this study. The *zitB* Zurbox sequence was shown below, along with computational Zur-box consensus obtained from znuA genes of 17 actinobacterial genomes (Schroder et al., 2010).

known CDF-type zinc exporters, as well as another putative CDF family exporter (SCO1310) encoded in the *S. coelicolor* genome, SCO6751 was grouped closely with *E. coli zitB* and *czcD* genes from *B. subtilis*, *Xanthomonas campestris*, *Mycobacterium smegmatis,* and *Corynebacterium glutamicum* (Fig. III-4.). Based on sequence similarity, metal-transport Function, and zinc-specific gene induction (see below), I named SCO6751 as *zitB*. The SCO1310 gene encoding another putative CDF family exporter was closely clustered with the *zitA* from *Mycobacterium tuberculosis* (Fig. III-4.). The *zitB* (SCO6751) gene is most likely transcribed as a monocistronic unit. The Zur binding was detected as a broad peak, which centered upstream of the coding region in the ChIP-chip analysis (Fig. III-5.). In order to verify its regulation by zinc and Zur, I monitored *zitB* transcripts from the wild type and *Δzur* cells treated with various divalent metal ions or zinc-chelator TPEN for 30 min. S1 mapping analysis demonstrated that it is induced specifically by Zn(II), and the induction is totally dependent on Zur, which functions as an activator (Fig. III-6). Zinc chelation by TPEN decreased its expression, and other divalent metal salts of Co(II), Cd(II), Fe(II), Mn(II), Ni(II), and Cu(II) at 0.1 mM did not induce *zitB* expression significantly (Fig. III-6). In the *Δzur* mutant, the basal level of *zitB* expression under non-treated condition decreased to about 20% level of the wild type value, indicating the contribution of Zur in activating *zitB* expression. TPEN further decreased the *zitB* mRNA level, suggesting that there may be some additional regulation other than Zur that acts on the *zitB* promoter under extreme metal depleting condition.

III.2.2. Overexpression of *zitB*hinders differentiation and causes a decrease in the content of Zn as well as Fe, Co, and Ni

The physiological function of ZitB was examined by overexpressing it on

Fig. III-4. Phylogenetic relationship of SCO6751 with other bacterial CDF-type transporters.

I compared the sequence of SCO6751 with those of several CDF-type efflux pumps of reported functions. The selected ones include $Zn^{2+}/Cd^{2+}/Fe^{2+}$ exporter FieF of *E. coli*, $Zn^{2+}/Cd^{2+}/Ni^{2+}/Cu^{2+}$ exporter ZitB of *E. coli*, and others such as ZitA of *Mycobacterium tuberculosis*, CzrB of *Thermus 44 hermophiles*, MamM of *Magnetospirillum. Gryphiswaldense* MSR-1, CzcDs of *B. subtilis* and *M. tuberculosis*. These sequences were aligned with Clustal W algorithm and visualized with MEGA7 software. Abbreviations and sequence sources are as follows. From *B. subtilis,* BsCzcD (NP_390542), BsYdfM (NP_388428), BsYeaB (NP_388513) ; from *Corynebacterium glutamicum*, CgCzcD (NP_600503); from *Cupriavidus metallidurans*, CmCzcD (CAA67085), CmDmeF (ABF07084), CmFieF (ABF10278); from *E. coli*, EcFieF (NP_418350), EcZitB(NP_415273); from *M. gryphiswaldense*, MgMamB (CDK99583), MgMamM (CAJ30120); from *M. smegmatis*, MsCzcD (YP_885161); from *M. tuberculosis H37Rv*, MtZitA (NP_216541); from *Rhizobium leguminosarum*, RL1175[17] (CAK06672), RL1351 (CAK06848); from *S. coelicolor A3(2)*, SCO0776 (NP_625078), SCO2772(NP_627002), SCO3024 (NP_627246), SCO1310 (NP_625596), SCO6751 (ScZitB; NP_630824); from *T. thermophiles*, TtCzrB (CAC83722); from *Xanthomonas campestris*, XcCzcD (WP_011036459).

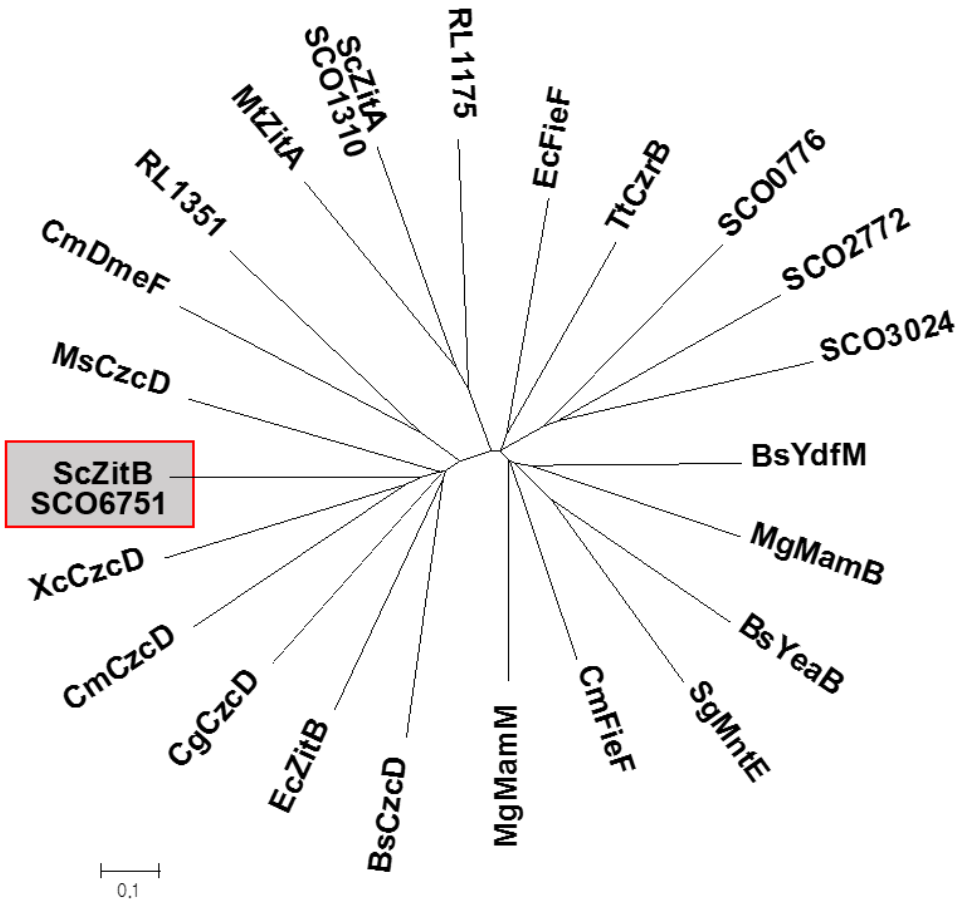
RL1175
ScZitA
SCO1310
MtZitA
RL1351
CmDmeF
MsCzcD
ScZitB
SCO6751
XcCzcD
CmCzcD
CgCzcD
EcZitB
BsCzcD
MgMamM
CmFieF
SgMntE
BsYeaB
MgMamB
BsYdfM
SCO3024
SCO2772
SCO0776
TtCztB
EcFieF
0.1

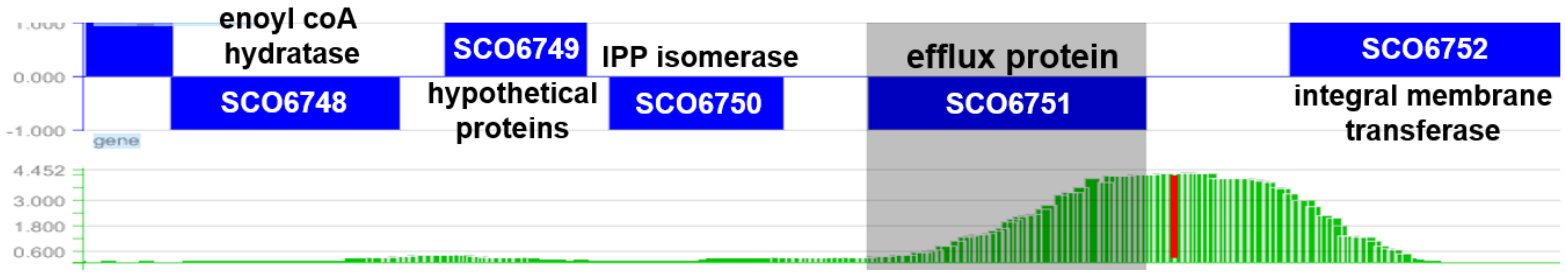

Fig. III-5. The location of Zur-box on the *zitB* gene relative to the transcription start site (TSS).

The ChIP-chip data for Zur binding near the SCO6751 gene. The position of Zur-box motif was shown in red in the middle of a broad peak of Zur-bound DNAs (green).

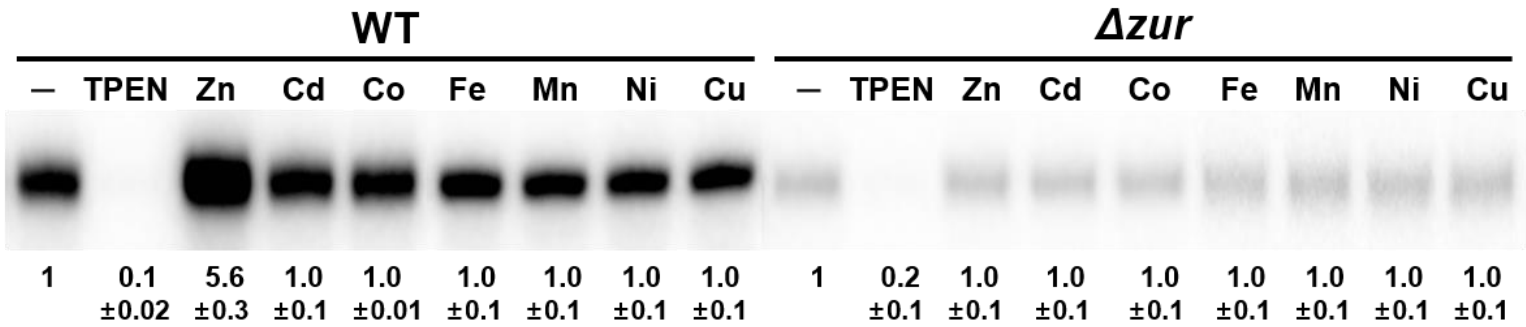

Fig. III-6. The zinc-specific and Zur-dependent induction of the *zitB* gene.

Transcripts from SCO6751 (*zitB*) gene were analyzed by S1 mapping. Exponentially grown wild type (WT) and *Δzur* mutant cells were treated with 6 μM TPEN or various metal salts ($ZnSO_4$, $CdCl_2$, $CoSO_4$, $FeSO_4$, $MnCl_2$, $NiSO_4$, and $CuSO_4$) at 100 μM for 30 min before cell harvest. The amount of *zitB* transcript was quantified and presented in relative value with that in non-treated sample as 1.0. Values from three independent experiments were presented as average with standard deviations. The P-values for all the measurements in TPEN and zinc treatment to WT and TPEN treatment to *zur* mutant were less than 0.001 by Student's t-test.

pSET-132 based integration vector. The strong *ermE* promoter-driven overexpression of *zitB* in the wild type *S. coelicolor* caused a defect in sporulation, showing a white phenotype, and reduced antibiotic production on R2YE plates (Fig. III-7A.). This coincides with previous observations that a defect in zinc homeostasis inhibits differentiation and antibiotic production. In *zitB*-overexpressing cells the level of *znuA* mRNA, which is derepressed upon zinc starvation, was elevated by about 5-fold in comparison with the wild type (Fig. III-7B.). This suggests that *zitB*-overexpression caused zinc-depletion in the cell. I then measured the total amounts of zinc and other divalent metals in the cell by ICP-MS analysis. Results in Fig. III-7C demonstrated that the *zitB* overexpression caused a marked reduction in the amount of total zinc and iron from 124,432 to 29,712 and 114,771 to 32,391 ppb, respectively. It also caused reduction in the less abundant cobalt and nickel from 2,384 to 812, and from 4,204 to 1,030 ppb, respectively. On the other hand, the amount of copper did not change. Cobalt and manganese were not detectable. These results indicate that ZitB indeed functions as an exporter for zinc, and for nickel and cobalt as well.

III.2.3. The *zitB* expression is activated by Zur in a biphasic manner

Since Zur controls both the uptake (*znuA*) and the export (*zitB*) genes for zinc, I compared the zinc responsiveness of Zur in regulating both genes. *S. coelicolor* cells exponentially grown in YEME were treated with TPEN (5 – 6.5 μM) or $ZnSO_4$ (up to 150 μM) for 30 min, followed by S1 mapping of the *znuA* and *zitB* transcripts. Consistent with the previous report, the *znuA* transcripts increased from nearly none to full expression level, as TPEN increased from 5 to 6.5 μM (Fig. III-8A.). When treated with TPEN, the *zitB* transcripts decreased as TPEN

increased, in an opposite direction to the *znuA* expression. The small amount of *zitB* expression in non-treated YEME further increased by adding $ZnSO_4$ up to 100 μM (Fig. III-8A.). Induction and repression patterns of *zitB* and *znuA* were confirmed by qRT-PCR (Fig. III-9.).

The relative expressions of *znuA* and *zitB* genes were plotted against the amount of zinc in the medium, by taking the maximally expressed level as 1.0 (Fig. III-8B.). The available zinc concentrations in the presence of TPEN were calculated by using the web-based solution tool WEBMAXC (http://web.stanford.edu/~cpatton/webmaxc/ webmaxcS.htm). YEME media, in the absence of added metal, contained 1.33 μM Zn^{2+} when analyzed by ICP-MS. The zinc-dependent *zitB* induction demonstrated a biphasic curve. At low zinc in the sub-femtomolar range, where the *znuA* expression changes from the full (1.0) to near zero level, the *zitB* increased from nearly zero to about 10% of the maximally induced level (phase I). At high zinc of over 10 μM, the *zitB* expression increased markedly, reaching to the maximal level at ~ 100 μM (phase II). Between 0.6 fM and 1.3 μM zinc, which correspond to 5 μM TPEN-treated and non-treated conditions, respectively, the *zitB* level stayed nearly constant. To compare the zinc-sensitivity of Zur regulation between the *znuA* and *zitB* genes in the sub-femtomolar range, I re-plotted the relative expression of the *zitB* gene in phase I by taking the non-treated or 5 μM TPEN-treated level as 1.0. The data (Fig. III-10.) demonstrated that, within this low zinc range, both the *znuA* and *zitB* expressions show nearly identical zinc-responsiveness. This suggests that under low zinc condition, Zur binds to both genes with similar sensitivities to zinc, whether it acted as an activator or a repressor.

Fig. III-7. Overexpression of *zitB* hinders differentiation and causes a decrease in the content of Zn as well as Fe, Co, and Ni.

(**A)** The *ermEp::zitB* construct on pSET162 plasmid (pZitB) was introduced into the chromosome of the wild type *S. coelicolor*. The pZitB containing strain showed defect in sporulation (white phenotype) and antibiotic production, whereas the wild type strain with or without the empty vector (pSET) demonstrated gray spore formation and blue antibiotic production.

(**B) E**pression of the *zitB* and *znuA* genes in pZitB containing strain. The *zitB* and *znuA* transcripts were analyzed by S1 mapping. The band intensity was quantified and presented as relative values obtained from three independent experiments and measured with P-values of less than 0.001 by Student's t-test.

(**C**) Intracellular amounts of divalent cations (Cu, Zn, Fe, Co, Ni) in the wild type cells with empty pSET162 vector or pZitB, as assayed by ICP-MS analysis. Mn and Cd were not detected. Average values from three biologically independent samples were presented in ppb (μg per L wet mycelium). Asterisks * and ** indicate measurements with P-values of less than 0.05 and 0.001, respectively, by Student's t-test

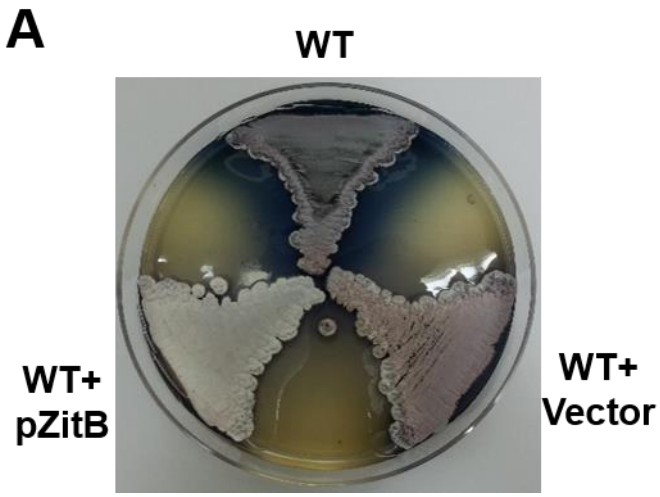
A
WT
WT+
pZitB
WT+
Vector

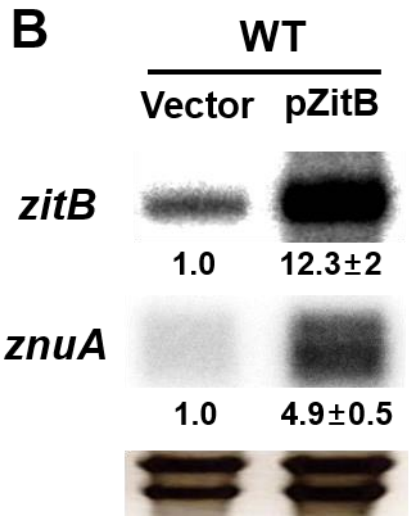
B
WT
Vector
pZitB
zitB
1.0
12.3±2
znuA
1.0
4.9±0.5

.

C

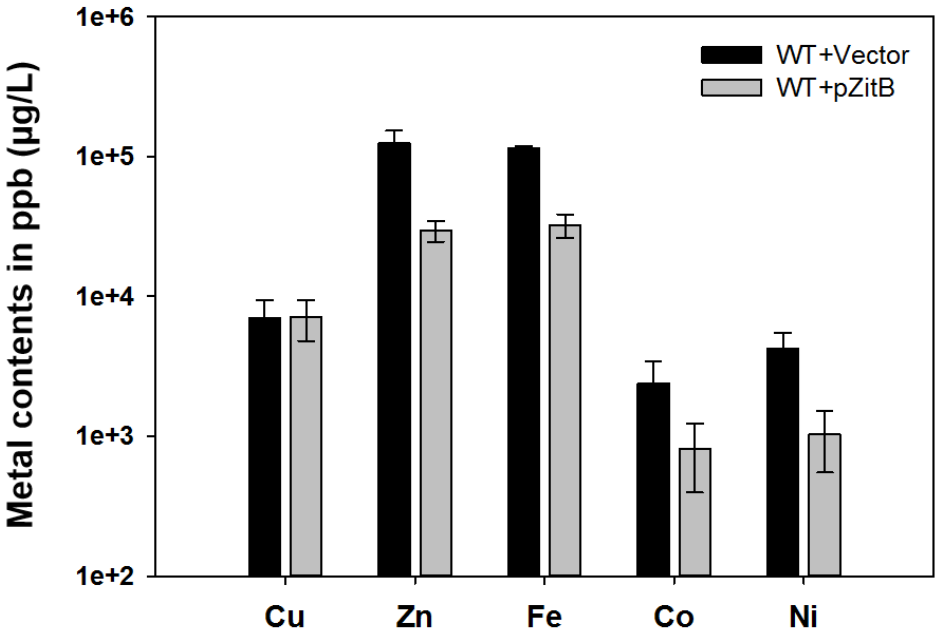
Metal contents in ppb (µg/L)
1e+6
1e+5
1e+4
1e+3
1e+2
WT+Vector
WT+pZitB
Cu
Zn
Fe
Co
Ni

III.2.4. The transcriptional start site for *zitB* promoter and prediction of the -10 and -35 region.

To understand how Zur positively regulates *zitB*, the transcription start site (TSS) of the *zitB* gene was determined by high-resolution S1 mapping, following induction with 100 μM $ZnSO_4$ for 1 h. The TSS (+1) was located at the C residue 50 nt upstream from the initiation codon (Fig. III-11A). The -10 (TTGACT) and -35 (TTGCCC) elements of the *zitB* promoter were predicted, and a Zur-box motif was localized 8 nt upstream from the -35 hexamer (Fig. III-11B.). The position of the Zur-box sequence was compatible with the role of Zur as an activator, not to inhibit RNA polymerase binding.

III.2.5. Location of Zur binding in the *zitB* promoter by footprinting

I then performed Dnase I footprinting of Zur binding on the *zitB* promoter DNA by capillary electrophoresis. Increasing amounts of Zur were incubated with 267 bp *zitB* DNA (from -228 to +39 nt relative to TSS) in the presence of 75 μM $ZnSO_4$. When compared with the DNA-only sample, the binding of Zur at 0.45 μM was enough to protect a region between -78 and -40 nt that harbors the Zur-box motif (Fig. III-12.). Zur at higher concentrations (up to 9 μM) protected further upstream region, up to -138 nt from the TSS, expanding the size of the footprint from 38 to 98 bp-long.

III.2.6. Zur binds with similar affinities to the core Zur-box DNAs of *zitB* and *znuA* genes

Since the zinc-responsiveness of the *zitB* induction in phase I was similar to that

of the *znuA* repression, I determined the binding affinity of Zur to both genes. EMSA experiments were done with increasing amounts of Zur on 25 bp of Zur-box DNA of each gene (Fig. III-13A.). Since the *znuA* gene contains two Zur-box sequences, I prepared both site 1 and site 2 DNA probes of 25 bp each. The EMSA assay at 5 μM $ZnSO_4$ with Zur from 0 to 90 nM showed that Zur bound to *znuA*-1, *znuA*-2, or *zitB* Zur-box DNA probes of 25 bp with comparable affinities. The shifted position of Zur-DNA complex band corresponds to the binding of a dimeric Zur on each DNA probe. The binding curve of the EMSA data demonstrated that Zur bound to the *znuA*-1 site with the highest affinity (Kd ~15 nM), whereas the binding affinity to *znuA*-2 and *zitB* was nearly identical with Kd of ~19 nM (Fig. III-13B.). The similarity in Kd values is consistent with the observation that Zur-binding was enriched with similar peak intensities at the *znuA* and *zitB* sites in ChIP-chip analysis.

III.2.7. Increase in Zn causes oligomeric Zur binding with extended footprints.

Since the amount of Zur protein stayed relatively constant in the cell, and since the *zitB* induction increased markedly at >10 μM zinc (phase II), I examined the Zur-DNA binding under varying zinc concentrations. Dnase I footprinting on *zitB* DNA was performed with fixed amount of Zur (2.7 μM) and varying $ZnSO_4$ from 2.5 to 10 μM. Results in Fig. III-14 demonstrated that the Zur-footprint extended further upstream as zinc increased, up to -138 nt from TSS. This expansion in Zur-binding region is likely to lie behind the induction of *zitB* by zinc in phase II. It can be postulated that high concentrations of zinc could have caused some changes in Zur and its DNA-binding behavior.

Fig. III-8. Zinc-responsive expression of the *zitB* gene in comparison with the zinc uptake (*znuA*) gene.

(**A**) S1 mapping analysis of *znuA* and *zitB* transcripts under TPEN or zinc-treated conditions. The wild type cells grown in YEME medium to exponential growth (OD_{600} of 0.4 to ~0.5) were treated for 30 min with TPEN (5.0 to 6.5 μM as indicated), $ZnSO_4$ (25-150 μM as indicated), or none, before cell harvest. Quantifications of S1 mapping results were done from 11 independent experiments for *znuA*, and 3 to 6 experiments for *zitB* transcript analysis. The relative expression values with standard deviations were presented, taking the untreated sample values as 1.0. The P-values for all the measurements were less than 0.001 by Student's t-test, except the *zitB* value for 5 μM TPEN treatment ($P > 0.8$).

(**B**) The relative expression levels of *znuA* and *zitB* mRNAs were plotted against the concentrations of zinc in the medium. The maximally expressed levels were drawn as equal heights in the y-axis for both *znuA* (●, solid circle; left axis) and *zitB* (○, open circle; right axis). The concentration of zinc in the TPEN-treated samples was calculated from the concentrations of treated TEPN (μM; in blue number). The added amount of Zn (μM) was indicated in purple. The amount of zinc in non-treated YEME medium (-) estimated by ICP-MS was 1.33 μM. The bi-phasic induction of the *zitB* gene was labeled as phase I (at subfemtomolar zinc) and phase II (at >micromolar zinc).

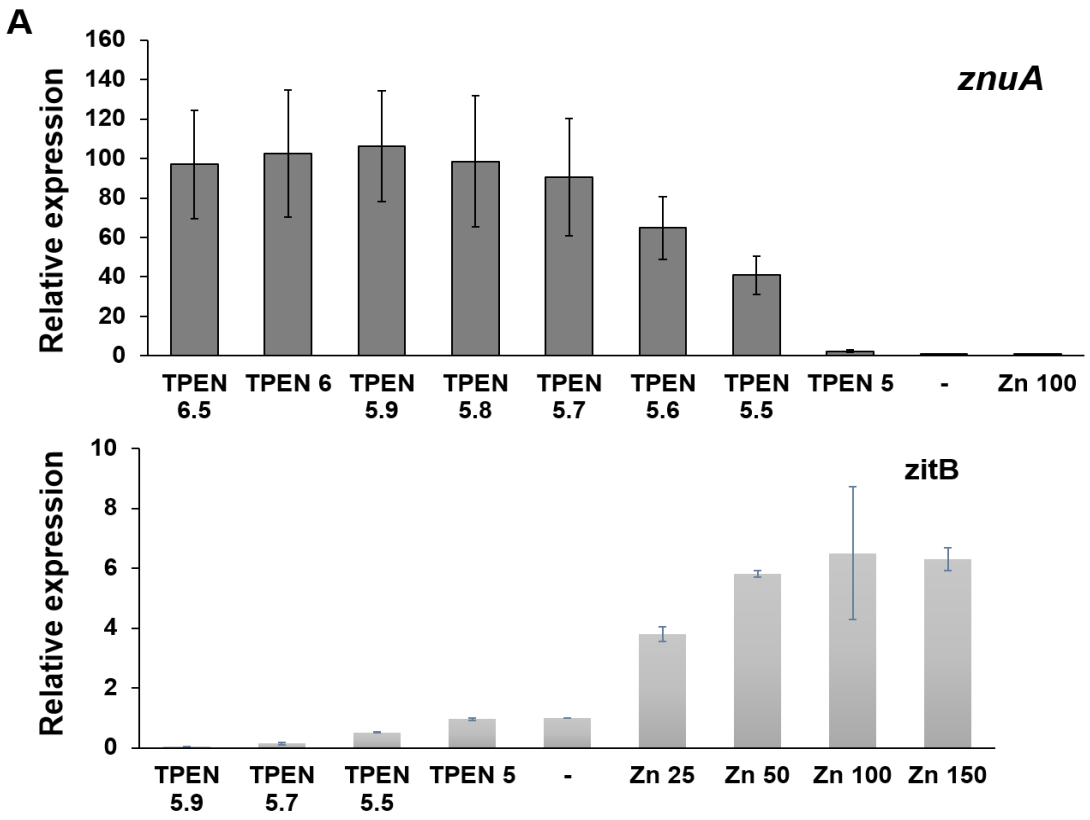
A
znuA
Relative expression
160
140
120
100
80
60
40
20
0
TPEN 6.5
TPEN 6
TPEN 5.9
TPEN 5.8
TPEN 5.7
TPEN 5.6
TPEN 5.5
TPEN 5
-
Zn 100
zitB
Relative expression
10
8
6
4
2
0
TPEN 5.9
TPEN 5.7
TPEN 5.5
TPEN 5
-
Zn 25
Zn 50
Zn 100
Zn 150

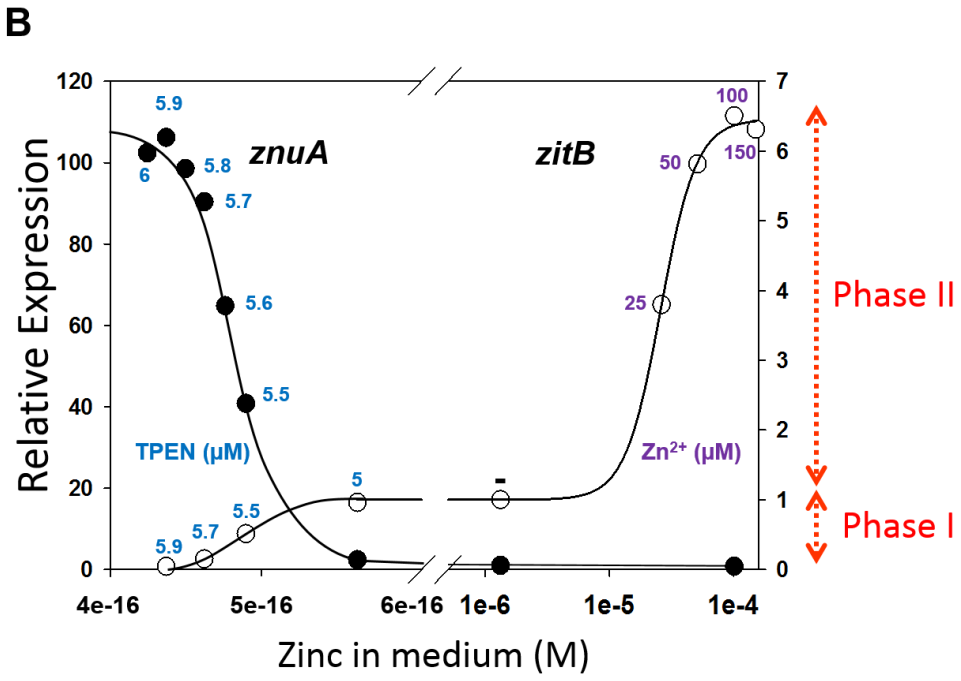
B
Relative Expression
120
100
80
60
40
20
0
7
6
5
4
3
2
1
0
znuA
zitB
5.9
6
5.8
5.7
5.6
5.5
5
5.9
5.7
5.5
TPEN (μM)
-
100
150
50
25
Zn2+ (μM)
Phase II
Phase I
4e-16
5e-16
6e-16
1e-6
1e-5
1e-4
Zinc in medium (M)

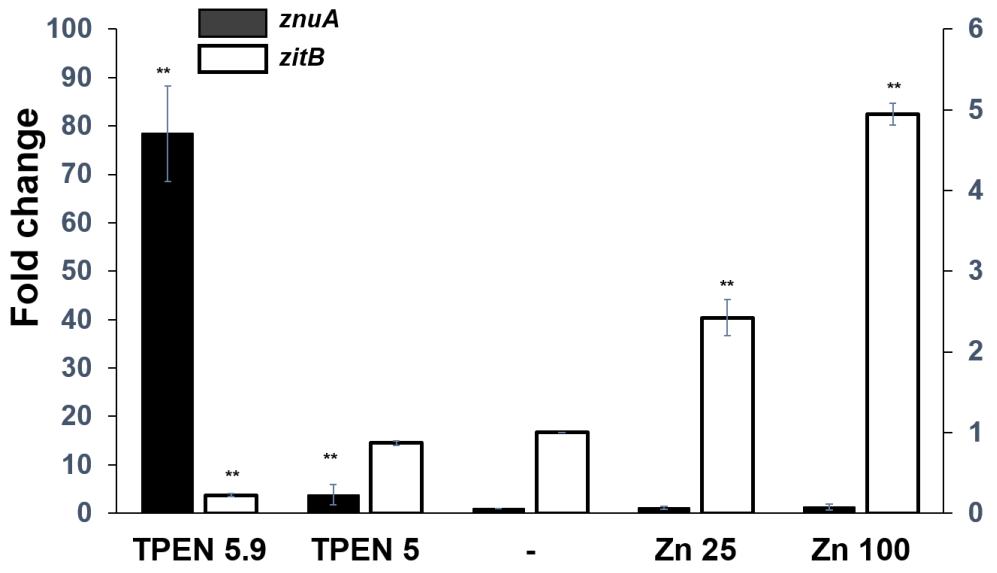

Fig. III-9. **Quantification of the *znuA* and *zitB* RNAs by qRT-PCR.**

The same RNA samples that were used in S1 mapping were evaluated by qRT-PCR. The forward (5′-GAACGTACGACGACGCCGCA-3′) and reverse (5′-CCGAGCTGTCGCTGGAGCAG-3′) primers were used to for znuA. The forward (5′-GGTACACACGAGGAGGCGGC-3′) and reverse (5′-GTGATCGACAGCGCCACGCG-3′) primers were used to for *zitB*. The qRT-PCR values were normalized to the constant reference gene (SCO0710) [20], and were presented as relative fold changes, by taking the untreated sample values as 1.0. Three independent RNA samples were obtained for qPCR analysis, using the Stratagene MX3000P QPCR system (Agilent Technologies). Asterisks (**) indicate measurements with P-values ≤0.001 by Student's t-test.

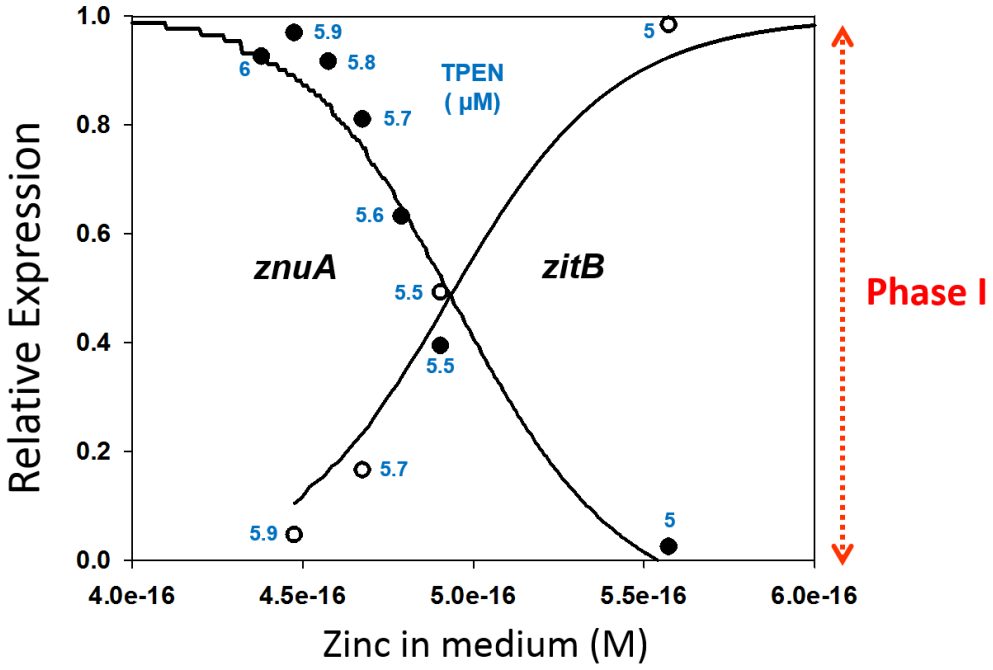

Fig. III-10. The zinc-dependent expression of the *zitB* and *znuA* gene at sub-femtomolar range of zinc concentrations.

For both genes, the maximal level of expression was taken as 1.0 for cells treated with TPEN (from 5 to 6 µM) in YEME medium. For the *zitB* gene, the maximal level of expression at phase I activation range occurred when TPEN was treated at 5 µM.

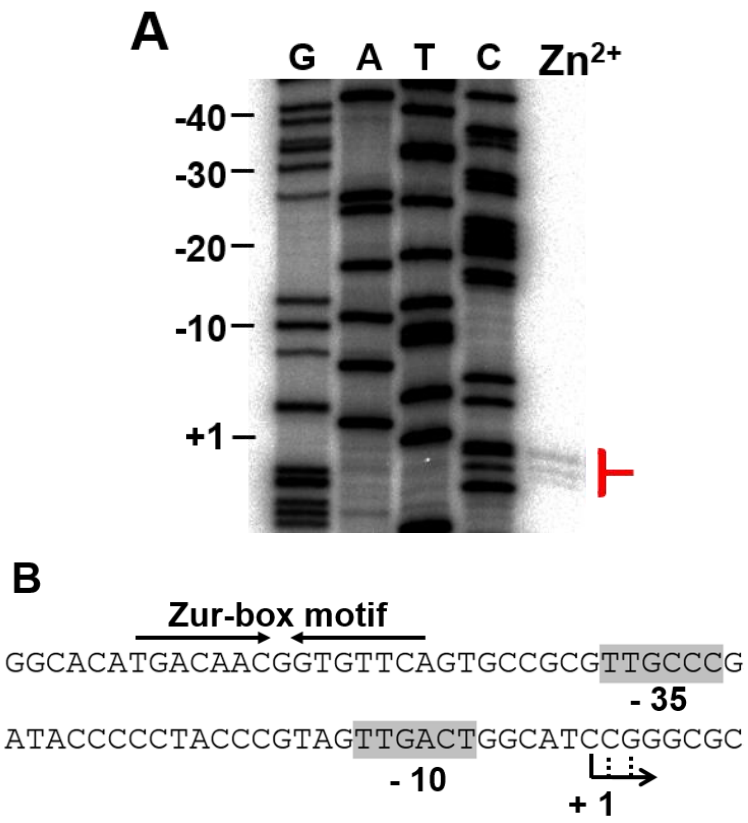

Fig. III-11. Determination of the *zitB* TSS and prediction of Zur-box location.

(**A**) Determination of the *zitB* TSS by high resolution S1 mapping. Exponentially grown cells were treated with $ZnSO_4$ at 100 µM for 1 h before RNA preparation. The 5′ end position of the *zitB* transcript (+1) was determined by electrophoresis of S1-protected DNAs on a 6% polyacrylamide gel containing 7 M urea, along with sequencing ladders generated with the SCC5F2A cosmid DNA and the same primer used to generate the S1 probe. The position of the longest protection was assigned as +1.

(**B**) The positions of the predicted -10 and -35 elements of the *zitB* promoter and the Zur-box motif.

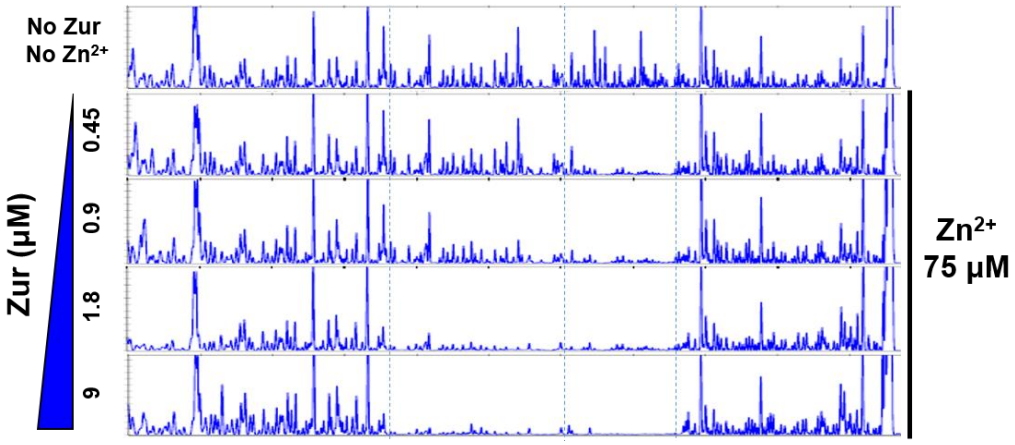

Fig. III-12. Footprinting analysis of Zur binding to the *zitB* promoter region.

Footprinting under varying Zur protein concentrations. The DNA probe containing the *zitB* gene from +39 to -228 nt relative to the transcription start site (+1) was incubated with increasing amounts of Zur (0.45, 0.9, 1.8 and 9.0 uM) in the presence of 75 μM $ZnSO_4$. The DNA probe only with no added Zur nor zinc was analyzed in parallel. The primary protection from -40 to -78, and the extended footprint at higher Zur up to -138 were indicated with dotted lines.

Fig. III-13. Binding of Zur to 25 bp DNA probes containing the core Zur-box motifs (in red italic) of the *znuA* (site 1 and site 2) or *zitB* promoters.

(**A**) EMSA between Zur and 25 bp DNA probes. Increasing amounts of purified Zur protein (0.9, 1.8, 2.7, 3.6, 9, 13.5, 18, 22.5, 27, 45 and 90 nM) were incubated in the presence of 5 μM $ZnSO_4$ with γ-^{32}P labeled synthetic DNA probes for *zitB*, *znuA* site1 and *znuA* site2 as indicated at the bottom.

(**B**) The binding curves (Hill plots) were generated from EMSA data for the *znuA* site 1 (filled circle, blue line), *znuA* site 2 (open circle, red dotted line), and *zitB* (filled triangle, black dotted line) probes. The Kd values were estimated to be 18.8, 15, and 19.3 nM for *znuA* site 1, *znuA* site 2, and *zitB*, respectively.

A

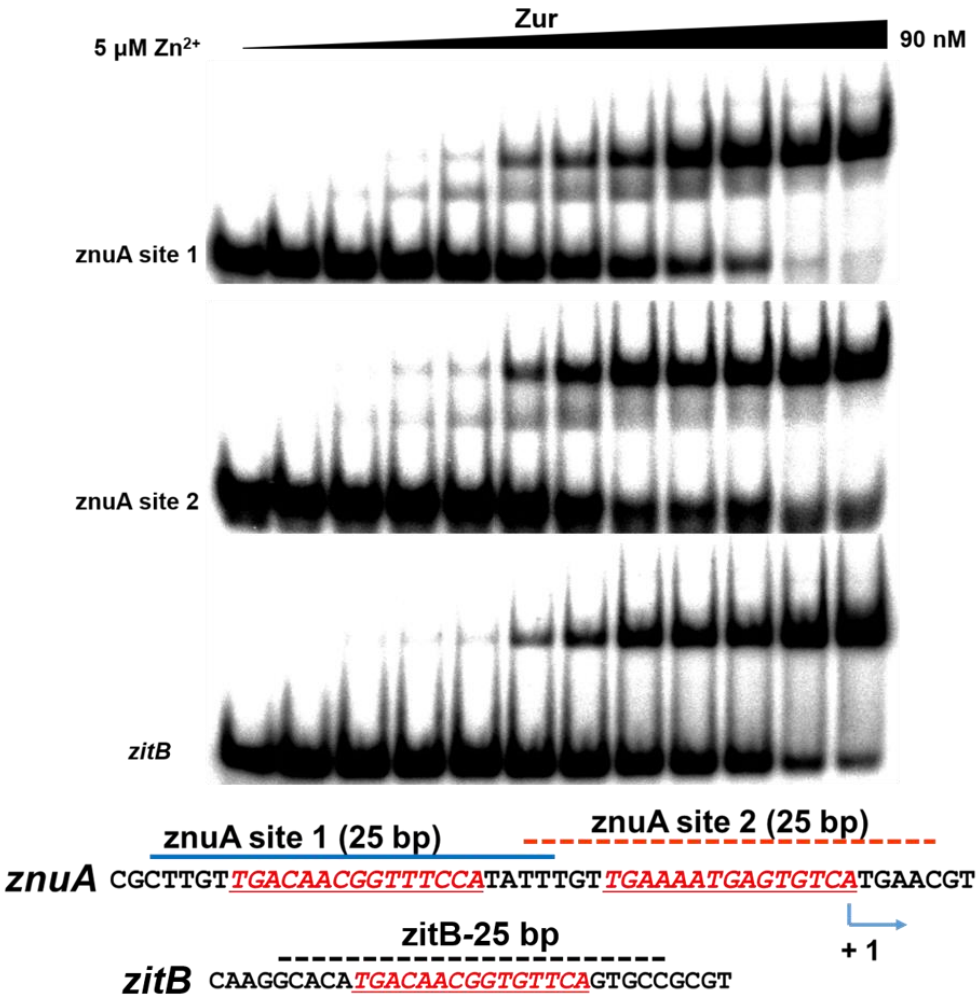
Zur
5 μM Zn2+
90 nM
znuA site 1
znuA site 2
zitB
znuA site 1 (25 bp)
znuA site 2 (25 bp)
znuA CGCTTGTTGACAACGGTTTCCATATTTGTTGAAAATGAGTGTCATGAACGT
+ 1
zitB-25 bp
zitB CAAGGCACATGACAACGGTGTTCAGTGCCGCGT

B

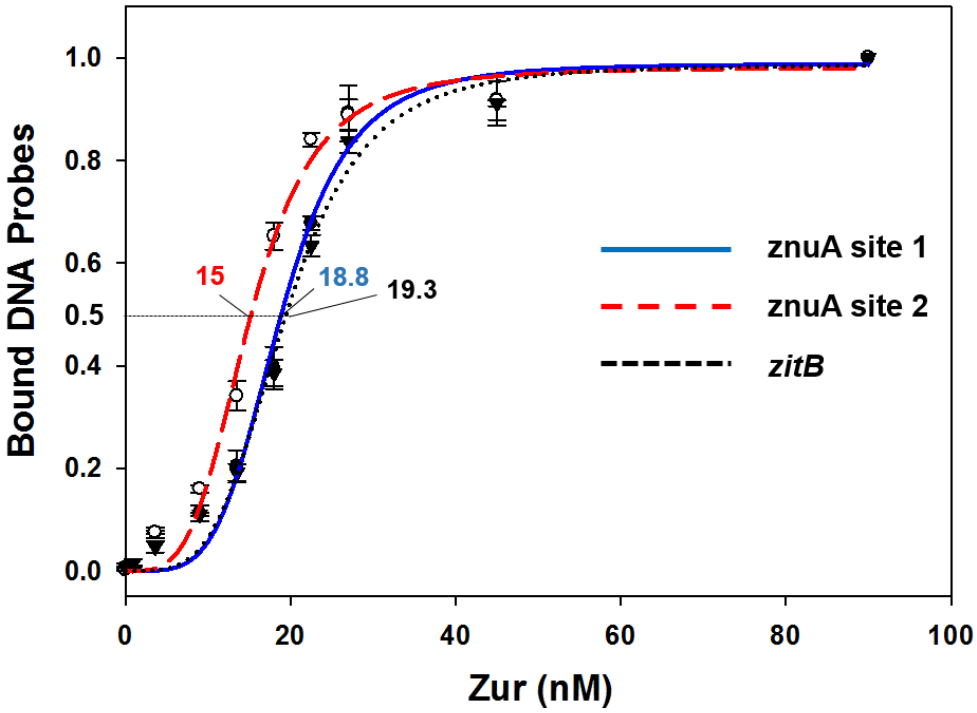
Bound DNA Probes
1.0
0.8
0.6
0.5
0.4
0.2
0.0
0
20
40
60
80
100
Zur (nM)
15
18.8
19.3
znuA site 1
znuA site 2
zitB

I examined whether high zinc induces Zur oligomerization in the absence of DNA. Addition of up to 0.5 mM $ZnCl_2$ to 10 μM Zur did not cause any change in mobility on 5% native PAGE (Fig. III-15.). Therefore, Zur appears not to form oligomers beyond dimer by itself under high zinc condition.

III.2.8. Zinc-dependent formation of multimeric Zur-*zitB* DNA complexes *in vitro* and the contribution of Zur-box upstream region on *zitB* activation *in vivo*.

As an initial step to unravel any changes that zinc might have caused to Zur and its binding to *zitB* DNA, I performed EMSA analysis with 33 bp *zitB* DNA containing the Zur-box motif in the middle, in comparison with the 25 bp probe. At sufficiently high concentration of zinc (20 μM) and Zur (90 nM), only a single complex band is formed on the 25 bp DNA probe (Fig. III-16A. lane 2). However, on the 33 bp DNA, longer by 4 nt at each end than the 25 bp probe, two retarded bands appeared as zinc increased (Fig. III-16A. lanes 4-11). I estimated the molecular weights of retarded bands by native PAGE with different percentages of polyacrylamide. The upper band on 33 bp probe matched the mobility of tetrameric Zur-DNA complex, most likely as a dimer of dimeric Zur, and the lower band corresponded to a dimeric Zur-DNA complex (Fig. III-17). I then examined Zur binding to 46 bp DNA (from -80 to -35 nt) by EMSA. The lower band on 46 bp probe corresponded to dimeric Zur-DNA complex, whereas the mobility of the upper band matched the molecular weights of either tetrameric or hexameric Zur-DNA complex within experimental error, as judged by native PAGE with different acrylamide percentages (Fig. III-18.). These results indicate that Zur has the ability to bind to *zitB* DNA as an oligomer, which is facilitated by zinc at high concentrations.

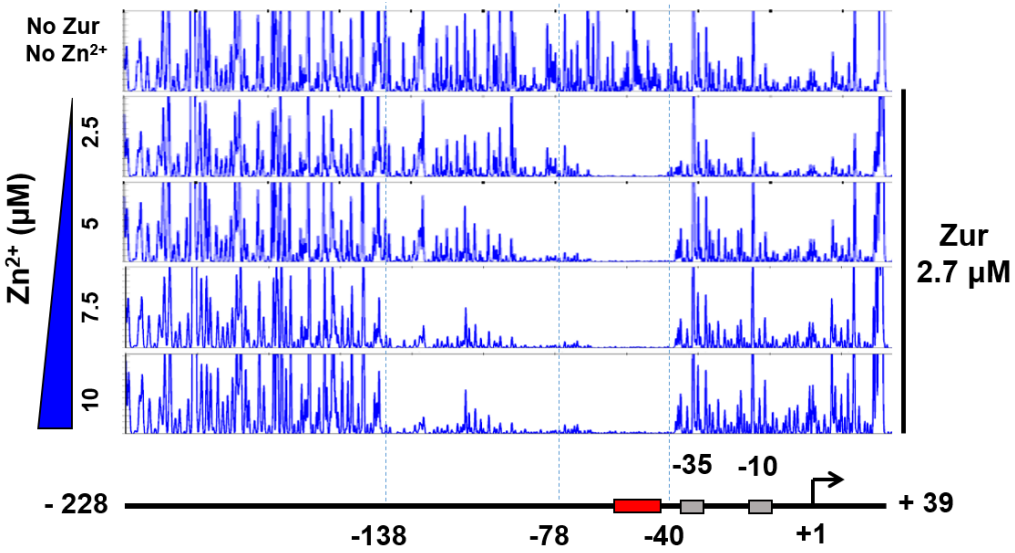

Fig. III-14. Increase in Zn dose dependent oligomeric Zur binding with extended footprints.

Footprinting under varying zinc concentrations. Dnase I footprinting analysis was done with the same DNA probe, but with fixed amount of Zur at 2.7 µM, and increasing amount of $ZnSO_4$ (2.5, 5.0, 7.5 and 10.0 µM) in each binding reaction. Zinc-dependent extension of Zur footprint on the *zitB* promoter was shown.

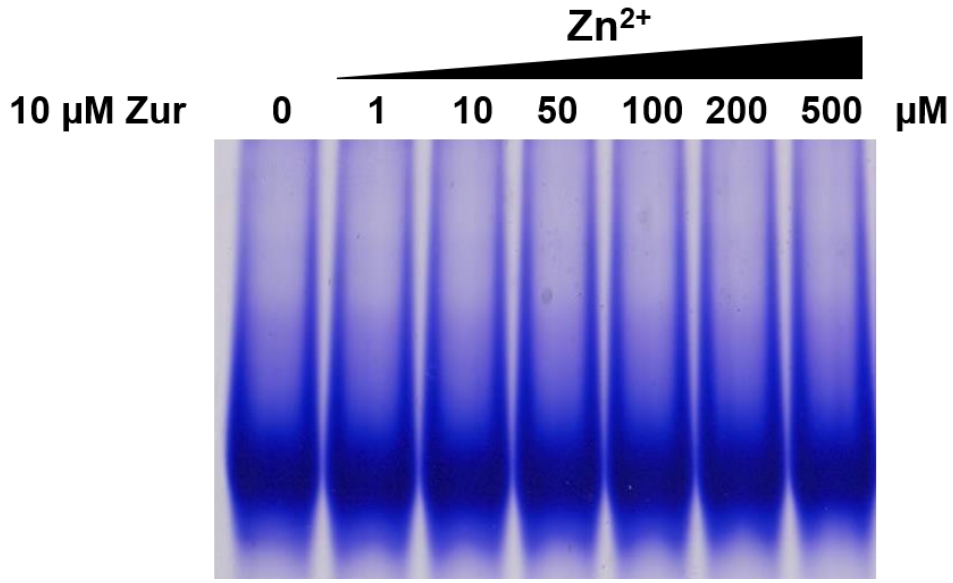

Fig. III-15. **Constant electrophoretic mobility of Zur on native PAGE over a wide range of zinc concentration changes.**

Increasing amounts of zinc (0 to 0.5 mM) were added to 10 μM Zur in the binding buffer, whose electrophoretic mobility change was examined on 5 % native PAGE.

Finally, I examined Zur binding by EMSA to a long 114 bp DNA probe (-148 to -35 nt) that encompasses the entire footprinted region (-138 to -40). As shown in Fig. III-16B, at a fixed amount of Zur (90 nM) and zinc at 10 and 20 μM (lanes 6 and 7), a further retarded band, whose mobility corresponded to either hexameric or octameric Zur-DNA complex (Fig. III-17.), appeared. On the same 114 bp DNA probe, when a higher amount of Zur was present at 900 nM, even at 10 μM zinc, super-shifted bands of highly retarded mobility were observed (Fig. III-19A.). Estimation of the extent of oligomerization was beyond the resolution limits by gel electrophoresis.

Interestingly, the footprint by Zur extended unidirectionally toward the upstream from the Zur-box as zinc increased (Fig. III-14.). Considering the symmetrically dimeric structure of Zur, it can be postulated that some sequence element in the upstream region may have contributed to oligomeric (or multiple) Zur binding. I examined Zur binding to DNA sequences upstream or downstream of the Zur box, using DNA EMSA results showed probes from -59 to -148 nt (up-probe) or from -29 to +50 nt (down-probe). The EMSA results showed that some oligomeric Zur binding was observed on the up-probe as zinc increased, whereas no binding was observed on the down-probe at all zinc concentrations (Fig. III-19B, C.). This clearly indicates that there is some sequence feature in the upstream of the Zur box of *zitB* promoter that facilitates oligomeric Zur binding.

III.2.9. Confirmation of zinc-dependent *zitB* activation via upstream sequences *in vivo* and *in vitro*

In order to confirm Zn-dependent Zur binding *in vivo* to the *zitB* promoter upstream region in the chromosome, I performed chromatin

Fig. III-16. Zinc-dependent formation of multimeric Zur-*zitB* DNA complexes *in vitro* and the contribution of Zur-box upstream region on *zitB* activation *in vivo*.

(**A**) EMSA analysis of Zur binding on 33 bp *zitB* DNA probe in comparison with the complex on 25 bp *zitB* DNA. Increasing amounts of zinc (0, 0.1, 0.5, 1.0, 2.5, 5, 10, 20 μM) were included in the binding buffer with 90 nM Zur. The molecular weights of the retarded bands were estimated from electrophoretic mobility on native PAGE with different acrylamide percentages (Fig. III-17.), and were marked as T (tetramer) or D (dimer).

(**B**) EMSA analysis on the 114 bp *zitB* probe (from -148 to -35 nt). Increasing amounts of zinc (0, 0.5, 1, 5, 10, 20 μM) were included in the binding buffer with 90 nM Zur. Based on the estimated molecular weights from native PAGE mobility, the retarded bands were indicated by O for octamer, and D for dimer.

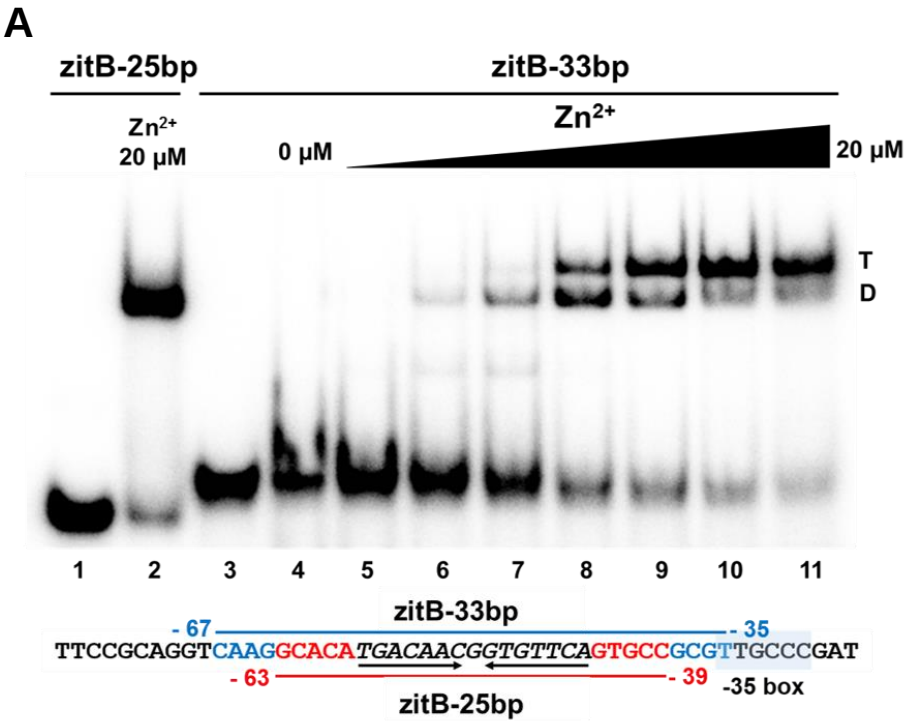
A
zitB-25bp
zitB-33bp
Zn2+
20 μM
Zn2+
0 μM
20 μM
T
D
1 2 3 4 5 6 7 8 9 10 11
zitB-33bp
- 67
- 35
TTCCGCAGGTCAAGGCACATGACAACGGTGTTCAGTGCCGCGTTGCCCGAT
- 63
- 39
-35 box
zitB-25bp

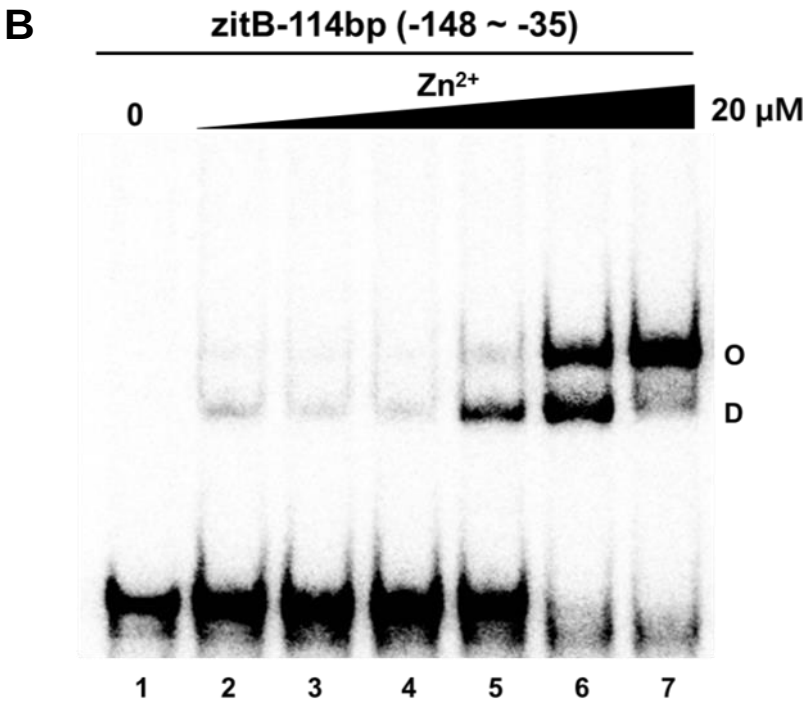
B
zitB-114bp (-148 ~ -35)
Zn2+
0
20 μM
O
D
1 2 3 4 5 6 7

Fig. III-17. Determination of the stoichiometry of Zur-DNA complexes by native PAGE mobility.

(**A**) Relative mobility of Zur-DNA complexes on DNA probes of 33, 46, or 120 bp probes on native PAGE on 5 to 9% polyacrylamide gels. Logarithms of relative mobility values (compared with bromophenol blue) of both upper and down complexes as well as standard proteins (BSA monomer, BSA dimer, Zur dimer) were plotted against acylamide percentages as described by Baichoo and Helmann (2002)[22]. Data points for each complex and standard protein were presented with color-coded legends.

(**B**) Estimation of molecular mass and the stoichiometry of Zur-DNA complex. The negative slope of the mobility change for each standard protein was re-plotted against their molecular weights to obtain a standard curve. The apparent molecular weight of each complex was estimated from the standard curve using the least squares regression. The best fitting line (R^2 of 0.9888; brown dotted line) was obtained by assuming the following stoichiometry of Zur for upper and down complex bands, respectively: On 33 bp DNA, tetrameric (47.2 kDa, blue) and dimeric (76.6 kDa, orange) Zur binding; on 46 bp DNA, tetrameric (86.3 kDa, pink triangle) and dimeric (57.9 kDa, red circle) Zur binding; On 120 bp probe, hexameric (162.4 kDa, purple triangle) and dimeric (103.6 kDa, green circle) binding. Another linear regression of data plots gave reasonably well-fitting curve (R^2 of 0.9804; blue dotted line), when the upper bands on longer probes (46 bp and 120 bp) were regarded as hexameric (115.7 kDa with 46 bp DNA; pink circle) and octameric (191.8 kDa with 120 bp DNA; purple circle) Zur-bound complexes, respectively.

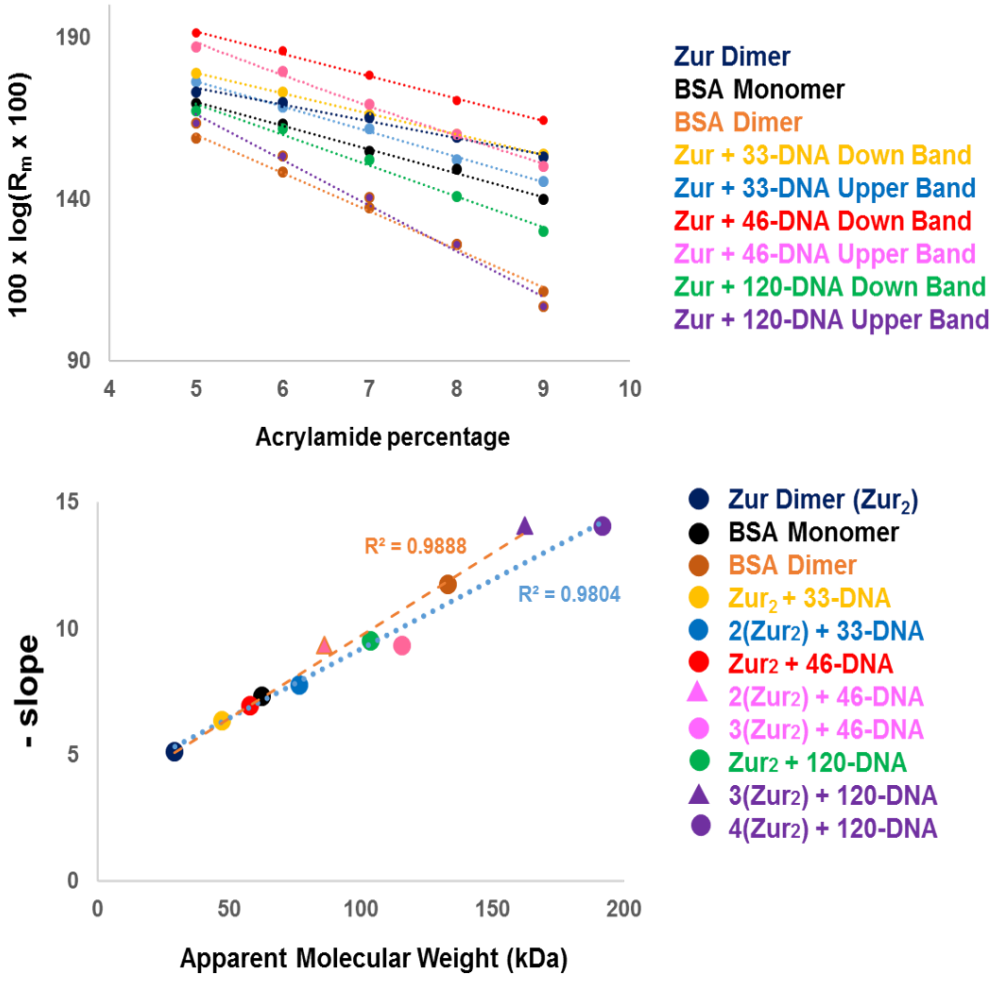
190
140
90
4
5
6
7
8
9
10
100 x log(Rm x 100)
Acrylamide percentage
Zur Dimer
BSA Monomer
BSA Dimer
Zur + 33-DNA Down Band
Zur + 33-DNA Upper Band
Zur + 46-DNA Down Band
Zur + 46-DNA Upper Band
Zur + 120-DNA Down Band
Zur + 120-DNA Upper Band
15
10
5
0
0
50
100
150
200
- slope
Apparent Molecular Weight (kDa)
R² = 0.9888
R² = 0.9804
Zur Dimer (Zur2)
BSA Monomer
BSA Dimer
Zur2 + 33-DNA
2(Zur2) + 33-DNA
Zur2 + 46-DNA
2(Zur2) + 46-DNA
3(Zur2) + 46-DNA
Zur2 + 120-DNA
3(Zur2) + 120-DNA
4(Zur2) + 120-DNA

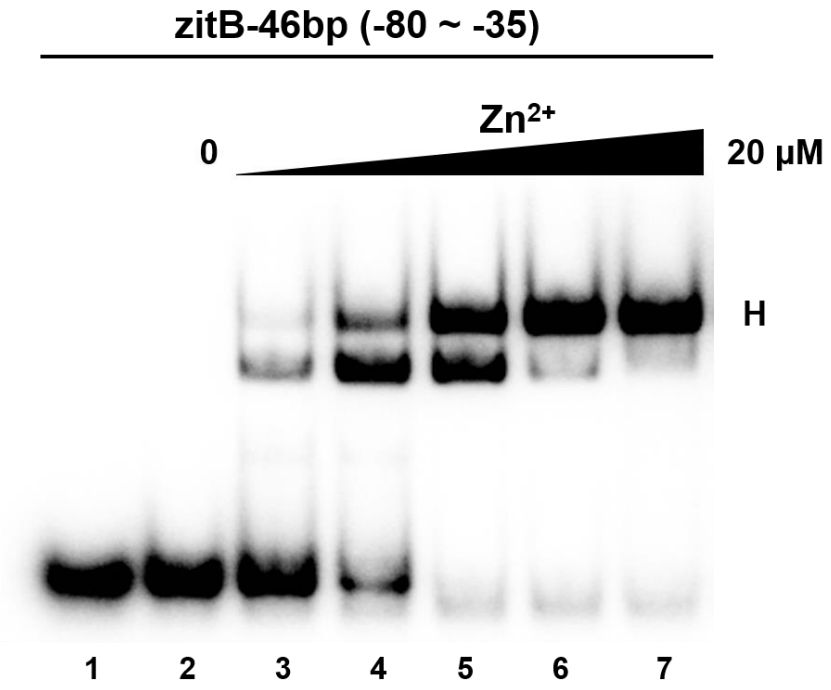

Fig. III-18. Binding of Zur to 46 bp DNA (from -80 to -35).

EMSA assay was performed for the binding reactions containing Increasing amounts of zinc (0, 0.5, 1, 5, 10, 20 μM) and 90 nM Zur. The upper and down complexes were labeled as T/H for tetramer or hexamer, and D for dimer, as estimated from the PAGE analysis on different acrylamide percentages (Fig. III-17.).

Fig. III-19. Zinc-dependent binding of Zur to 114 bp *zitB* probe at high concentration of Zur (900 nM).

(**A**) EMSA of Zur binding to 114 bp probe (from -148 to -35 nt from TSS) at 900 nM Zur with increasing concentrations of zinc (0.1, 0.5, 1, 5, 10, 20, 30, 50, 75, 90 μM) in the binding reaction. Formation of super-shifted bands appear at >10 μM zinc.

(**B**) EMSA of Zur binding (900 nM) to upstream DNA probe (-148 to -59) devoid of Zur-box motif. The same binding conditions as in (A) were used.

(**C**) EMSA of Zur binding (900 nM) to downstream DNA probe (-29 to +50) devoid of Zur-box motif. The same binding conditions as in (A) were used.

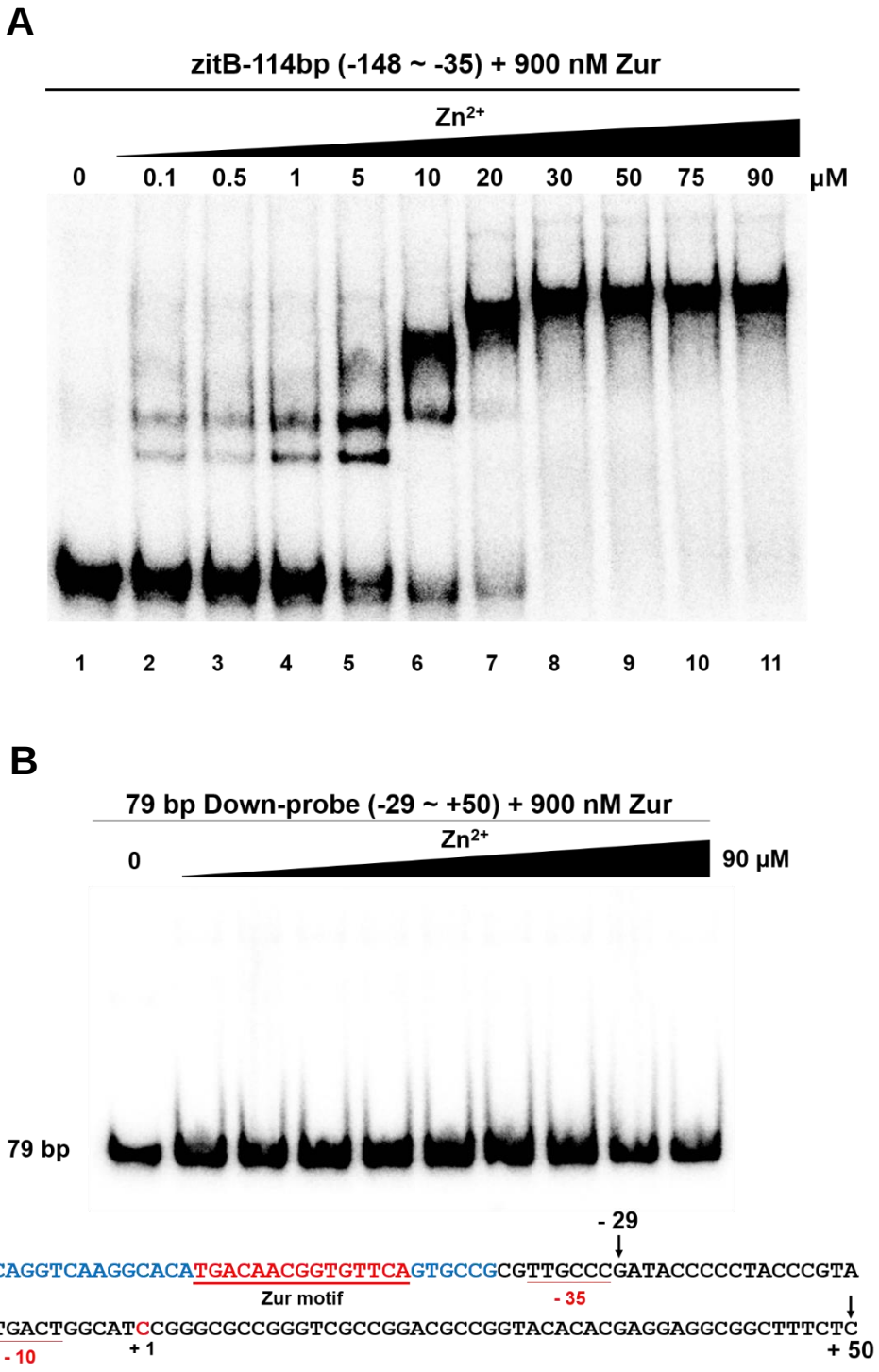
A
zitB-114bp (-148 ~ -35) + 900 nM Zur
Zn2+
0 0.1 0.5 1 5 10 20 30 50 75 90 μM
1 2 3 4 5 6 7 8 9 10 11
B
79 bp Down-probe (-29 ~ +50) + 900 nM Zur
Zn2+
0
90 μM
79 bp
- 29
CGCAGGTCAAGGCACATGACAACGGTGTTCAGTGCCGCGTTGCCCGATACCCCCTACCCGTA
Zur motif
- 35
GTTGACTGGCATCCGGGCGCCGGGTCGCCGGACGCCGGTACACACGAGGAGGCGGCTTTCTC
- 10
+ 1
+ 50

C

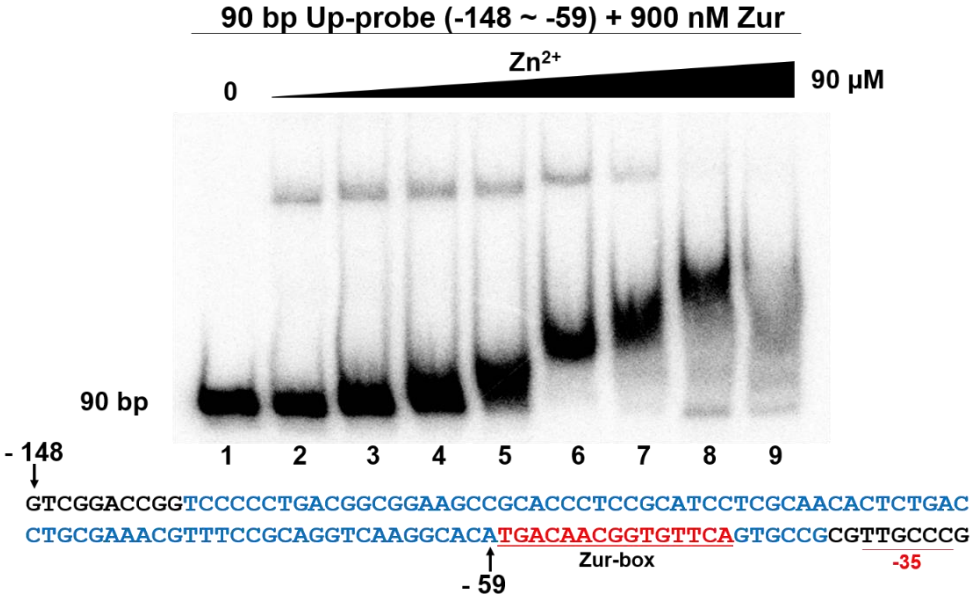
90 bp Up-probe (-148 ~ -59) + 900 nM Zur
Zn2+
0
90 μM
90 bp
1 2 3 4 5 6 7 8 9
- 148
GTCGGACCGGTCCCCCTGACGGCGGAAGCCGCACCCTCCGCATCCTCGCAACACTCTGAC
CTGCGAAACGTTTCCGCAGGTCAAGGCACATGACAACGGTGTTCAGTGCCGCGTTGCCCG
Zur-box
-35
- 59

immunoprecipitation with anti-Zur antibody. *S. coelicolor* cells treated with 0.1 mM $ZnSO_4$ were examined along with non-treated wild type and *Δzur* cells. About 500 bp region of the *zitB* gene from -348 to +155 nt (relative to TSS) was screened by qPCR, by using 8 sets of overlapping primers, each pair of which producing 70-90 bp PCR products that encompass the whole region. ChIP results (Fig. III-20.) indicated clearly that Zur binding occurred preferentially to the promoter upstream region rather than to the downstream region. It also showed that 0.1 mM zinc addition substantially increased Zur binding, compared with the non-treated (~1 μM zinc in the media) sample.

The effectiveness of the *zitB* upstream region in zinc-dependent gene activation was examined *in vivo* by using a heterologous reporter gene encoding β-glucuronides (GUS). Recombinant p*zitB*-GUS fusion plasmids that contain the *zitB* regulatory region up to -60 or -228 nt were constructed on pSET152-based integration vector (Fig. III-21.). Following chromosomal integration through the *att* site, the reporter gene expression was assessed after zinc treatment. The S1 mapping of GUS transcripts demonstrated that the *zitB* regulatory region with the Zur-box motif only (up to -60) allowed only marginal gene activation, whereas the *zitB* upstream sequence up to -228 nt enabled full activation of the reporter gene expression (Fig. III-21.).

Finally, I performed run-off transcription assay with purified Zur to examine its ability to activate *zitB* transcription *in vitro*. The *zitB* promoter sequence deviates farther from the prominent promoter consensus sequence recognizable by the housekeeping sigma factor HrdB, whereas *znuA* promoter matches well with the consensus (Jeong *et al*., 2016,; Fig. III-22.). The *zitB* promoter lacks the critical A residue at position -11, and is likely to be recognized very weakly by HrdB, if not recognized by another alternate sigma factor. Transcription from the 339-bp *zitB* DNA template (-287 to +52) was allowed to occur in the presence

of *E. coli* RNA polymerase core enzyme and the sigma factor HrdB of *S. coelicolor*, fixed amount of Zur (50 nM) and varying amounts of $ZnSO_4$ from 0 to 20 μM. Transcription from the *znuA* template (-107 to +87) was examined in parallel. Results in Fig. 5d demonstrated that Zur activated *zitB* transcription directly under high zinc (15 and 20 μM) conditions, but not under lower zinc, supporting the proposal that the phase II activation can occur by Zur binding only. In contrast, the *znuA* gene was highly transcribed under no-zinc condition, but was repressed efficiently by 1 μM zinc, consistent with *in vivo* observations (Fig. III-23.). The failure to detect *zitB* transcription under lower zinc condition could be due to non-optimal composition of RNA polymerase holoenzyme for the weak *zitB* promoter. Otherwise, there still remains the possibility that some additional factor(s) may also contribute to activate *zitB* under low zinc condition (phase I).

III.3. ZitB orthologues in other bacteria.

III.3.1. zitB orthologue in *Mycobacterium smegmatis and Corynebacterium glutamicum*

I performed the finding of zitB orthologue in *Mycobacterium smegmatis and Corynebacterium glutamicum*. MS0755 is the ZitB orthologue in *Mycobacterium smegmatis and* Ncgl1232 is the orthologue in *Corynebacterium glutamicum*. I could find the putative Zur binding motif at upstream about 30~50 nt from transcription start site, respectively (Fig. III-24.).

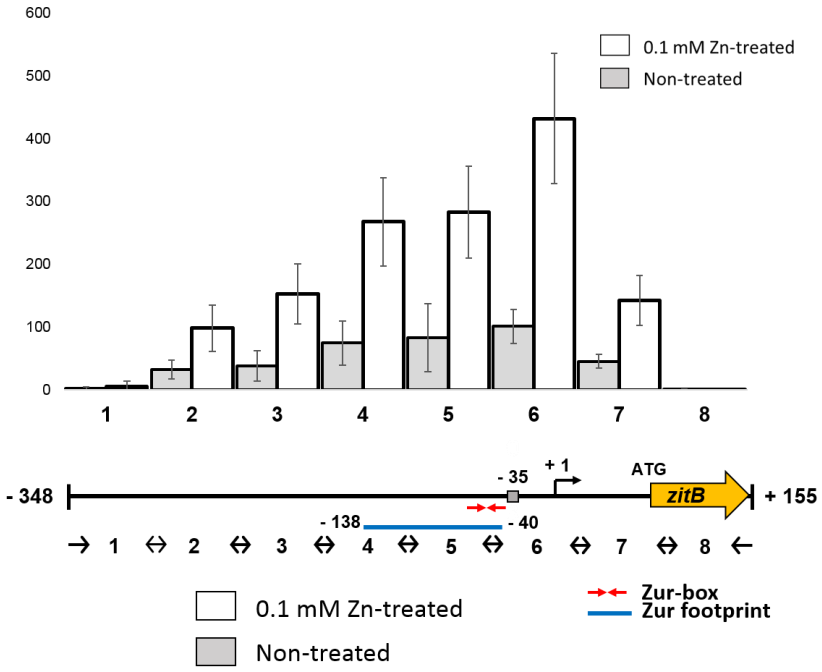

Fig. III-20. ChIP analysis of zinc-dependent binding of Zur around the *zitB* promoter region *in vivo*.

Quantitative PCR (qPCR) was performed for the chromatin samples immunoprecipitated with anti-Zur antibody. Wild type cells were either non-treated or treated with 0.1 mM $ZnSO_4$. Overlapping primers were used to for regions 1 (88 bp, -348 ~ -260), 2 (72 bp, -280 ~ -208), 3 (71 bp, -228 ~ -157), 4 (87 bp, -177 ~ -90), 5 (75 bp, -110 ~ -35), 6 (94 bp, -55 ~ +39), 7 (65 bp, +18 ~ +83), and 8 (93 bp, +62 ~ +155). Relative enrichments were presented by taking the value from *Δzur* sample as 1.0. Three independent ChIP samples were obtained for qPCR analysis, using the Stratagene MX3000P QPCR system (Agilent Technologies). Asterisks (**) indicate measurements with P-values ≤ 0.001 by Student's t-test.

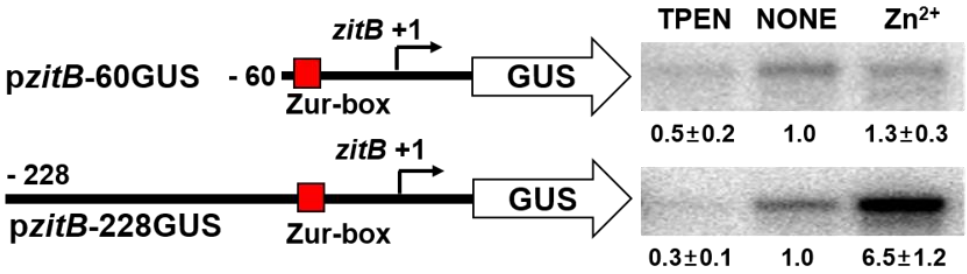

Fig. III-21. The confirmation of the *zitB* upstream region in zinc-dependent gene activation.

Expression of GUS reporter gene linked with the *zitB* promoter region from +50 to -60 nt (p*zitB*-60GUS) or to -228 nt (p*zitB*-228GUS). *S. coelicolor* cells containing the chromosomally integrated reporter gene were either non-treated or treated with 10 μM TPEN or 100 μM $ZnSO_4$ for 30 min. Quantitation of S1 mapping results were done from 3 independent experiments, and the relative expression values were presented by taking the non-treated level as 1.0. The P-values of all the relative measurements except zinc treated p*zitB*-60GUS were ≤0.001 by Student's t-test.

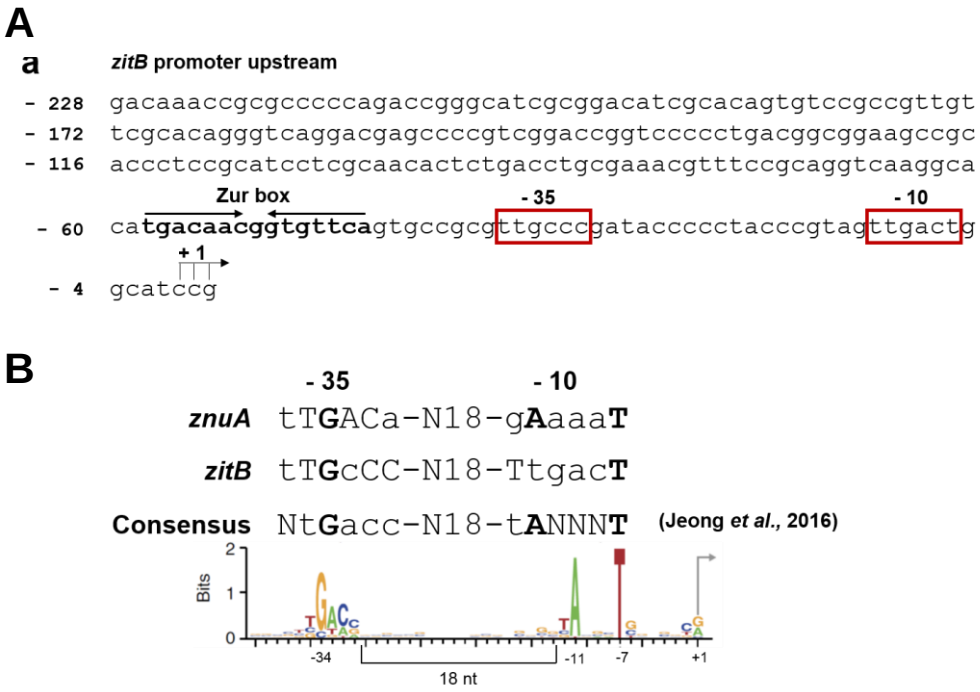

Fig. III-22. Sequence features of the *zitB* promoter region.

(**A**) Promoter upstream sequences of the *zitB* gene.

(**B**) Comparison of the -35 and -10 elements of the *zitB* promoter with those of *znuA* and the prominent promoters, whose transcription start sites (TSS) have been determined in the genome of *S. coelicolor*. The bold capitals denote most conserved nucleotides. The nucleotide positions in the prominent promoter consensus logo were numbered based on the most frequently observed distances from the TSS.

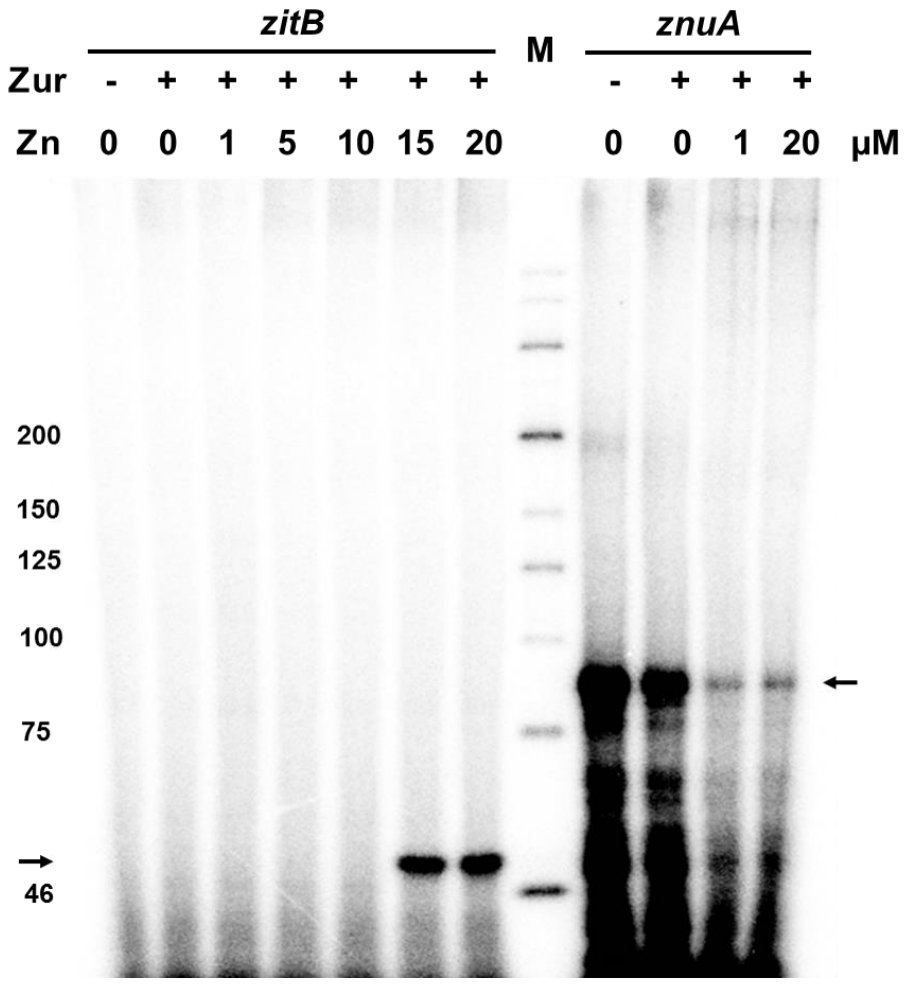

Fig. III-23. ***In vitro*** **transcription assay of** ***zitB*** **and** ***znuA*****.**

In vitro transcription assays of the *zitB* and *znuA* promoters in the presence of purified Zur (50 nM) and RNA polymerase core enzyme (*E. coli*) and the housekeeping sigma factor HrdB (*S. coelicolor*). Varying amounts of $ZnSO_4$ (0, 1, 5, 10, 15 and 20 µM) were added in the transcription buffer. Predicted lengths of the *zitB* and *znuA* transcripts are 52 nt (left arrow) and 87 nt (right arrow), respectively.

III.3.2. EMSA assay with S.coelicolor and confirmation of RNA expression

In order to confirm the ZitB ortholgue genes are putative direct targets of Zur, I performed Zur binding assay and S1 nuclease mapping. Zur bound the MS0755 and Ncgl1232 promoter region (Fig. III-25.). And the genes are induced by zinc concentreation (Fig. III-26.). All together, the genes have the possibility of Zur target in each species.

III.4. Finding new Zur target genes & classification of the zinc-responsive genes.

III.4.1 Zur ChIP-sequencing analysis.

I perfomed ChIP-sequencing to get better quality results compared to ChIP-chip. Cells were either untreated or treated with $ZnSO_4$ (100 μM) for 1 h before obtaining cell extracts. The analysis of the ChIP samples showed that the peaks located in through the genome (Fig. III-27.). These peaks showed the known Zur target genes as *znuA, znuB2/C2, rpmF, rpmG/B*, SCO7676, 7681/7682 in a gene cluster for synthesizing enterobactin-type zincophore and *zitB* in this study. Among the peasks, the position of the significantly enriched peaks were similar each other. However, I found the Zur binding extension in zinc treated one than no treated one. The phenomenon of binding was shown on *zitB* and *znuA* promoter region. (Fig. III-28.). The result suggests that I condn't find the new Zur target genes and Zur can perform multimerized structure in zinc excess condition *in vivo*.

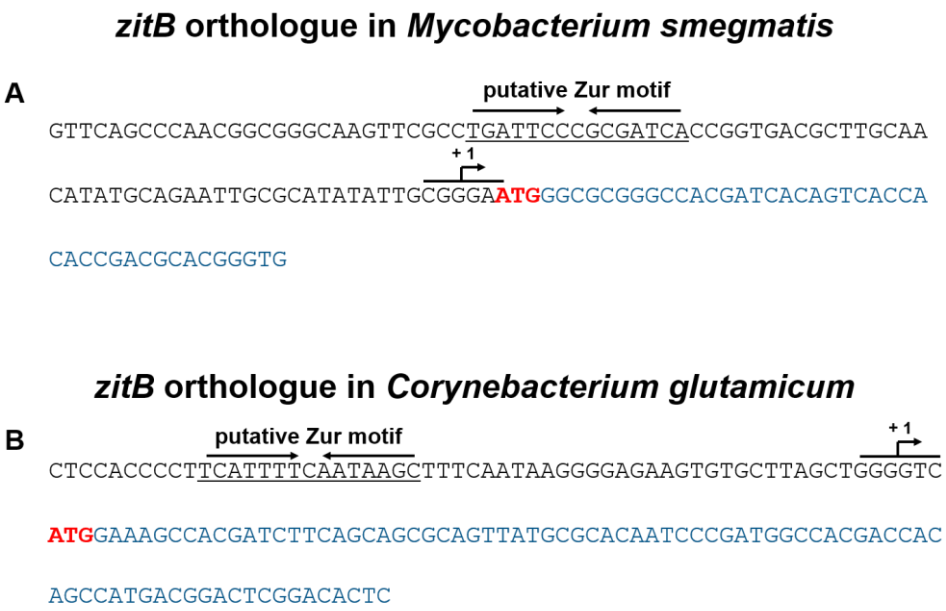

Fig. III-24. ZitB orthologue in *Mycobacterium smegmatis* and *Corynebacterium glutamicum*.

(**A**) ZitB orthologue in *Mycobacterium smegmatis*. Transcription start site (TSS) locate on near ATG start codon and Putative Zur motif is 50 nt upstream from TSS.

(**B**) ZitB orthologue in *Corynebacterium glutamicum*. Transcription start site (TSS) locate on near ATG start codon and Putative Zur motif is about 30 nt upstream from TSS.

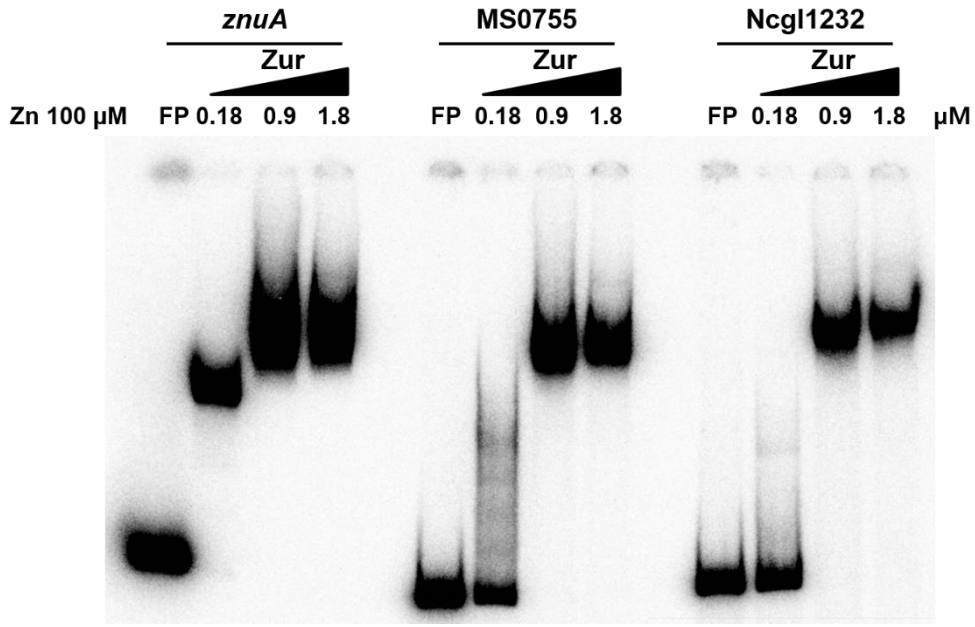

Fig. III-25. EMSA assay of the ZitB orthologue in *Mycobacterium smegmatis* (MS0755) and *Corynebacterium glutamicum* (Ncgl1232).

Increasing amounts of purified Zur protein (0.18 to 1.8 µM) were incubated in the presence of 100 µM $ZnSO_4$ with γ-^{32}P labeled DNA probes for *znuA*, MS0755 and Ncgal1232.

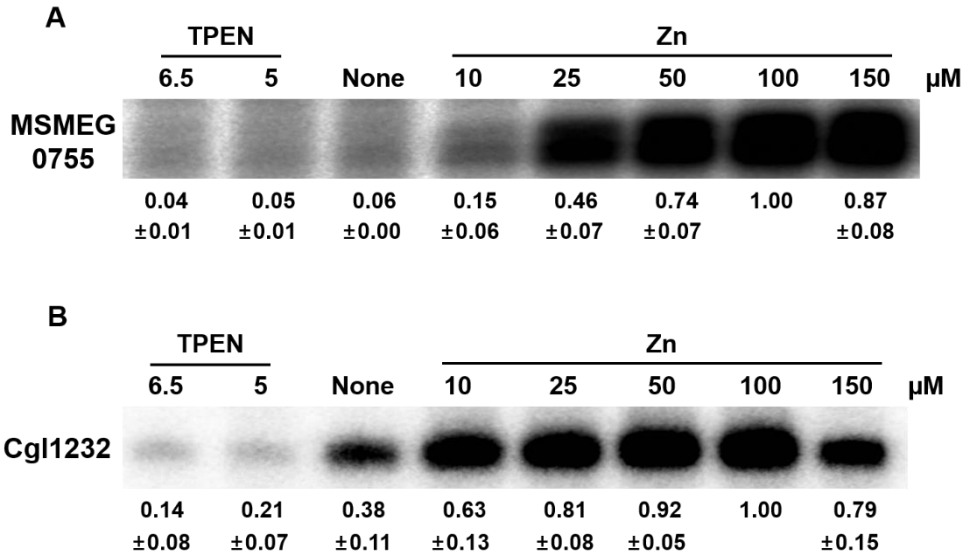

Fig. III-26. Confirmation of RNA expression of MS0755 and Ncgl1232 dependent zinc concentration.

(**A** and **B**) S1 mapping analysis of MS0755 and Ncgl1232 transcripts under TPEN or zinc-treated conditions. The wild type cells grown in YEME medium to exponential growth (OD_{600} of 0.4 to ~0.5) were treated for 30 min with TPEN (5.0 to 6.5 μM as indicated), $ZnSO_4$ (10-150 μM as indicated), or none, before cell harvest. Quantifications of S1 mapping results were done from 3 independent experiments, repectively.

III.4.2. RNA sequencing analysis.

I performed RNA sequencing duplicated of wild type-untreated, wild type-treated with 50 μM TPEN treated for 50 min and *△zur* for finding new zur targets. The samples were confirmed by S1 mapping and RNA quality in gel. The RPKM value of each samples were compared by scatter plot (Fig. III-29). I analyzed 1.5 fold change up-regulation or 0.66 fold change down-regulation limitation TPEN treated in comparison with the wild type-untreated of the RPKM value followed KEGG pathway (Fig. III-30.). The portion of ABC transporters or valine, Leucine and Isoleucine degradation pathway were taken up highly in up-regulation. The portion of ribosome and pyrimidine or purine metabolism were taken up highly in down-regulation. But portion of the functions are taken up below 1% in genome, respectively. This result suggests that this genes were essential or unnecessary for survival in metal-depleted condition.

III.5. Classification of the genes inducted by metal depletion.

Metals affect bacterial physiology in diverse ways, as catalytic cofactors, structural or regulatory components of proteins, etc. When in excess, they disrupt cell physiology as toxic agents, and hence its homeostasis needs be strictly achieved in all life forms. In *Streptomyces coelicolor*, several metalloregulators were identified, among which a zinc-responsive regulator of the Fur family has been reported to be a primary regulator for zinc homeostasis, which is important for differentiation and antibiotic production.

Fig. III-27. The Zur binding peaks of the Zur ChIP-sequencing.

The peaks indicate the Zur binding region in the whole genome. No-treated or 100 μM zinc-treated one are shown by green or blue, respectively. The red arrows indicate the known Zur target genes or blue arrow is the genes studied in this work

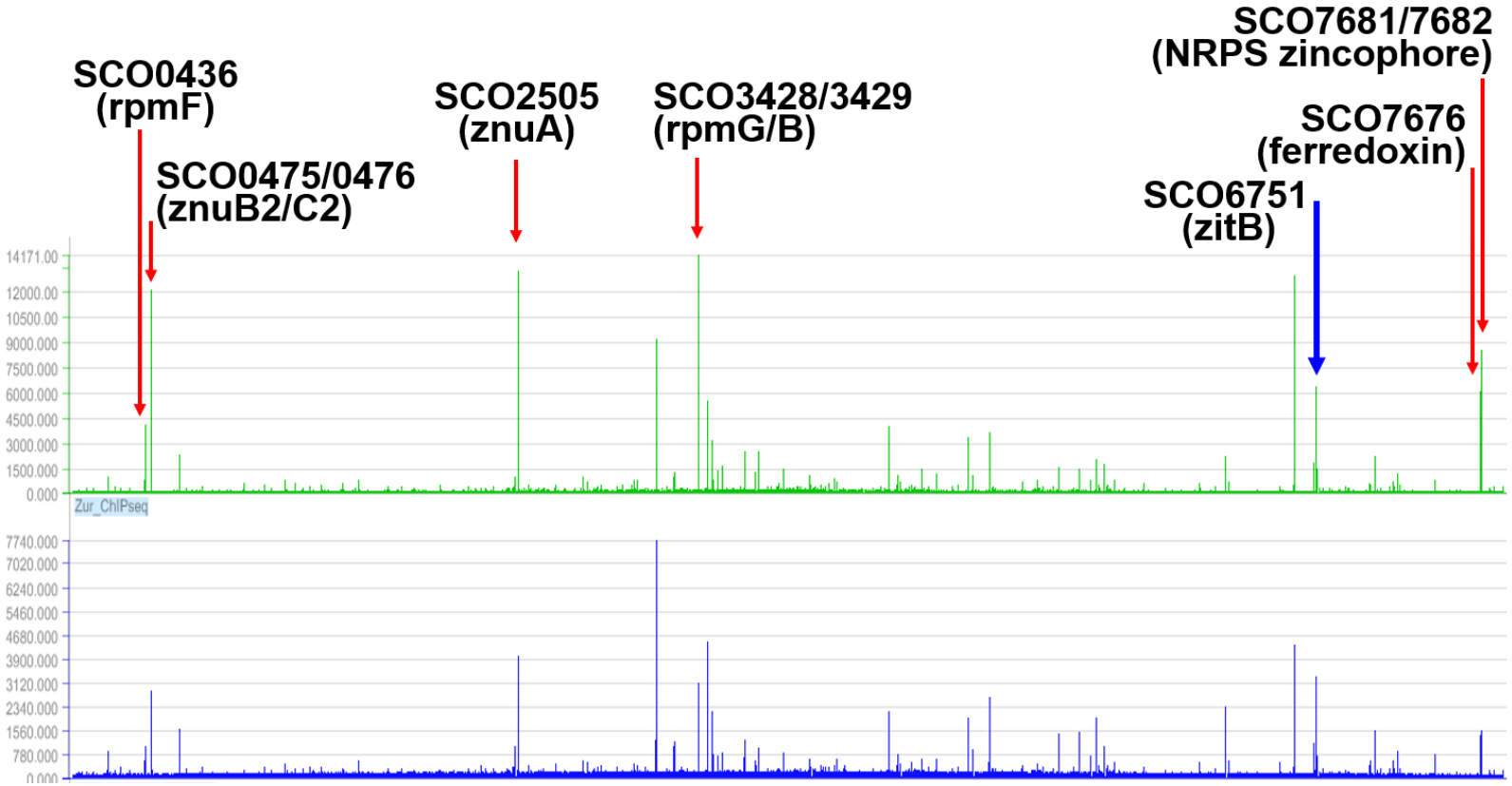
SCO0436
(rpmF)
SCO0475/0476
(znuB2/C2)
SCO2505
(znuA)
SCO3428/3429
(rpmG/B)
SCO6751
(zitB)
SCO7676
(ferredoxin)
SCO7681/7682
(NRPS zincophore)
14171.00
12000.00
10500.00
9000.000
7500.000
6000.000
4500.000
3000.000
1500.000
0.000
Zur_ChIPseq
7740.000
7020.000
6240.000
5460.000
4680.000
3900.000
3120.000
2340.000
1560.000
780.000

Fig. III-28. Zur binding peaks of *zitB* and *znuA* on promoter region.

(**A** and **B**) The peak of Zur biding is located at zitB and *znuA* promoter region. The green peak is No-treated one and the blue is 100 μM zinc treated one, respectively.

A

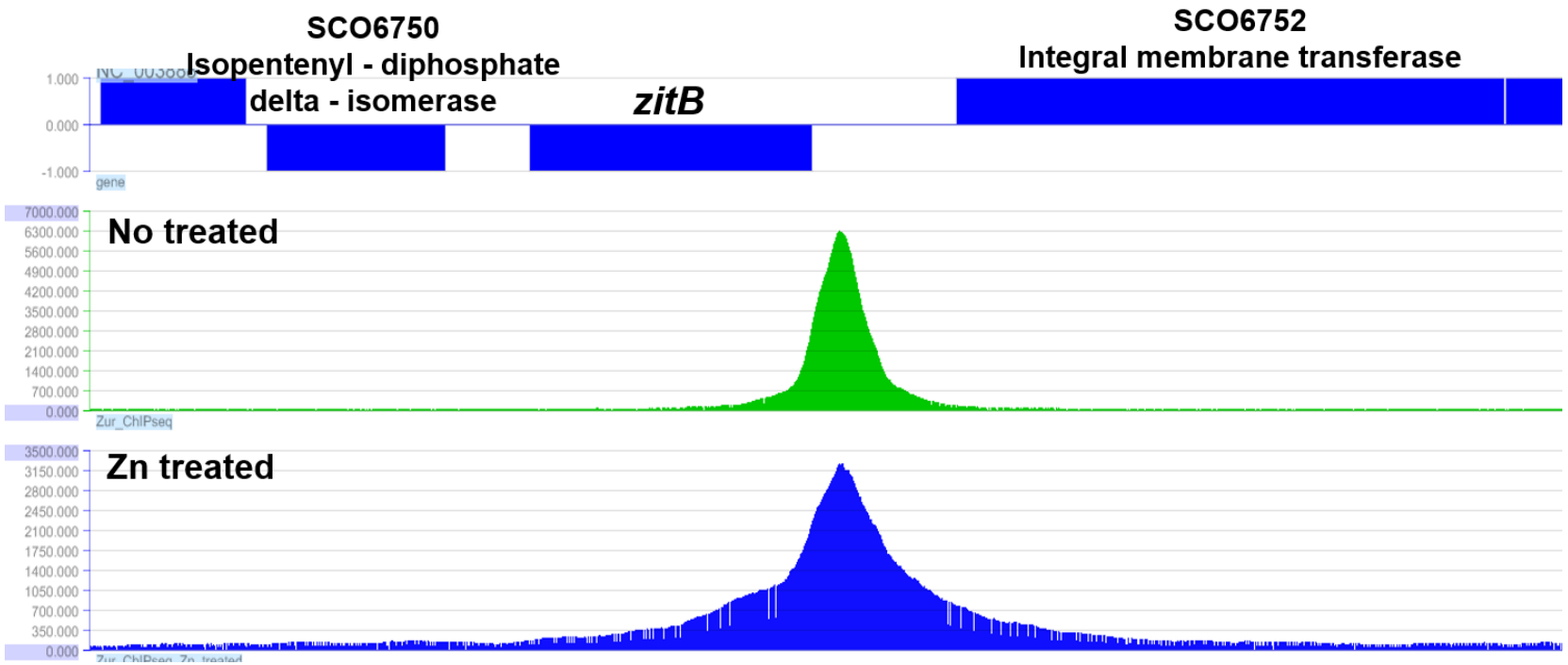
SCO6750
Isopentenyl - diphosphate
delta - isomerase
zitB
SCO6752
Integral membrane transferase
1.000
0.000
-1.000
gene
No treated
7000.000
6300.000
5600.000
4900.000
4200.000
3500.000
2800.000
2100.000
1400.000
700.000
0.000
Zur_ChIPseq
Zn treated
3500.000
3150.000
2800.000
2450.000
2100.000
1750.000
1400.000
1050.000
700.000
350.000
0.000

B

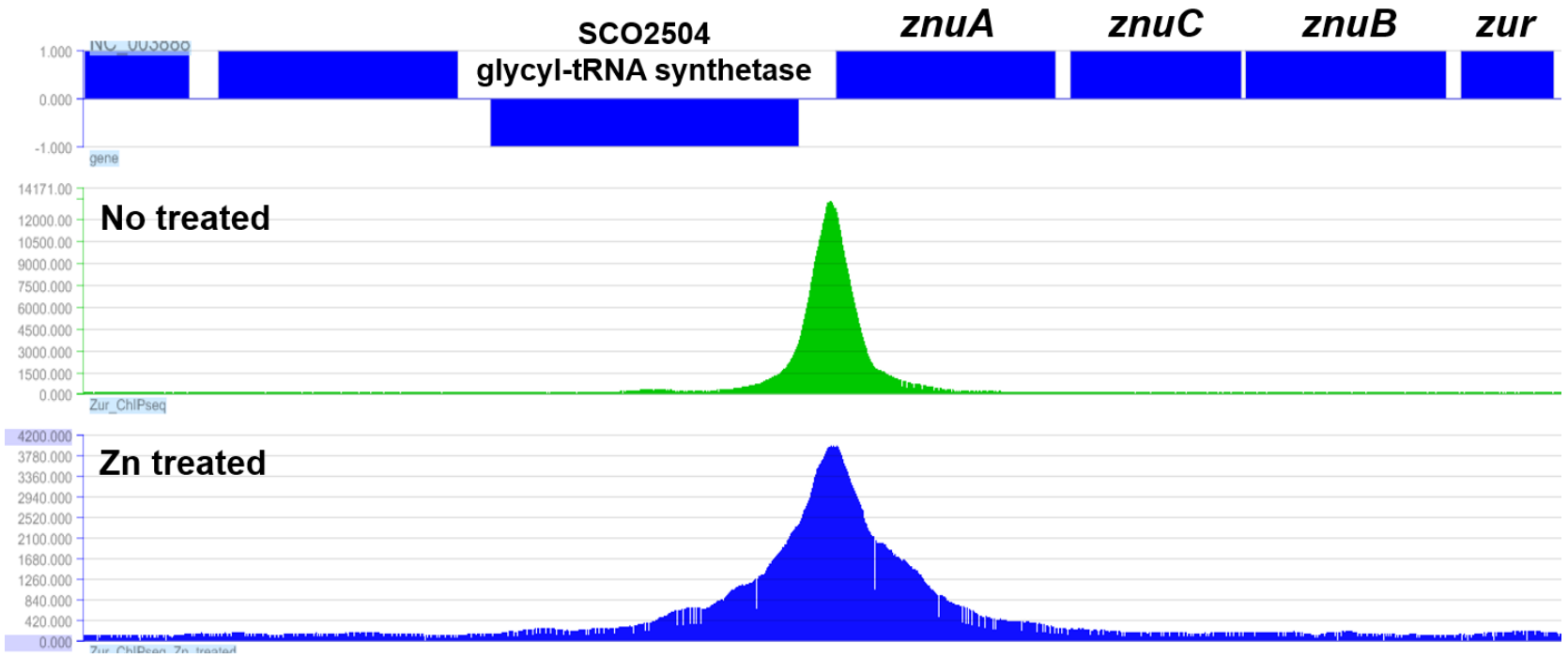
SCO2504
glycyl-tRNA synthetase
znuA
znuC
znuB
zur
1.000
0.000
-1.000
gene
14171.00
12000.00
10500.00
9000.000
7500.000
6000.000
4500.000
3000.000
1500.000
0.000
No treated
Zur_ChIPseq
4200.000
3780.000
3360.000
2940.000
2520.000
2100.000
1680.000
1260.000
840.000
420.000
0.000
Zn treated

Fig. III-29. Scatter plotting of the RNA sequencing.

The plotting are shown as correlation of the samples duplicated. X-axis is 1st sample and Y-axis 2nd sample, respectively.

WT None

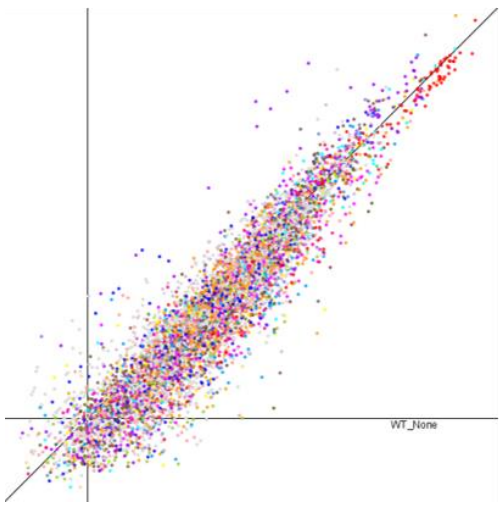

WT TPEN

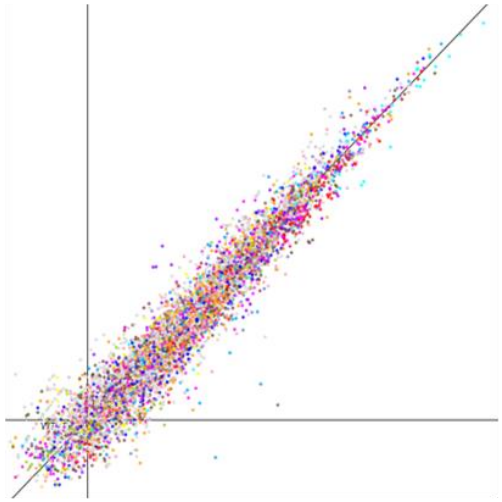

ΔZur None

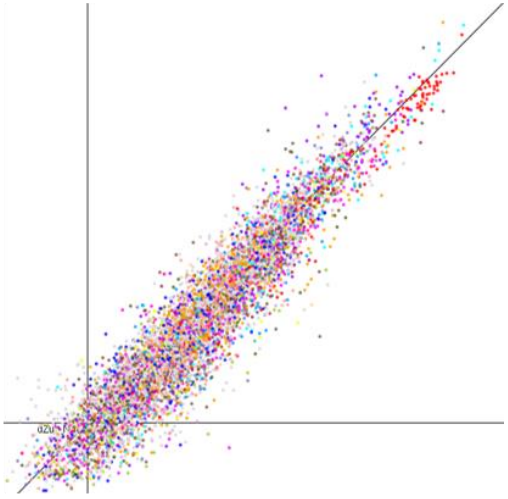

Fig. III-30. Analysis of the gene expression change by metal depletion followed KEGG pathway.

(**A**) Over 1.6 fold change up-regulation genes are 173 genes. The peaks show the portion (left Y-axis) of function of whole genome (blue peaks) and the up-regulation genes (orange peaks).

(**B**) Below 0.66 fold change down-regulation genes are total 177 genes. The right Y-axis is p-value of the duplicated RNA-sequencing result.

A

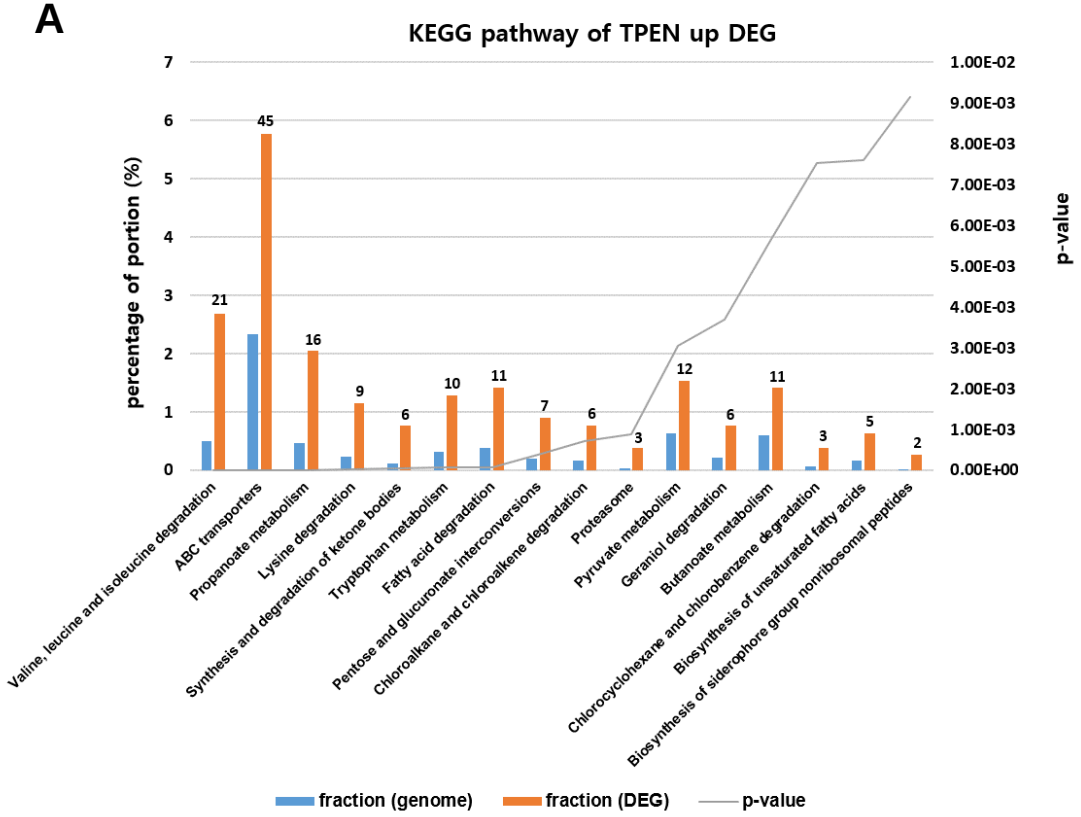
KEGG pathway of TPEN up DEG
percentage of portion (%)
p-value
0
1
2
3
4
5
6
7
0.00E+00
1.00E-03
2.00E-03
3.00E-03
4.00E-03
5.00E-03
6.00E-03
7.00E-03
8.00E-03
9.00E-03
1.00E-02
21
45
16
9
6
10
11
7
6
3
12
6
11
3
5
2
Valine, leucine and isoleucine degradation
ABC transporters
Propanoate metabolism
Lysine degradation
Synthesis and degradation of ketone bodies
Tryptophan metabolism
Fatty acid degradation
Pentose and glucuronate interconversions
Chloroalkane and chloroalkene degradation
Proteasome
Pyruvate metabolism
Geraniol degradation
Butanoate metabolism
Chlorocyclohexane and chlorobenzene degradation
Biosynthesis of unsaturated fatty acids
Biosynthesis of siderophore group nonribosomal peptides
fraction (genome)
fraction (DEG)
p-value

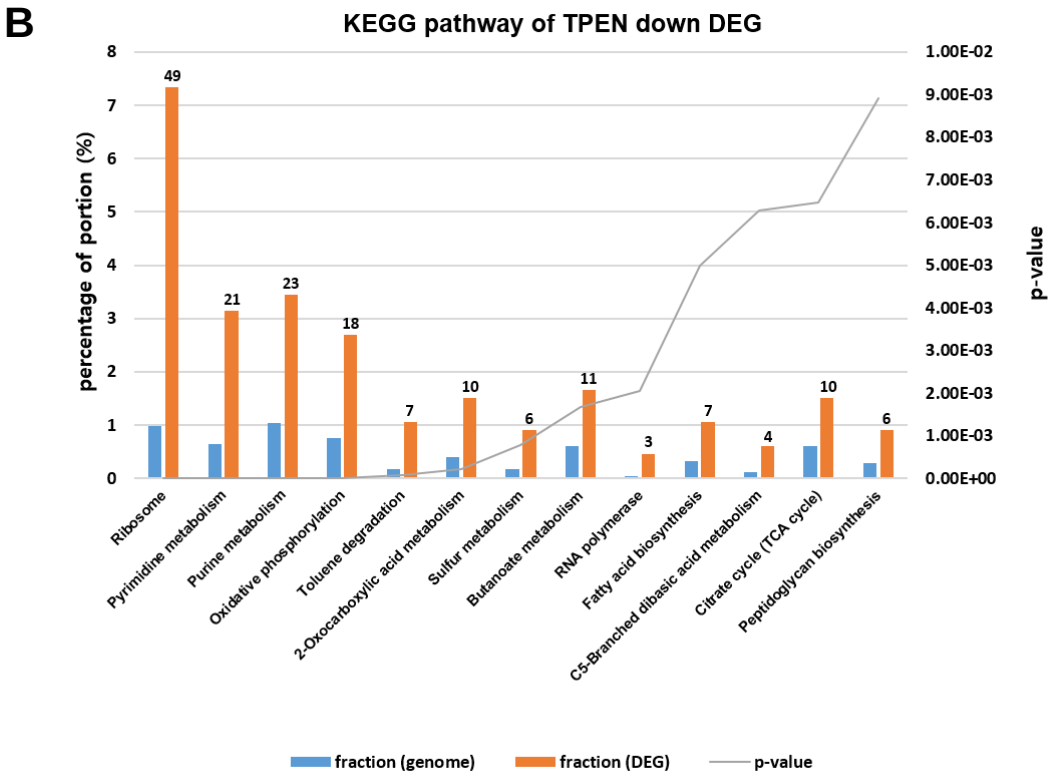
B
KEGG pathway of TPEN down DEG
percentage of portion (%)
p-value
0
1
2
3
4
5
6
7
8
0.00E+00
1.00E-03
2.00E-03
3.00E-03
4.00E-03
5.00E-03
6.00E-03
7.00E-03
8.00E-03
9.00E-03
1.00E-02
49
21
23
18
7
10
6
11
3
7
4
10
6
Ribosome
Pyrimidine metabolism
Purine metabolism
Oxidative phosphorylation
Toluene degradation
2-Oxocarboxylic acid metabolism
Sulfur metabolism
Butanoate metabolism
RNA polymerase
Fatty acid biosynthesis
C5-Branched dibasic acid metabolism
Citrate cycle (TCA cycle)
Peptidoglycan biosynthesis
fraction (genome)
fraction (DEG)
p-value

A handful of its target genes that encode zinc-uptake and mobilization systems have been identified to be negatively regulated by zinc-bound Zur.

I divided two class of the inducted genes regulated by solely Zur or Zur and co-regulator. Class I is the genes regulated by Zur and Class II is the genes regulated by Zur and co-regulator(s). This classification was decided with RNA-sequencing and ChIP-sequencing analysis and experimental result until now. Class I genes were already known including as *znuA, znuB2/C2, rpmF, rpmG/B*, SCO7676, 7681/7682 in a gene cluster for synthesizing enterobactin-type zincophore and *zitB*. Class II genes were decided with up-regulation genes treated TPEN from RNA sequencing and Zur binding from ChIP-sequencing. Metal depletion is sensed by various regulators such as fur family. But, I could not confirm the co-regulators because of too many and complicated. Class II genes are composed of SCO1121 is annotated; secreted protein, SCO1421; hypothetical protein, SCO1540; hypothetical protein, SCO1793; Spo0M-homologous protein, SCO1966; exonuclease ABC subunit B, SCO2310; integral membrane efflux protein, SCO3538; hypothetical protein, SCO3761; hypothetical protein, SCO4200; hypothetical protein, SCO4256; hydrolytic protein, SCO4258; hydrolytic protein, SCO4798; peptidase, SCO5476; oligopeptide transport membrane protein, SCO5656 hypothetical protein, SCO6644; solute binding protein. I confirmed the Class II genes sensed various metal after metal depletion by S1 mapping (Fig. III-31.). Basically, all Class II genes were inducted by metal depletion. And I checked the expression change of the genes after treating various metals.

Fig. III-31. Transcripts from class II genes were analyzed by S1 mapping.

Exponentially grown wild type (WT) and *Δzur* mutant cells were treated with 20 μM TPEN for 50 min and then various metal salts ($ZnSO_4$, $FeSO_4$, $CuSO_4$, $MnCl_2$ and NiSO) at 50 μM for 20 min before cell harvest. The amount of gene transcript was quantified and presented in relative value with that in non-treated sample as 1.0.

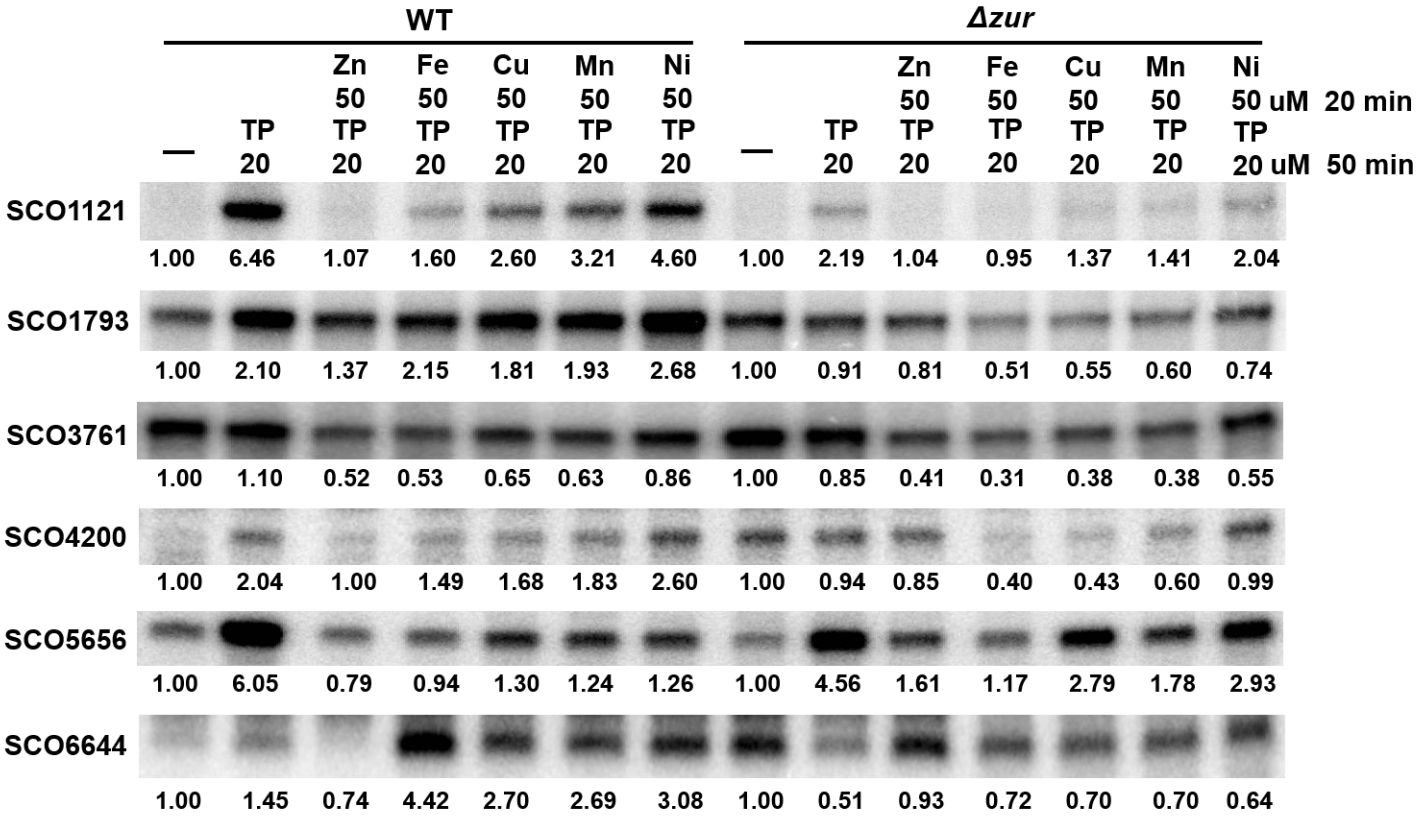
WT
Δzur
— TP 20 Zn 50 TP 20 Fe 50 TP 20 Cu 50 TP 20 Mn 50 TP 20 Ni 50 TP 20
— TP 20 Zn 50 TP 20 Fe 50 TP 20 Cu 50 TP 20 Mn 50 TP 20 Ni 50 uM TP 20 uM 20 min 50 min
SCO1121
1.00 6.46 1.07 1.60 2.60 3.21 4.60 1.00 2.19 1.04 0.95 1.37 1.41 2.04
SCO1793
1.00 2.10 1.37 2.15 1.81 1.93 2.68 1.00 0.91 0.81 0.51 0.55 0.60 0.74
SCO3761
1.00 1.10 0.52 0.53 0.65 0.63 0.86 1.00 0.85 0.41 0.31 0.38 0.38 0.55
SCO4200
1.00 2.04 1.00 1.49 1.68 1.83 2.60 1.00 0.94 0.85 0.40 0.43 0.60 0.99
SCO5656
1.00 6.05 0.79 0.94 1.30 1.24 1.26 1.00 4.56 1.61 1.17 2.79 1.78 2.93
SCO6644
1.00 1.45 0.74 4.42 2.70 2.69 3.08 1.00 0.51 0.93 0.72 0.70 0.70 0.64

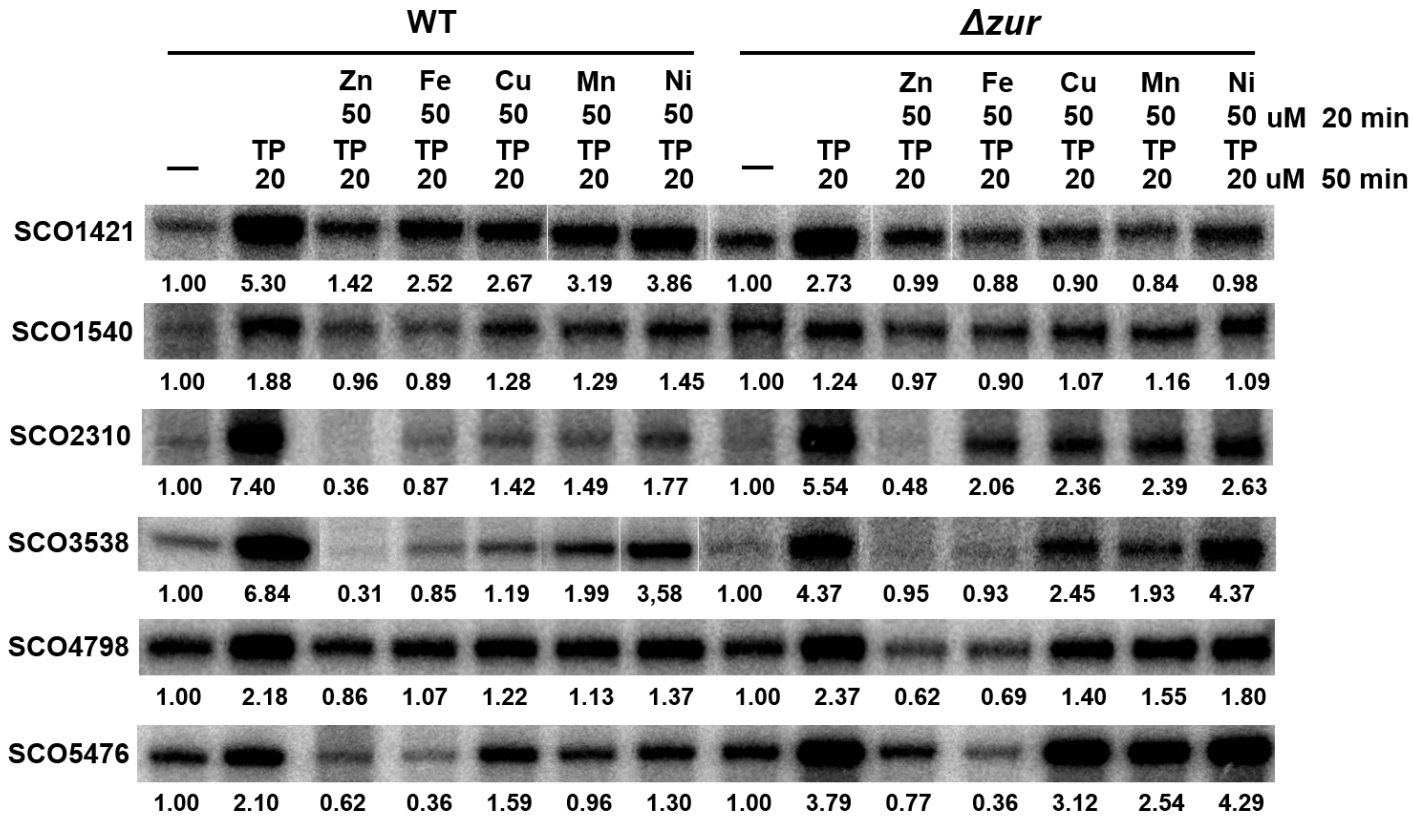
WT
Δzur
Zn 50
Fe 50
Cu 50
Mn 50
Ni 50
50 uM 20 min
— TP 20 TP 20 TP 20 TP 20 TP 20 TP 20
— TP 20 TP 20 TP 20 TP 20 TP 20 TP 20
20 uM 50 min
SCO1421
1.00 5.30 1.42 2.52 2.67 3.19 3.86 1.00 2.73 0.99 0.88 0.90 0.84 0.98
SCO1540
1.00 1.88 0.96 0.89 1.28 1.29 1.45 1.00 1.24 0.97 0.90 1.07 1.16 1.09
SCO2310
1.00 7.40 0.36 0.87 1.42 1.49 1.77 1.00 5.54 0.48 2.06 2.36 2.39 2.63
SCO3538
1.00 6.84 0.31 0.85 1.19 1.99 3,58 1.00 4.37 0.95 0.93 2.45 1.93 4.37
SCO4798
1.00 2.18 0.86 1.07 1.22 1.13 1.37 1.00 2.37 0.62 0.69 1.40 1.55 1.80
SCO5476
1.00 2.10 0.62 0.36 1.59 0.96 1.30 1.00 3.79 0.77 0.36 3.12 2.54 4.29

III.6. A comparison between ChIP-chip and ChIP-sequencing.

III.6.1. Possibility that Zur is nucleoid associated protein (NAP) through HU, H-NS and IHF comparison.

I wonder that the possibility that Zur is nucleoid associated protein (NAP). Because Zur bind genome wide on genome from ChIP-chip result. The total peaks that present Zur binding region are about 17,200 peaks (Fig. III-2A.). Our result shows the amount of Zur is about 3.7 μM in a cell (Fig. III-1.). Follwed these results, Zur exists in large quantities as a transcription regulator in a cell. Also, this result informed that Zur has possibility of NAP of H-NS. However, the proteins known as NAP are present huge amount in a cell. For example, HU is a small (10 kDa) bacterial histone-like protein that resembles the eukaryotic Histone H2B. HU acts similarly to a histone by inducing negative supercoiling into circular DNA with the assistance of topoisomerase. The protein has been implicated in DNA replication, recombination, and repair. With an α-helical hydrophobic core and two positively charged β-ribbon arms, HU binds non-specifically to dsDNA with low affinity but binds to altered DNA—such as junctions, nicks, gaps, forks, and overhangs—with high affinity. There are about 28,000 Hus in the cell in the nomal condition and about 85,000 in the nutrient-rich condition.

Also, H-NS is about 15.6 kDa and assists in the regulation of bacterial transcription in bacteria by repressing and activating certain genes. H-NS binds to DNA with an intrinsic curvature. In *E. coli*, H-NS binds to a P1 promoter decreasing rRNA production during stationary and slow growth periods. RNA polymerase and H-NS DNA binding protein have overlapping binding sites; it is thought that H-NS regulates rRNA production by acting on the transcription initiation site. It has been found that H-NS and RNA polymerase both bind to

the P1 promoter and form a complex. When H-NS is bound with RNA polymerase to the promoter region, there are structural differences in the DNA that are accessible. It has also been found that H-NS can affect translation as well by binding to mRNA and causing its degradation. There are about 28,000 H-NSs in the cell in the nomal condition and about 85,000 in the nutrient-rich condition.

And, Integration host factor, IHF, is a nucleoid-associated protein that is required for recombination between the λ phage and *E.coli* DNA. It is a 20 kDa heterodimer, composed of α and β subunits that binds to specific sequences and bends specific sites on λ DNA. The β arms of IHF have Proline residues that help stabilize the DNA kinks. These kinks can help compact DNA and allow for supercoiling. The mode of binding to DNA depends on environmental factors, such as the concentration of ions present. With a high concentration of KCl, there is weak DNA bending. It has been found that sharper DNA bending occurs when the concentration of KCl is less than 100 mM, and IHF is not concentrated. There are about 10,000 H-NSs in the cell in the nomal condition and about 15,000 in the nutrient-rich condition. Overall, based on the above comparison, it is unlikely that Zur would be NAP.

III.6.2. A comparison between ChIP-chip and ChIP-sequencing.

I perfomed ChIP-sequencing to get better quality results compared to ChIP-chip (Fig. III-27.). The number of peaks is all 370. This means that the ChIP-sequencing is more specific and quality than ChIP-chip. I performed the comparison with 1% peaks of ChIP-chip and whole peaks of ChIP-sequencing (Fig. III-32.). 172 peaks of ChIP-chip and 370 peaks of ChIP-sequencing venn diagram show 140 over-rapped peaks which include known Zur target genes. The predicted Zur binding motif of ChIP-chip and ChIP-sequencing are similar.

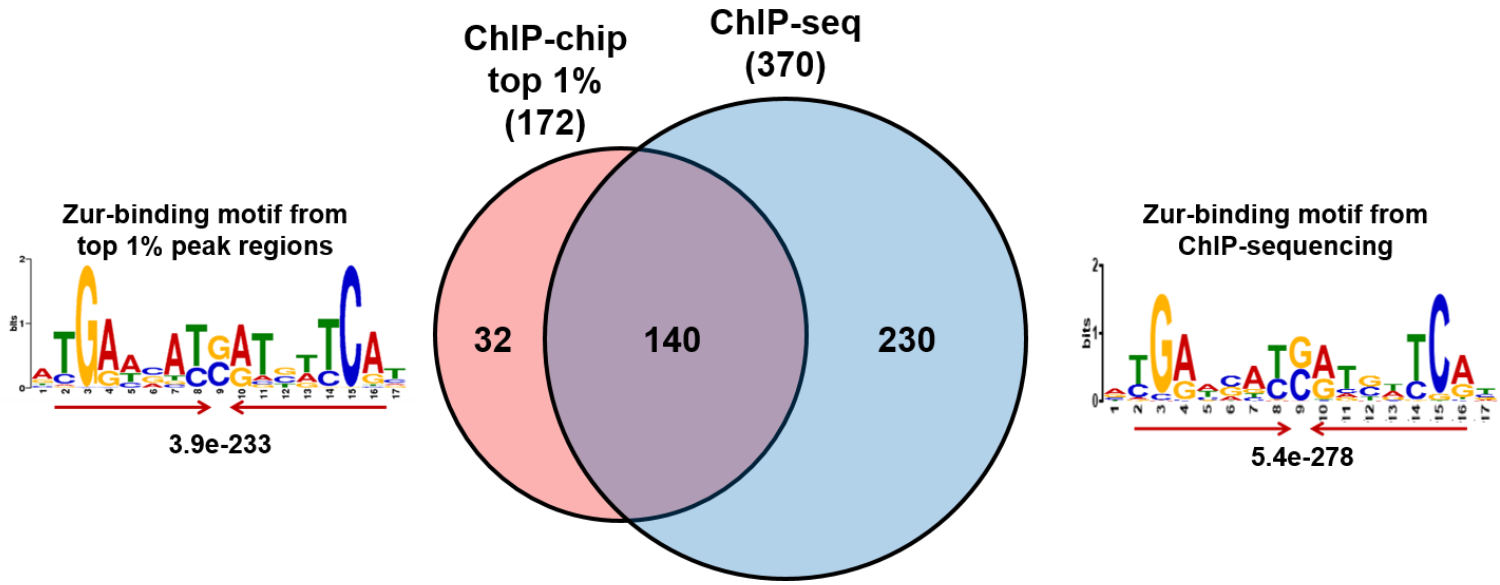

Fig. III-32. Venn diagram of top 1% ChIP-chip peaks and whole peaks of ChIP-sequencing.

The pink circle represents the number of 1% peaks of ChIP-chip and the blue circle represents the number of peaks of ChIP-sequencing. The numbers show the numbers of peaks of the section.

CHAPTER IV

DISCUSSION

Cation diffusion facilitator (CDF) family transporters are distributed across three domains of life, and contribute to metal homeostasis by extruding divalent metal ions (Cubillas *et al*., 2013; Paulsen and Saier, 1997). In this study I found that the synthesis of ZitB, which shows close sequence similarity to *E. coli* ZitB and CzcDs from various bacteria (clade IX of the Zn transporter subfamily) (Cubillas *et al*., 2013), is induced by zinc in a Zur-dependent manner in *S. coelicolor*. The cellular phenotype of ZitB overproduction indicated that ZitB extrudes zinc, as well as nickel and cobalt, but not copper (Fig. III-7.). The amount of total zinc in *S. coelicolor* cells grown in YEME medium was estimated to be about 2.1 mM (Fig. III-7.). Considering the amount of zinc in the medium (1.33 μM), this reveals more than 1000-fold zinc concentration in the cell. This level is higher than the "zinc quota" of *E. coli*, yeast, and some mammalian cells, estimated to be 0.1-0.5 mM (Eide, 2006) Therefore, *S. coelicolor* cells growing in YEME medium may already contain surplus zinc to be extruded through exporters such as ZitB.

The finding that a single metalloregulator regulates both the uptake and export genes, in response to the availability of the specific metal, is unprecedented. In all bacterial systems reported so far, regulators for the uptake and export genes are different, with different metal-binding affinities (Reyes-Caballero *et al*., 2011), except in *Xanthomonas campestris*, where Zur was reported to activate a putative metal-exporter gene[7]. Zur is the most prevalent regulator for zinc uptake genes in bacteria, except in *Streptococcus pneumoniae* where AdcR, a MarR family repressor, regulates zinc uptake genes (Reyes-Caballero H, *et al.,* 2010). In *E. coli, B. subtilis,* and *S. coelicolor*, Zur responds to zinc at fM range (Outten and O'Halloran, 2001; Shin *et al*., 2011; Ma *et al*., 2011). As judged from the affinity of the specific metal that allosterically changes DNA-binding activity of the regulator (metal-responsiveness), the efflux regulators respond to zinc at

femtomolar (ZntR in *E. coli* (Outten and O'Halloran, 2001)), picomolar (CzrA in *S. aureus* (Pennella *et al*., 2006)), and up to nM ranges (AztR in Anabaena PCC7120 (Liu *et al*., 2005)). In my study, I demonstrated that Zur responds to (binds) zinc at sub-fM range to repress zinc uptake genes fully and activate the zinc export gene (*zitB*) partially (phase I activation). Zur further responds to µM zinc, resulting in oligomeric Zur binding to the *zitB* promoter upstream region, and activates *zitB* expression to the full level. This is an ingenious way of utilizing a single metalloregulator over a wide concentration range of the specific cognate metal. The Zur-box sequence is conserved upstream of the *zitB* homologues in other actinomycetes. Therefore, it is likely that similar zinc homeostatic regulation may occur in other actinobacteria such as *Mycobacterium* and *Corynebacterium* spp. Sequences upstream from the Zur-box up to -138 nt did not show any pronounced conserved feature among these bacteria. Further systematic studies to identify as yet uncharacterized sequence feature within the Zur-box upstream region of *zitB* are in need.

There are numerous examples of DNA-binding proteins that can act both as a repressor and an activator, depending on its binding site relative to the promoter elements. Among metalloregulators, Fur and Zur are known to play a dual role (Delany *et al*., 2004; Pawlik *et al*., 2012; Troxell and Hassan, 2013). Even though Fur acts mostly as a repressor of its target genes, it is reported to activate some genes by binding to the promoter upstream region in *Neisseria meningitides*, *Helicobacter pylori*, and *Salmonella enterica*. In the Fur-activated genes, Fur binds to the Fur-box sequence located about 100 to 200 bp upstream of the transcription start site. This far distance is not suitable to allow a direct contact between an activator and RNA polymerase on linear DNA, without a looping mechanism. Oligomeric Fur binding at high protein concentrations (in the presence of Mn^{2+}) *in vitro* has been proposed to repress aerobactin genes (de

Lorenzo *et al*., 1987; Escolar *et al*., 2000) and the *sodA* gene for MnSOD (Tardat and Touati, 1993), and to activate the *hilD* gene encoding T3SS virulence factor by binding at -147 ~ -219 upstream from TSS (Teixido *et al*., 2011). The physiological relevance of oligomeric Fur binding at high protein concentrations is not certain. Whereas the dimeric Fur can oligomerize both in the presence and absence of DNA (Frechon and Le Cam, 1994; Le Cam *et al*., 1994), Streptomyces dimeric Zur in our study did not form oligomers in the absence of DNA. In the case of *X. campestris* Zur (Huang *et al*., 2008) the binding site upstream of the putative efflux gene showed a different sequence motif distant from the Zur-box consensus found in zinc-uptake genes. In *Neisseria meningitidis,* Zur was proposed to activate two genes encoding putative alcohol dehydrogenase and NosR-related protein, respectively, based on transcriptome analysis (Pawlik *et al*., 2012). Meningococcal Zur was found to bind to the Zur-box sequence located at 140 nt upstream from the translational start codon of the putative alcohol dehydrogenase gene, where the binding position relative to the promoter elements is unknown (Pawlik *et al*., 2012). The close proximity of the Zur-box in the *zitB* promoter of *S. coelicolor*, spaced 8 nt upstream from the -35 region, suggests that Zur may contact RNA polymerase to activate transcription. The possibility of the activator to recruit RNA polymerase via alpha subunits (class I activation mechanism) or to contact the domain 4 of sigma factor (class II activation), as best demonstrated for CRP/CAP in *E. coli*, can be considered (Browning and Busby, 2016).

What could be the mode of Zur binding on the *zitB* promoter in phase I and phase II activations? Previous studies have focused on the high affinity zinc binding to Zur, relevant under low zinc conditions. Binding of a zinc to the "structural" site enable the formation of dimeric Zur (Zn_2-Zur_2) that lack DNA-binding activity. In *S. coelicolor* Zur, additional zinc ions occupy two "regulatory"

sites with sub-femtomolar sensitivities, transforming it to DNA binding-competent forms (Zn_4-Zur_2, Zn_6-Zur_2), and enabling graded expression of its target genes in response to sub-femtomolar range of "free" zinc (Shin *et al*., 2011). In *B. subtilis,* sequential binding of zinc to one "regulatory" site in Zur is proposed to transforms it to partially (Zn_3-Zur_2) or fully active (Zn_4-Zur_2) conformation, also enabling graded gene expression of its target genes (Ma *et al*., 2011; Shin and Helmann, 2016).

In phase I activation mode, where free zinc is present at femtomolar range, the three high-affinity zinc-binding sites (one structural and two regulatory) of *S. coelicolor* Zur will be fully occupied by zinc, and the functional Zur will bind to both *znuA* and *zitB* promoter sites as a dimer, fully repressing *znuA* and partially activating *zitB* expression (phase I; Fig. III-8, Fig. III-10.). The binding mode is likely to be the Zur_2-DNA complex observed on the 25 bp *zitB* DNA probe, or on longer probes under low zinc conditions (Fig. III-16.). A molecular model of the Zur_2-DNA complex is presented in Fig. IV-1A. As the level of zinc increases to micromolar range, oligomeric Zur binding occurs. Formation of tetrameric Zur-DNA complex was captured on the 33 bp DNA probe, whose molecular structure could be modelled as in Fig. IV-1B. In this tetrameric Zur binding model, the specific DNA interaction appears different from the mode for dimeric Zur binding. On longer *zitB* probes at micromolar zinc, formation of hexameric or octameric Zur bindings were captured by EMSA with limited amount of Zur. From EMSA, the formation of super-retarded complex with higher concentration of Zur indicates the possibility of multimerization of Zur, with or without DNA conformational change, to underlie the activation mechanism of phase II. A schematic mode of gene activation was presented in Fig. IV-1C. Considering the requirement of high zinc concentrations for Zur multimerization, Zur might have additional zinc binding sites with low zinc

avidity and the occupation of those sites at high zinc concentrations might favor Zur multimerization.

In this study, I revealed a novel way of a specific metal to change the binding mode and activity of its cognate metalloregulator, hence regulating its homeostatic genes ranging from uptake to efflux functions. Whether and how, if any, the low-affinity zinc binding at micromolar concentrations transforms the structure of Zur to facilitate its cooperative binding to DNA as oligomers is a challenging question to solve in the future. Identification of the cryptic sequence feature that facilitates upward oligomeric binding of Zur in the *zitB* promoter is yet another interesting question to solve in the near future.

Fig. IV-1. A scheme for zinc-dependent changes in the binding mode of Zur on *zitB* DNA.

(**A**) A structural model for the Zur_2-DNA (25 bp) complex and (**B**) a model for Zur_4 -DNA (33 bp) complex. The blue regions in DNA represent the 15 bp Zur-box motif. The two figures were prepared with the same DNA orientation, to show the distinct binding modes of dimeric vs. tetrameric Zur.

(**C**) A schematic model for the change in the binding mode of Zur on *zitB* promoter region as zinc level increases. The dimeric Zur with three high affinity zinc-binding sites occupied by zinc at femtomolar range $(Zn_3Zur)_2$ was indicated in red, whereas the oligomers of dimeric Zur with possibly more zinc binding at low-affinity site(s) were presented in purple.

A

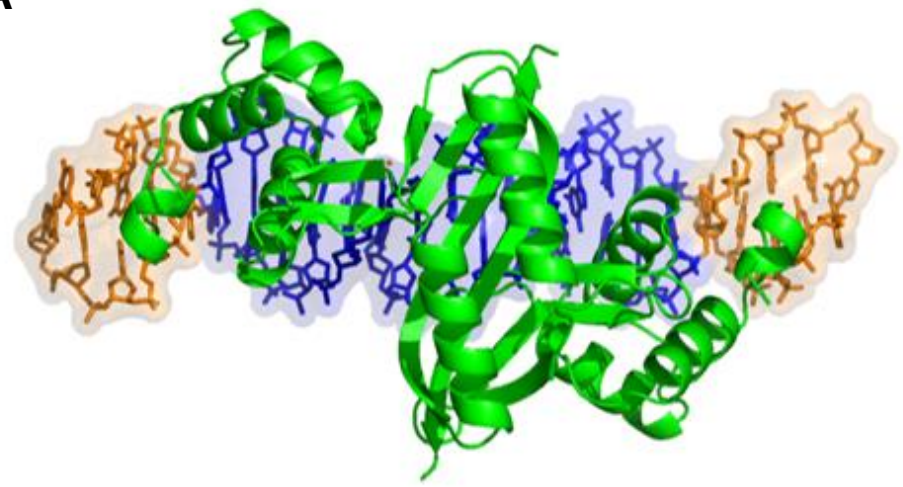

B

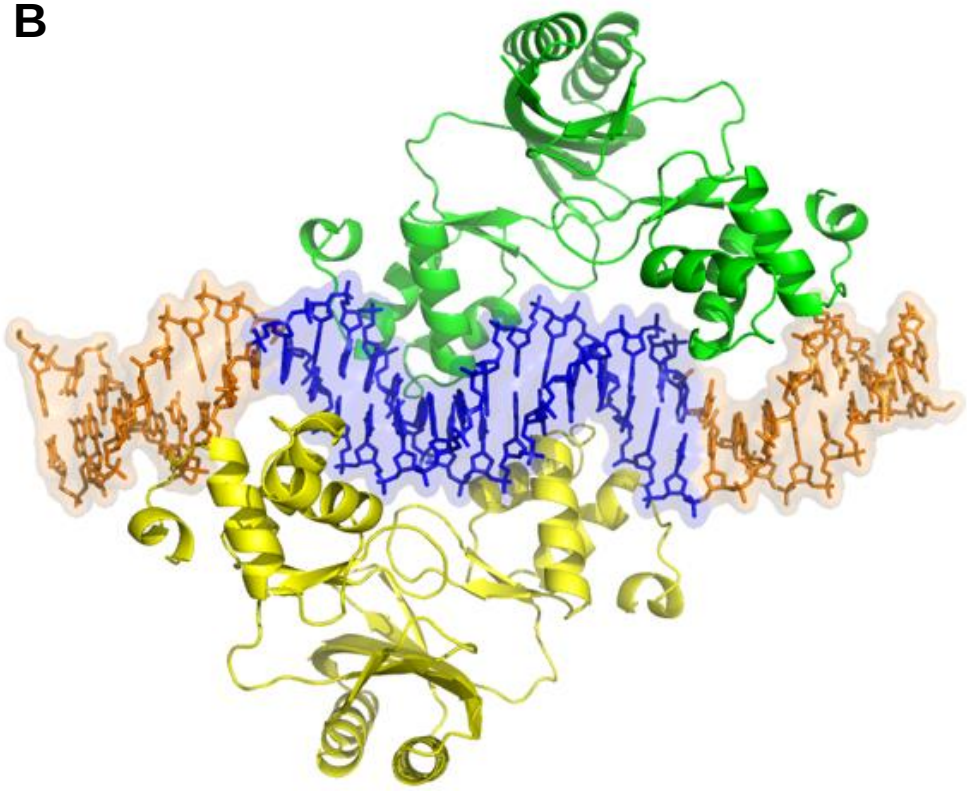

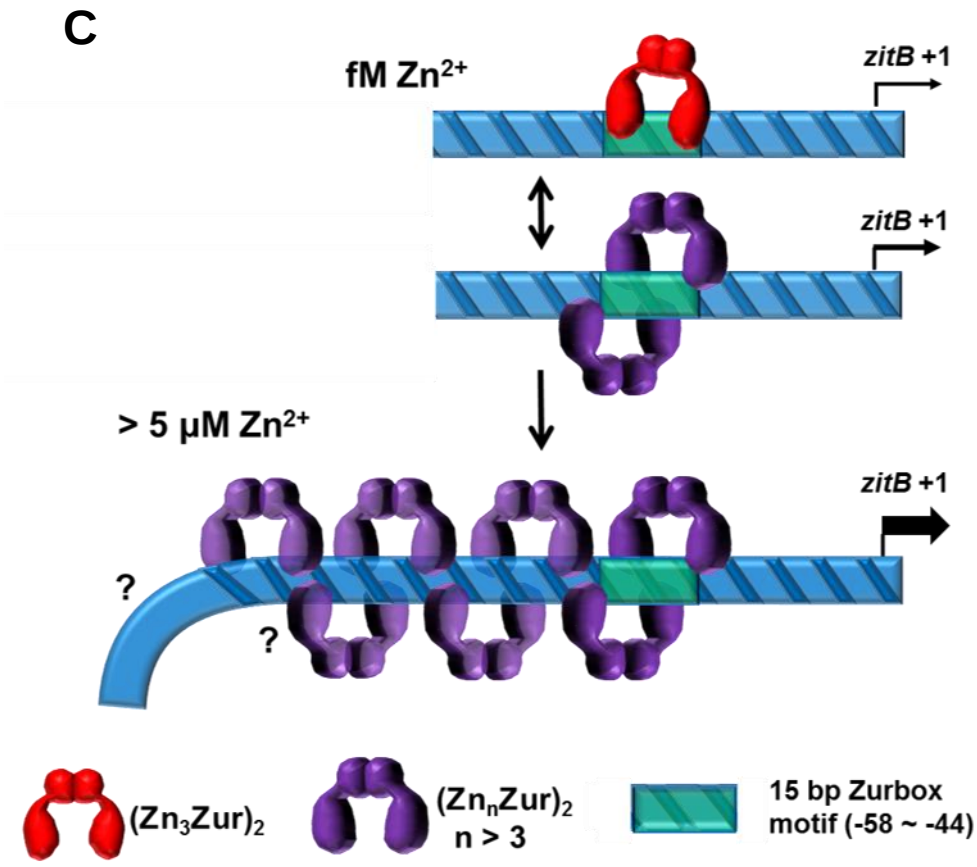
C
fM Zn2+
zitB +1
zitB +1
> 5 μM Zn2+
zitB +1
?
?
(Zn3Zur)2
(ZnnZur)2
n > 3
15 bp Zurbox
motif (-58 ~ -44)

REFERENCES

Aagaard, A. & P. Brzezinski, (2001) Zinc ions inhibit oxidation of cytochrome c oxidase by oxygen. *FEBS Lett* **494**: 157-160.

Ahn, B. E., J. Cha, E. J. Lee, A. R. Han, C. J. Thompson & J. H. Roe, (2006) Nur, a nickel-responsive regulator of the Fur family, regulates superoxide dismutases and nickel transport in *Streptomyces coelicolor*. *Mol Microbiol* **59**: 1848-1858.

Akanuma, G., H. Nanamiya, Y. Natori, N. Nomura & F. Kawamura, (2006) Liberation of zinc-containing L31 (RpmE) from ribosomes by its paralogous gene product, YtiA, in *Bacillus subtilis*. *J Bacteriol* **188**: 2715-2720.

Alberts, I. L., K. Nadassy & S. J. Wodak, (1998) Analysis of zinc binding sites in protein crystal structures. *Protein Sci* **7**: 1700-1716.

Almiron, M., A. J. Link, D. Furlong & R. Kolter, (1992) A novel DNA-binding protein with regulatory and protective roles in starved *Escherichia coli*. *Genes Dev* **6**: 2646-2654.

Bae, J. B., J. H. Park, M. Y. Hahn, M. S. Kim & J. H. Roe, (2004) Redox-dependent changes in RsrA, an anti-sigma factor in *Streptomyces coelicolor*: zinc release and disulfide bond formation. *J Mol Biol* **335**: 425-435.

Bagg, A. & J. B. Neilands, (1987a) Ferric uptake regulation protein acts as a repressor, employing iron (II) as a cofactor to bind the operator of an iron transport operon in *Escherichia coli*. *Biochemistry* **26**: 5471-5477.

Bagg, A. & J. B. Neilands, (1987b) Molecular mechanism of regulation of siderophore-mediated iron assimilation. *Microbiol Rev* **51**: 509-518.

Bellini, P. & A. M. Hemmings, (2006) In vitro characterization of a bacterial manganese uptake regulator of the fur superfamily. *Biochemistry* **45**: 2686-2698.

Bentley, S. D., K. F. Chater, A. M. Cerdeno-Tarraga, G. L. Challis, N. R. Thomson, K. D. James, D. E. Harris, M. A. Quail, H. Kieser, D. Harper, A. Bateman, S. Brown, G. Chandra, C. W. Chen, M. Collins, A. Cronin, A. Fraser, A. Goble, J. Hidalgo, T. Hornsby, S. Howarth, C. H. Huang, T. Kieser, L. Larke, L. Murphy, K. Oliver, S. O'Neil, E. Rabbinowitsch, M. A. Rajandream, K. Rutherford, S. Rutter, K. Seeger, D. Saunders, S. Sharp, R. Squares, S. Squares, K. Taylor, T. Warren, A. Wietzorrek, J. Woodward, B. G. Barrell, J. Parkhill & D. A. Hopwood, (2002) Complete genome sequence of the model actinomycete *Streptomyces coelicolor* A3(2). *Nature* **417**: 141-147.

Braun, V., (2003) Iron uptake by *Escherichia coli*. *Front Biosci* **8**: s1409-1421.

Bray, T. M. & W. J. Bettger, (1990) The physiological role of zinc as an antioxidant. *Free Radic Biol Med* **8**: 281-291.

Bsat, N. & J. D. Helmann, (1999) Interaction of *Bacillus subtilis* Fur (ferric uptake repressor) with the *dhb* operator in vitro and in vivo. *J Bacteriol* **181**: 4299-4307.

Bsat, N., A. Herbig, L. Casillas-Martinez, P. Setlow & J. D. Helmann, (1998) *Bacillus subtilis* contains multiple Fur homologues: identification of the iron uptake (Fur) and peroxide regulon (PerR) repressors. *Mol Microbiol* **29**: 189-198.

Campbell, E. A., R. Greenwell, J. R. Anthony, S. Wang, L. Lim, K. Das, H. J.

Sofia, T. J. Donohue & S. A. Darst, (2007) A conserved structural module regulates transcriptional responses to diverse stress signals in bacteria. *Mol Cell* **27**: 793-805.

Canneva, F., M. Branzoni, G. Riccardi, R. Provvedi & A. Milano, (2005) Rv2358 and FurB: two transcriptional regulators from *Mycobacterium tuberculosis* which respond to zinc. *J Bacteriol* **187**: 5837-5840.

Carmel-Harel, O. & G. Storz, (2000) Roles of the glutathione- and thioredoxin-dependent reduction systems in the *Escherichia coli* and *Saccharomyces cerevisiae* responses to oxidative stress. *Annu Rev Microbiol* **54**: 439-461.

Chater, K. F. (1984) Morphological and physiological differentiation in Streptomyces. In Microbial Development (Ed. R. Losick and L. Shapiro). Cold Spring Harbor Laboratory Press. pp89-116.

Chen, L., L. Keramati & J. D. Helmann, (1995) Coordinate regulation of *Bacillus subtilis* peroxide stress genes by hydrogen peroxide and metal ions. *Proc Natl Acad Sci U S A* **92**: 8190-8194.

Chung, H. J., J. H. Choi, E. J. Kim, Y. H. Cho & J. H. Roe, (1999) Negative regulation of the gene for Fe-containing superoxide dismutase by an Ni-responsive factor in *Streptomyces coelicolor*. *J Bacteriol* **181**: 7381-7384.

Coleman, J. E., (1998) Zinc enzymes. *Curr Opin Chem Biol* **2**: 222-234.

Culotta, V. C., (2000) Superoxide dismutase, oxidative stress, and cell metabolism. *Curr Top Cell Regul* **36**: 117-132.

Datsenko, K. A. & B. L. Wanner, (2000) One-step inactivation of chromosomal

genes in *Escherichia coli* K-12 using PCR products. *Proc Natl Acad Sci U S A* **97**: 6640-6645.

Delany, I., R. Rappuoli & V. Scarlato, (2004) Fur functions as an activator and as a repressor of putative virulence genes in *Neisseria meningitidis*. *Mol Microbiol* **52**: 1081-1090.

Delany, I., G. Spohn, R. Rappuoli & V. Scarlato, (2001) The Fur repressor controls transcription of iron-activated and -repressed genes in *Helicobacter pylori*. *Mol Microbiol* **42**: 1297-1309.

Delany, I., G. Spohn, R. Rappuoli & V. Scarlato, (2003) An anti-repression Fur operator upstream of the promoter is required for iron-mediated transcriptional autoregulation in *Helicobacter pylori*. *Mol Microbiol* **50**: 1329-1338.

Demain, A. L., Aharonowitz, Y., and Martin, J. -F. (1983) Metabolic control of secondary biosynthetic pathways. In Vining, L.C. (Ed.), Biochemistry and Genetic Regulation of Commercially Important Antibiotics. Addison-Wesley, London, pp. 49-72.

Diaz-Mireles, E., M. Wexler, G. Sawers, D. Bellini, J. D. Todd & A. W. Johnston, (2004) The Fur-like protein Mur of *Rhizobium leguminosarum* is a Mn(2+)-responsive transcriptional regulator. *Microbiology* **150**: 1447-1456.

Diaz-Mireles, E., M. Wexler, J. D. Todd, D. Bellini, A. W. Johnston & R. G. Sawers, (2005) The manganese-responsive repressor Mur of *Rhizobium leguminosarum* is a member of the Fur-superfamily that recognizes an unusual operator sequence. *Microbiology* **151**: 4071-4078.

Escolar, L., J. Perez-Martin & V. de Lorenzo, (1998) Binding of the fur (ferric uptake regulator) repressor of *Escherichia coli* to arrays of the GATAAT sequence. *J Mol Biol* **283**: 537-547.

Falchuk, K. H., (1993) Zinc in developmental biology: the role of metal dependent transcription regulation. *Prog Clin Biol Res* **380**: 91-111.

Friedman, Y. E. & M. R. O'Brian, (2004) The ferric uptake regulator (Fur) protein from *Bradyrhizobium japonicum* is an iron-responsive transcriptional repressor in vitro. *J Biol Chem* **279**: 32100-32105.

Fuangthong, M. & J. D. Helmann, (2003) Recognition of DNA by three ferric uptake regulator (Fur) homologs in *Bacillus subtilis*. *J Bacteriol* **185**: 6348-6357.

Fuangthong, M., A. F. Herbig, N. Bsat & J. D. Helmann, (2002) Regulation of the *Bacillus subtilis* fur and perR genes by PerR: not all members of the PerR regulon are peroxide inducible. *J Bacteriol* **184**: 3276-3286.

Gaballa, A. & J. D. Helmann, (1998) Identification of a zinc-specific metalloregulatory protein, Zur, controlling zinc transport operons in *Bacillus subtilis*. *J Bacteriol* **180**: 5815-5821.

Gaballa, A., T. Wang, R. W. Ye & J. D. Helmann, (2002) Functional analysis of the *Bacillus subtilis* Zur regulon. *J Bacteriol* **184**: 6508-6514.

Gilbert, H. F., (1990) Molecular and cellular aspects of thiol-disulfide exchange. *Adv Enzymol Relat Areas Mol Biol* **63**: 69-172.

Gralnick, J. & D. Downs, (2001) Protection from superoxide damage associated with an increased level of the YggX protein in *Salmonella enterica*. *Proc Natl*

Acad Sci U S A **98**: 8030-8035.

Guedon, E. & J. D. Helmann, (2003) Origins of metal ion selectivity in the DtxR/MntR family of metalloregulators. *Mol Microbiol* **48**: 495-506.

Gust, B., G. L. Challis, K. Fowler, T. Kieser & K. F. Chater, (2003) PCR-targeted Streptomyces gene replacement identifies a protein domain needed for biosynthesis of the sesquiterpene soil odor geosmin. *Proc Natl Acad Sci U S A* **100**: 1541-1546.

Hahn, J. S., S. Y. Oh, K. F. Chater, Y. H. Cho & J. H. Roe, (2000a) H2O2-sensitive fur-like repressor CatR regulating the major catalase gene in *Streptomyces coelicolor*. *J Biol Chem* **275**: 38254-38260.

Hahn, J. S., S. Y. Oh & J. H. Roe, (2000b) Regulation of the *furA* and *catC* operon, encoding a ferric uptake regulator homologue and catalase-peroxidase, respectively, in *Streptomyces coelicolor* A3(2). *J Bacteriol* **182**: 3767-3774.

Hamza, I., S. Chauhan, R. Hassett & M. R. O'Brian, (1998) The bacterial irr protein is required for coordination of heme biosynthesis with iron availability. *J Biol Chem* **273**: 21669-21674.

Hanahan, D., (1983) Studies on transformation of *Escherichia coli* with plasmids. *J Mol Biol* **166**: 557-580.

Hantke, K., (1981) Regulation of ferric iron transport in *Escherichia coli* K12: isolation of a constitutive mutant. *Mol Gen Genet* **182**: 288-292.

Hantke, K., (1987) Selection procedure for deregulated iron transport mutants (fur) in *Escherichia coli* K 12: fur not only affects iron metabolism. *Mol Gen Genet*

210: 135-139.

Hantke, K., (2001) Iron and metal regulation in bacteria. *Curr Opin Microbiol* **4**: 172-177.

Harding, M. M., (2002) Metal-ligand geometry relevant to proteins and in proteins: sodium and potassium. *Acta Crystallogr D Biol Crystallogr* **58**: 872-874.

Hayashi, K., T. Ohsawa, K. Kobayashi, N. Ogasawara & M. Ogura, (2005) The H2O2 stress-responsive regulator PerR positively regulates srfA expression in *Bacillus subtilis*. *J Bacteriol* **187**: 6659-6667.

Herbig, A. F. & J. D. Helmann, (2001) Roles of metal ions and hydrogen peroxide in modulating the interaction of the *Bacillus subtilis* PerR peroxide regulon repressor with operator DNA. *Mol Microbiol* **41**: 849-859.

Hopwood, D. A., Bibb, M. J., Chater, K. F., Kieser, T., Bruton, C. J., Kieser, H. M., Lydiate, D. J., Smith, C. P., Ward, J. M., and Schrempf, H. (1985) Genetic manipulation of Streptomyces: a laboratory manual. John Innes Foundation, Norwich, Enlgand.

Horsburgh, M. J., M. O. Clements, H. Crossley, E. Ingham & S. J. Foster, (2001) PerR controls oxidative stress resistance and iron storage proteins and is required for virulence in *Staphylococcus aureus*. *Infect Immun* **69**: 3744-3754.

Imlay, J. A., S. M. Chin & S. Linn, (1988) Toxic DNA damage by hydrogen peroxide through the Fenton reaction in vivo and in vitro. *Science* **240**: 640-642.

Imlay, J. A. & S. Linn, (1988) DNA damage and oxygen radical toxicity. *Science* **240**: 1302-1309.

Inaoka, T., Y. Matsumura & T. Tsuchido, (1999) SodA and manganese are essential for resistance to oxidative stress in growing and sporulating cells of *Bacillus subtilis*. *J Bacteriol* **181**: 1939-1943.

Kang, J. G., M. S. Paget, Y. J. Seok, M. Y. Hahn, J. B. Bae, J. S. Hahn, C. Kleanthous, M. J. Buttner & J. H. Roe, (1999) RsrA, an anti-sigma factor regulated by redox change. *EMBO J* **18**: 4292-4298.

Kelemen, G. H., G. L. Brown, J. Kormanec, L. Potuckova, K. F. Chater & M. J. Buttner, (1996) The positions of the sigma-factor genes, *whiG* and *sigF*, in the hierarchy controlling the development of spore chains in the aerial hyphae of *Streptomyces coelicolor* A3(2). *Mol Microbiol* **21**: 593-603.

Keyer, K. & J. A. Imlay, (1996) Superoxide accelerates DNA damage by elevating free-iron levels. *Proc Natl Acad Sci U S A* **93**: 13635-13640.

Kieser, T., M. J. Bibb, M. J. Buttner, K. F. Chater, and D. A. Hopwood. (2000) Practical Streptomyces Genetics. The John Innes Foundation., Norwich.

Kim, I. K., C. J. Lee, M. K. Kim, J. M. Kim, J. H. Kim, H. S. Yim, S. S. Cha & S. O. Kang, (2006) Crystal structure of the DNA-binding domain of BldD, a central regulator of aerial mycelium formation in *Streptomyces coelicolor* A3(2). *Mol Microbiol* **60**: 1179-1193.

Knott, G. D. (1979) MLAB-a mathematical modeling tool. Computer Programs in Biomedicine 10:271-280.

Laue, T. M., Shah, B, Ridgeway, T. M, and Pelleitier, S. L. (1992) Analytical Ultracentrifugation in Biochemistry and Polymer Science, pp 90-125. Royal Society of Chemistry, Cambridge.

Lee, C. J., H. S. Won, J. M. Kim, B. J. Lee & S. O. Kang, (2007) Molecular domain organization of BldD, an essential transcriptional regulator for developmental process of *Streptomyces coelicolor* A3(2). *Proteins* **68**: 344-352.

Lee, J. W. & J. D. Helmann, (2006) The PerR transcription factor senses H2O2 by metal-catalysed histidine oxidation. *Nature* **440**: 363-367.

Lee, J. W. & J. D. Helmann, (2007) Functional specialization within the Fur family of metalloregulators. *Biometals* **20**: 485-499.

Lewin, A. C., P. A. Doughty, L. Flegg, G. R. Moore & S. Spiro, (2002) The ferric uptake regulator of *Pseudomonas aeruginosa* has no essential cysteine residues and does not contain a structural zinc ion. *Microbiology* **148**: 2449-2456.

Li, W., A. R. Bottrill, M. J. Bibb, M. J. Buttner, M. S. Paget & C. Kleanthous, (2003) The Role of zinc in the disulphide stress-regulated anti-sigma factor RsrA from *Streptomyces coelicolor*. *J Mol Biol* **333**: 461-472.

Lin, S. J. & V. C. Culotta, (1996) Suppression of oxidative damage by *Saccharomyces cerevisiae* ATX2, which encodes a manganese-trafficking protein that localizes to Golgi-like vesicles. *Mol Cell Biol* **16**: 6303-6312.

Lucarelli, D., S. Russo, E. Garman, A. Milano, W. Meyer-Klaucke & E. Pohl, (2007) Crystal structure and function of the zinc uptake regulator FurB from *Mycobacterium tuberculosis*. *J Biol Chem* **282**: 9914-9922.

Maciag, A., E. Dainese, G. M. Rodriguez, A. Milano, R. Provvedi, M. R. Pasca, I. Smith, G. Palu, G. Riccardi & R. Manganelli, (2007) Global analysis of the *Mycobacterium tuberculosis* Zur (FurB) regulon. *J Bacteriol* **189**: 730-740.

MacNeil, D. J., K. M. Gewain, C. L. Ruby, G. Dezeny, P. H. Gibbons & T. MacNeil, (1992) Analysis of *Streptomyces avermitilis* genes required for avermectin biosynthesis utilizing a novel integration vector. *Gene* **111**: 61-68.

Makarova, K. S., V. A. Ponomarev & E. V. Koonin, (2001) Two C or not two C: recurrent disruption of Zn-ribbons, gene duplication, lineage-specific gene loss, and horizontal gene transfer in evolution of bacterial ribosomal proteins. *Genome Biol* **2**: RESEARCH 0033.

Masse, E. & S. Gottesman, (2002) A small RNA regulates the expression of genes involved in iron metabolism in *Escherichia coli*. *Proc Natl Acad Sci U S A* **99**: 4620-4625.

Matsumoto, A., Ishizuka, H., Beppu, T., and Horinouchi, S. (1995) Involvement of a small ORF downstream of the *afsR* gene in the regulation of secondary metabolism in *Streptomyces coelicolor* A3(2). Actinomycetologica 9: 37-43.

McCarthy, A. J. & S. T. Williams, (1992) Actinomycetes as agents of biodegradation in the environment--a review. *Gene* **115**: 189-192.

Merrick, M. J., (1976) A morphological and genetic mapping study of bald colony mutants of *Streptomyces coelicolor*. *J Gen Microbiol* **96**: 299-315.

Milano, A., M. Branzoni, F. Canneva, A. Profumo & G. Riccardi, (2004) The Mycobacterium tuberculosis Rv2358-furB operon is induced by zinc. *Res Microbiol* **155**: 192-200.

Mills, D. A., B. Schmidt, C. Hiser, E. Westley & S. Ferguson-Miller, (2002) Membrane potential-controlled inhibition of cytochrome c oxidase by zinc. *J Biol Chem* **277**: 14894-14901.

Mills, S. A. & M. A. Marletta, (2005) Metal binding characteristics and role of iron oxidation in the ferric uptake regulator from Escherichia coli. *Biochemistry* **44**: 13553-13559.

Nanamiya, H., G. Akanuma, Y. Natori, R. Murayama, S. Kosono, T. Kudo, K. Kobayashi, N. Ogasawara, S. M. Park, K. Ochi & F. Kawamura, (2004) Zinc is a key factor in controlling alternation of two types of L31 protein in the *Bacillus subtilis* ribosome. *Mol Microbiol* **52**: 273-283.

Nathan, C. & M. U. Shiloh, (2000) Reactive oxygen and nitrogen intermediates in the relationship between mammalian hosts and microbial pathogens. *Proc Natl Acad Sci U S A* **97**: 8841-8848.

Nodwell, J. R., K. McGovern & R. Losick, (1996) An oligopeptide permease responsible for the import of an extracellular signal governing aerial mycelium formation in *Streptomyces coelicolor*. *Mol Microbiol* **22**: 881-893.

Onaka, H., T. Nakagawa & S. Horinouchi, (1998) Involvement of two A-factor receptor homologues in *Streptomyces coelicolor* A3(2) in the regulation of secondary metabolism and morphogenesis. *Mol Microbiol* **28**: 743-753.

Outten, C. E. & T. V. O'Halloran, (2001) Femtomolar sensitivity of metalloregulatory proteins controlling zinc homeostasis. *Science* **292**: 2488-2492.

Outten, C. E., D. A. Tobin, J. E. Penner-Hahn & T. V. O'Halloran, (2001) Characterization of the metal receptor sites in *Escherichia coli* Zur, an ultrasensitive zinc(II) metalloregulatory protein. *Biochemistry* **40**: 10417-10423.

Paget, M. S., J. G. Kang, J. H. Roe & M. J. Buttner, (1998) sigmaR, an RNA

polymerase sigma factor that modulates expression of the thioredoxin system in response to oxidative stress in *Streptomyces coelicolor* A3(2). *EMBO J* **17**: 5776-5782.

Paget, M. S., V. Molle, G. Cohen, Y. Aharonowitz & M. J. Buttner, (2001) Defining the disulphide stress response in *Streptomyces coelicolor* A3(2): identification of the sigmaR regulon. *Mol Microbiol* **42**: 1007-1020.

Panina, E. M., A. A. Mironov & M. S. Gelfand, (2003) Comparative genomics of bacterial zinc regulons: enhanced ion transport, pathogenesis, and rearrangement of ribosomal proteins. *Proc Natl Acad Sci U S A* **100**: 9912-9917.

Patzer, S. I. & K. Hantke, (1998) The ZnuABC high-affinity zinc uptake system and its regulator Zur in *Escherichia coli*. *Mol Microbiol* **28**: 1199-1210.

Patzer, S. I. & K. Hantke, (2000) The zinc-responsive regulator Zur and its control of the znu gene cluster encoding the ZnuABC zinc uptake system in *Escherichia coli*. *J Biol Chem* **275**: 24321-24332.

Pohl, E., J. C. Haller, A. Mijovilovich, W. Meyer-Klaucke, E. Garman & M. L. Vasil, (2003) Architecture of a protein central to iron homeostasis: crystal structure and spectroscopic analysis of the ferric uptake regulator. *Mol Microbiol* **47**: 903-915.

Pope, M. K., B. Green & J. Westpheling, (1998) The *bldB* gene encodes a small protein required for morphogenesis, antibiotic production, and catabolite control in *Streptomyces coelicolor*. *J Bacteriol* **180**: 1556-1562.

Potuckova, L., G. H. Kelemen, K. C. Findlay, M. A. Lonetto, M. J. Buttner & J. Kormanec, (1995) A new RNA polymerase sigma factor, sigma F, is required

for the late stages of morphological differentiation in *Streptomyces spp*. *Mol Microbiol* **17**: 37-48.

Ratledge, C. & L. G. Dover, (2000) Iron metabolism in pathogenic bacteria. *Annu Rev Microbiol* **54**: 881-941.

Redenbach, M., H. M. Kieser, D. Denapaite, A. Eichner, J. Cullum, H. Kinashi & D. A. Hopwood, (1996) A set of ordered cosmids and a detailed genetic and physical map for the 8 Mb *Streptomyces coelicolor* A3(2) chromosome. *Mol Microbiol* **21**: 77-96.

Rudolph, G., H. Hennecke & H. M. Fischer, (2006a) Beyond the Fur paradigm: iron-controlled gene expression in rhizobia. *FEMS Microbiol Rev* **30**: 631-648.

Rudolph, G., G. Semini, F. Hauser, A. Lindemann, M. Friberg, H. Hennecke & H. M. Fischer, (2006b) The Iron control element, acting in positive and negative control of iron-regulated *Bradyrhizobium japonicum* genes, is a target for the Irr protein. *J Bacteriol* **188**: 733-744.

Sambrook, J., Fritsch, E. F., and Maniatis, T. (1989) Molecular cloning. A laboratory manual. 2nd ed. Cold Spring Harbor, New York: Cold Spring Harbor Laboratory Press.

Schwede, T., J. Kopp, N. Guex & M. C. Peitsch, (2003) SWISS-MODEL: An automated protein homology-modeling server. *Nucleic Acids Res* **31**: 3381-3385.

Shin JH, Oh SY, Kim SJ, Roe JH, (2007) The zinc-responsive regulator Zur controls a zinc uptake system and some ribosomal proteins in *Streptomyces coelicolor* A3(2). *J Bacteriol*. **189**:4070-7.

Smith, C. P. (1991) Methods for mapping transcribed DNA sequences. In Essential molecular biology, A practical approach, pp237-252. Edited by Brown, T. A. New York : Oxford University Press.

Stadtman, E. R., (1992) Protein oxidation and aging. *Science* **257**: 1220-1224.

Storz, G. & J. A. Imlay, (1999) Oxidative stress. *Curr Opin Microbiol* **2**: 188-194.

Studier, F. W., (1991) Use of bacteriophage T7 lysozyme to improve an inducible T7 expression system. *J Mol Biol* **219**: 37-44.

Tenhaken, R., A. Levine, L. F. Brisson, R. A. Dixon & C. Lamb, (1995) Function of the oxidative burst in hypersensitive disease resistance. *Proc Natl Acad Sci U S A* **92**: 4158-4163.

Tottey, S., D. R. Harvie & N. J. Robinson, (2005) Understanding how cells allocate metals using metal sensors and metallochaperones. *Acc Chem Res* **38**: 775-783.

Touati, D., M. Jacques, B. Tardat, L. Bouchard & S. Despied, (1995) Lethal oxidative damage and mutagenesis are generated by iron in delta fur mutants of *Escherichia coli*: protective role of superoxide dismutase. *J Bacteriol* **177**: 2305-2314.

Traore, D. A., A. El Ghazouani, S. Ilango, J. Dupuy, L. Jacquamet, J. L. Ferrer, C. Caux-Thang, V. Duarte & J. M. Latour, (2006) Crystal structure of the apo-PerR-Zn protein from *Bacillus subtilis*. *Mol Microbiol* **61**: 1211-1219.

Wilderman, P. J., N. A. Sowa, D. J. FitzGerald, P. C. FitzGerald, S. Gottesman, U. A. Ochsner & M. L. Vasil, (2004) Identification of tandem duplicate

regulatory small RNAs in *Pseudomonas aeruginosa* involved in iron homeostasis. *Proc Natl Acad Sci U S A* **101**: 9792-9797.

Yang, J., H. R. Panek & M. R. O'Brian, (2006a) Oxidative stress promotes degradation of the Irr protein to regulate haem biosynthesis in *Bradyrhizobium japonicum*. *Mol Microbiol* **60**: 209-218.

Yang, J., I. Sangwan, A. Lindemann, F. Hauser, H. Hennecke, H. M. Fischer & M. R. O'Brian, (2006b) *Bradyrhizobium japonicum* senses iron through the status of haem to regulate iron homeostasis and metabolism. *Mol Microbiol* **60**: 427-437.

Finney LA, O'Halloran TV, (2003) Transition metal speciation in the cell: insights from the chemistry of metal ion receptors. *Science* **300**, 931-936.

Reyes-Caballero H, Campanello GC, Giedroc DP, (2011) Metalloregulatory proteins: metal selectivity and allosteric switching. *Biophys Chem* **156**, 103-114.

Foster AW, Osman D, Robinson NJ, (2014) Metal preferences and metallation. *J Biol Chem* **289**, 28095-28103.

Waldron KJ, Rutherford JC, Ford D, Robinson NJ, (2009) Metalloproteins and metal sensing. *Nature* **460**, 823-830.

Giedroc DP, Arunkumar AI, (2007) Metal sensor proteins: nature's metalloregulated allosteric switches. *Dalton Trans*, 3107-3120.

Ma Z, Jacobsen FE, Giedroc DP, (2009) Coordination chemistry of bacterial metal transport and sensing. *Chem Rev* **109**, 4644-4681.

Huang DL, *et al*, (2008) The Zur of *Xanthomonas campestris* functions as a repressor and an activator of putative zinc homeostasis genes via recognizing two distinct sequences within its target promoters. *Nucleic acids research* **36**, 4295-4309.

Riccardi G, Milano A, Pasca MR, Nies DH, (2008) Genomic analysis of zinc homeostasis in *Mycobacterium tuberculosis*. *FEMS Microbiol Lett* **287**, 1-7.

Xu FF, Imlay JA, (2012) Silver(I), mercury(II), cadmium(II), and zinc(II) target exposed enzymic iron-sulfur clusters when they toxify *Escherichia coli*. *Appl Environ Microbiol* **78**, 3614-3621.

Braymer JJ, Giedroc DP, (2014) Recent developments in copper and zinc homeostasis in bacterial pathogens. *Curr Opin Chem Biol* **19**, 59-66.

Hantke K, (2005) Bacterial zinc uptake and regulators. *Curr Opin Microbiol* **8**, 196-202.

Panina EM, Mironov AA, Gelfand MS, (2003) Comparative genomics of bacterial zinc regulons: enhanced ion transport, pathogenesis, and rearrangement of ribosomal proteins. *Proceedings of the National Academy of Sciences of the United States of America* **100**, 9912-9917.

Outten CE, O'Halloran TV, (2001) Femtomolar sensitivity of metall-oregulatory proteins controlling zinc homeostasis. *Science* **292**, 2488-2492.

Wang D, Hosteen O, Fierke CA, (2012) ZntR-mediated transcription of *zntA* responds to nanomolar intracellular free zinc. *J Inorg Biochem* **111**, 173-181.

Shin JH, Jung HJ, An YJ, Cho YB, Cha SS, Roe JH, (2011) Graded expression of

zinc-responsive genes through two regulatory zinc-binding sites in Zur. *Proceedings of the National Academy of Sciences of the United States of America* **108**, 5045-5050.

Ma Z, Gabriel SE, Helmann JD, (2011) Sequential binding and sensing of Zn(II) by *Bacillus subtilis* Zur. *Nucleic acids research* **39**, 9130-9138.

Kallifidas D, Pascoe B, Owen GA, Strain-Damerell CM, Hong HJ, Paget MS, (2010) The zinc-responsive regulator Zur controls expression of the coelibactin gene cluster in *Streptomyces coelicolor*. *Journal of bacteriology* **192**, 608-611.

Hesketh A, Kock H, Mootien S, Bibb M, (2009) The role of *absC*, a novel regulatory gene for secondary metabolism, in zinc-dependent antibiotic production in *Streptomyces coelicolor* A3(2). *Molecular microbiology* **74**, 1427-1444.

Shin JH, Oh SY, Kim SJ, Roe JH, (2007) The zinc-responsive regulator Zur controls a zinc uptake system and some ribosomal proteins in *Streptomyces coelicolor* A3(2). *Journal of bacteriology* **189**, 4070-4077.

Owen GA, Pascoe B, Kallifidas D, Paget MS, (2007) Zinc-responsive regulation of alternative ribosomal protein genes in *Streptomyces coelicolor* involves *zur* and sigmaR. *Journal of bacteriology* **189**, 4078-4086.

Shahab N, Flett F, Oliver SG, Butler PR, (1996) Growth rate control of protein and nucleic acid content in *Streptomyces coelicolor* A3(2) and *Escherichia coli* B/r. *Microbiology* **142 (Pt 8)**, 1927-1935.

Schroder J, Jochmann N, Rodionov DA, Tauch A, (2010) The Zur regulon of *Corynebacterium glutamicum ATCC 13032*. *BMC Genomics* **11**, 12.

Jeong Y, *et al,* (2016) The dynamic transcriptional and translational landscape of the model antibiotic producer *Streptomyces coelicolor* A3(2). *Nat Commun* **7**, 11605.

Cubillas C, Vinuesa P, Tabche ML, Garcia-de los Santos A, (2013) Phylogenomic analysis of Cation Diffusion Facilitator proteins uncovers Ni2+/Co2+ transporters. *Metallomics : integrated biometal science* **5**, 1634-1643.

Paulsen IT, Saier MH, Jr, (1997) A novel family of ubiquitous heavy metal ion transport proteins. *J Membr Biol* **156**, 99-103.

Eide DJ, (2006) Zinc transporters and the cellular trafficking of zinc. *Biochim Biophys Acta* **1763**, 711-722.

Reyes-Caballero H, *et al,* (2010) The metalloregulatory zinc site in *Streptococcus pneumoniae* AdcR, a zinc-activated MarR family repressor. *J Mol Biol* **403**, 197-216.

Pennella MA, Arunkumar AI, Giedroc DP, (2006) Individual metal ligands play distinct functional roles in the zinc sensor *Staphylococcus aureus* CzrA. *J Mol Biol* **356**, 1124-1136.

Liu T, Golden JW, Giedroc DP, (2005) A zinc(II)/lead(II)/cadmium(II)-inducible operon from the *Cyanobacterium anabaena* is regulated by AztR, an alpha3N ArsR/SmtB metalloregulator. *Biochemistry* **44**, 8673-8683.

Delany I, Rappuoli R, Scarlato V, (2004) Fur functions as an activator and as a repressor of putative virulence genes in *Neisseria meningitidis*. *Molecular microbiology* **52**, 1081-1090.

Pawlik MC, Hubert K, Joseph B, Claus H, Schoen C, Vogel U, (2012) The zinc-responsive regulon of *Neisseria meningitidis* comprises 17 genes under control of a Zur element. *Journal of bacteriology* **194**, 6594-6603.

Troxell B, Hassan HM, (2013) Transcriptional regulation by Ferric Uptake Regulator (Fur) in pathogenic bacteria. *Front Cell Infect Microbiol* **3**, 59.

Gilbreath JJ, West AL, Pich OQ, Carpenter BM, Michel S, Merrell DS, (2012) Fur activates expression of the 2-oxoglutarate oxidoreductase genes (*oorDABC*) in *Helicobacter pylori*. *Journal of bacteriology* **194**, 6490-6497.

Teixido L, Carrasco B, Alonso JC, Barbe J, Campoy S, (2011) Fur activates the expression of *Salmonella enterica* pathogenicity island 1 by directly interacting with the *hilD* operator in vivo and in vitro. *PloS one* **6**, e19711.

de Lorenzo V, Wee S, Herrero M, Neilands JB, (1987) Operator sequences of the aerobactin operon of plasmid ColV-K30 binding the ferric uptake regulation (fur) repressor. *Journal of bacteriology* **169**, 2624-2630.

Escolar L, Perez-Martin J, de Lorenzo V, (2000) Evidence of an unusually long operator for the *fur* repressor in the aerobactin promoter of *Escherichia coli*. *J Biol Chem* **275**, 24709-24714.

Tardat B, Touati D, (1993) Iron and oxygen regulation of *Escherichia coli* MnSOD expression: competition between the global regulators Fur and ArcA for binding to DNA. *Molecular microbiology* **9**, 53-63.

Frechon D, Le Cam E, (1994) Fur (ferric uptake regulation) protein interaction with target DNA: comparison of gel retardation, footprinting and electron microscopy analyses. *Biochem Biophys Res Commun* **201**, 346-355.

Le Cam E, Frechon D, Barray M, Fourcade A, Delain E, (1994) Observation of binding and polymerization of Fur repressor onto operator-containing DNA with electron and atomic force microscopes. *Proceedings of the National Academy of Sciences of the United States of America* **91**, 11816-11820.

Browning DF, Busby SJ, (2016) Local and global regulation of transcription initiation in bacteria. *Nat Rev Microbiol* **14**, 638-650.

Shin JH, Helmann JD, (2016) Molecular logic of the Zur-regulated zinc deprivation response in *Bacillus subtilis*. *Nat Commun* **7**, 12612.

Kieser T, Bibb MJ, Buttner MJ, Chater KF, Hopwood DA, (2000) *Practical Streptomyces Genetics*. John Innes Foundation.

Bibb MJ, Janssen GR, Ward JM, (1985) Cloning and analysis of the promoter region of the erythromycin resistance gene (*ermE*) of *Streptomyces erythraeus*. *Gene* **38**, 215-226.

Kim MS, Hahn MY, Cho Y, Cho SN, Roe JH, (2009) Positive and negative feedback regulatory loops of thiol-oxidative stress response mediated by an unstable isoform of sigmaR in actinomycetes. *Molecular microbiology* **73**, 815-825.

Myronovskyi M, Welle E, Fedorenko V, Luzhetskyy A, (2011) Beta-glucuronidase as a sensitive and versatile reporter in actinomycetes. *Appl Environ Microbiol* **77**, 5370-5383.

Kim MS, *et al*, (2012) Conservation of thiol-oxidative stress responses regulated by SigR orthologues in actinomycetes. *Molecular microbiology* **85**, 326-344.

Dufour YS, Landick R, Donohue TJ, (2008) Organization and evolution of the biological response to singlet oxygen stress. *J Mol Biol* **383**, 713-730.

Bieda M, Xu X, Singer MA, Green R, Farnham PJ, (2006) Unbiased location analysis of E2F1-binding sites suggests a widespread role for E2F1 in the human genome. *Genome Res* **16**, 595-605.

Kang JG, Hahn MY, Ishihama A, Roe JH, (1997) Identification of sigma factors for growth phase-related promoter selectivity of RNA polymerases from *Streptomyces coelicolor* A3(2). *Nucleic acids research* **25**, 2566-2573.

Deng Z, *et al,* (2015) Mechanistic insights into metal ion activation and operator recognition by the ferric uptake regulator. *Nat Commun* **6**, 7642.

Gilston BA, *et al,* (2014) Structural and mechanistic basis of zinc regulation across the *E. coli* Zur regulon. *PLoS Biol* **12**, e1001987.

Biasini M, *et al,* (2014) SWISS-MODEL: modelling protein tertiary and quaternary structure using evolutionary information. *Nucleic acids research* **42**, W252-258.

국문초록

Zur는 다양한 박테리아에서 아연에 특이적으로 작용하는 Fur family의 하나로서, 세포내의 아연 항상성을 유지시키기 위해 target 유전자들의 발현을 조절한다. 흙 속에서 생존하는 *Streptomyces coelicolor*는 네 개의 Fur family가 존재하고 Zur의 경우 zinc uptake transporter인 *znuACB* operon 뒤 쪽에 존재한다. 아연의 항상성을 유지하기 위해 *znuACB* operon과 리보좀 단백질이 Zur에 의해 조절된다. 또한, 아연을 세포 내에서 밖으로 수송할 수 있는 efflux protein인 SCO6751을 조절한다는 것을 밝혔고 SCO6751은 *zitB*라고 명명되었다. 현재까지, *Streptomyces coelicolor*의 경우 Zur가 전사 억제자로써의 역할을 한다고 알려져 있었지만, 이와는 반대인 *zitB*의 조절 기작의 경우 아연이 풍부한 상황에서만 반응하는 전사 유도자로써의 역할을 한다는 것을 밝혔다. *zitB*를 과 발현 시켰을 경우 포자를 형성하지 못하는 표현형을 확인할 수 있었고 야생형에 비해 항생제의 생산이 줄어드는 것을 확인할 수 있었으며 YEME 배지에서의 성장 속도와 최종 성장이 야생형보다 떨어지는 것을 확인하였다. 또한, 야생형에 비해 세포내의 금속 이온들의 양이 줄어들었는데, 아연 뿐만 아니라 철, 니켈, 코발트의 양까지 약 30% 이하로 줄어드는 것을 확인하였다. Zur가 서로 상반되는 기능을 하는 *znuA*와 *zitB*를 조절하기 때문에 아연의 농도에 따른 각 유전자의 발현 양을 비교해 보았을 때 *znuA*의 경우 아연의 농도가 fM의 범위에서만 조절을 받았고 *zitB*의 경우 fM의 범위에서 한번 발현이 유도되고 (Phase I), μM의 단위에서 한번 더 발현이 강하게 유도 (Phase II)되는 것을 확인하였다. 이러한 현상이 각 유전자의 Zur 결합서열의 차이에 일어나는지를 확인하기 위해 각 유전자의 Zur 결합서열만을 가지고 EMSA assay를 수행했을 때 Zur와 결합서열의 결합력은 동일한 것으로 확인할 수 있었다. 즉, 하나의 전사 조절자가 반대되는 기능을 가진 아연수송단백질을 세포 내 넓은 범위의 아연농도에 따라 각 유전자를 조절한다는 것을 새롭게 밝혔다. *zitB*의 어느 부위에 Zur가 결합

하는지 확인하기 위해 High resolution S1 mapping을 통해 *zitB*의 전사시작점을 확인하였고 ChIP-chip분석을 통해 Zur 결합서열을 도출해 내어 Zur 결합서열이 -35 부위의 upstream에 존재한다는 것을 확인하였다. DNaseI footprinting assay를 통해 실제로 예상한 부위에 결합하는지 확인하였고 Zur와 아연의 농도가 증가할수록 upstream방향으로만 Zur가 결합하여 늘어나는 것을 확인 할 수 있었다. 즉, 아연의 농도가 증가함에 따라 Zur가 multimerization을 형성하며 upstream방향으로 늘어나면서 *zitB*의 발현을 조절할 것이라는 가설을 세웠고 실제로 그러한지 확인하기 위해 native PAGE assay를 통해 DNA가 길어질수록 Zur가 multimerization을 형성하는 것을 확인하였다. 이것이 실제 세포 내에서 일어나는 현상인지 확인하기 위해 YEME 배지에서 일반상황과 아연이 풍부한 상황에서의 Zur 결합이 어떻게 달라지는 지를 확인하기 위해 ChIP-qPCR을 수행했고 실제로 세포 내에서 아연이 풍부한 상황에서 Zur가 upstream 방향으로 늘어나는 것을 확인 할 수 있었다. 또한, 야생형에는 없는 유전자인 β-glucuronides (GUS) 유전자를 이용하여 Zur가 결합하는 위치까지의 *zitB* promoter부위와 늘어나는 부위를 포함한 *zitB* promoter를 각각 클로닝하여 야생형에 도입해 보았을 때 아연이 충분한 조건에서 Zur가 결합하여 늘어나는 부위를 포함한 *zitB* promoter의 경우에만 GUS 유전자의 발현이 유도되는 것을 확인하였다. 또한, 이러한 현상이 Zur에 의해서만 일어나는지 확인하기 위해 *in vitro* transcription assay를 통해 아연이 충분한 조건에서 housekeeping sigma factor인 HrdB, RNA polymerase 그리고 Zur에 의해서 *zitB*의 발현이 유도된다는 것을 확인하였다. 이러한 결과들을 바탕으로 DNA와 Zur의 구조적 결합 모델을 예상해 볼 수 있었다.

주요어: *Streptomyces coelicolor*, Fur family, Zur, 아연항상성, *znuA*, zinc-exporter, *zitB*, 전사유도조절기작, Zur multimerization.